Coupled-cluster theory in quantum chemistry

Rodney J. Bartlett and Monika Musiał*

Quantum Theory Project, Departments of Chemistry and Physics, University of Florida, Gainesville, Florida 32611-8435, USA

(Published 22 February 2007)

Today, coupled-cluster theory offers the most accurate results among the practical *ab initio* electronic-structure theories applicable to moderate-sized molecules. Though it was originally proposed for problems in physics, it has seen its greatest development in chemistry, enabling an extensive range of applications to molecular structure, excited states, properties, and all kinds of spectroscopy. In this review, the essential aspects of the theory are explained and illustrated with informative numerical results.

DOI: 10.1103/RevModPhys.79.291 PACS number(s): 01.30.Rr, 31.15.Dv, 71.15.Qe, 31.25.Jf

CONTENTS

I. PERSPECTIVE ON THE MOLECULAR ELECTRONIC PROBLEM

As the recent developments in coupled-cluster (CC) theory have been mostly accomplished in quantum chemistry circles, we begin with a quote from Ken Wilson (1989):

> "*Ab initio quantum chemistry is an emerging computational area that is fifty years ahead of lattice gauge theory…and a rich source of new ideas and new approaches to the computation of many fermion systems.*"

Driving these developments are the types of problems addressed by quantum chemists, as shown in Fig. 1. Primary among these are potential-energy surfaces (PES) which describe the behavior of the electronic energy with respect to the locations of the nuclei, subject to the underlying Born-Oppenheimer or clamped nuclei approximation. As shown, these PES can be for ground or electronic excited states. At the equilibrium geometry, $\nabla E(\mathbf{R})=0$ defines the molecular structure. The second derivatives $\nabla\nabla E(\mathbf{R})$ determine whether the critical point is a minimum or a saddle point.

In addition, from the ground- and excited-state wave functions one obtains all properties that arise from a solution to the vibrational Schrödinger equation that gives the frequencies, and, with the derivatives of the dipole moment, the infrared intensities. The derivatives of the dipole polarizability define the Raman intensities. Electronic excited states are also accessible along with electronic and photoelectron spectra.

For the more kinetic aspects of chemistry, the basic concept is a reaction path that is defined as a multidimensional path along which all vibrational degrees of freedom are optimum except one, which defines a path toward products. The latter might have a saddle point as shown, which defines a transition state and its activation barriers. From that information, it is possible to obtain rate constants and state-to-state cross sections.

In addition, properties that arise from the one-particle density matrix, such as dipole moments, hyperfine coupling constants, and electric-field gradients, are readily available. Also, one obtains second- and higher-order properties such as the dipole polarizability and NMR chemical shifts and coupling constants. From even higher-order electric-field derivatives, one obtains hyperpolarizabilities, which determine nonlinear optical

*Permanent address: Institute of Chemistry, University of Silesia, Szkolna 9, 40-006 Katowice, Poland.

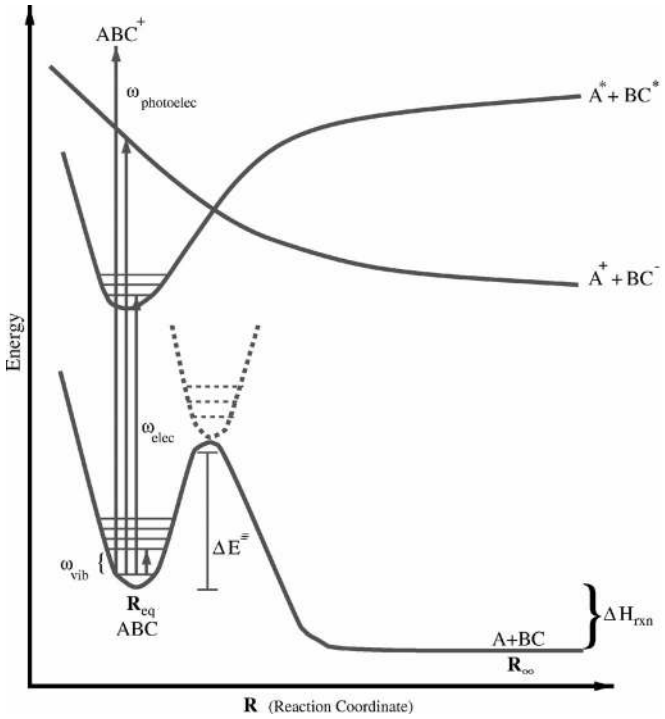

FIG. 1. The nature of quantum chemical problems.

behavior. From derivatives relative to atomic displacements in molecules, one obtains anharmonic effects on vibrational-rotational spectra. The two-particle density matrix, besides having a role in the energy, is also essential for spin operators such as $\hat{S}^2$ and spin-orbit effects in particular.

Consequently, the objective is an accurate solution of the Schrödinger equation for molecules composed of comparatively light elements. When relativistic effects are essential, the solution of the Dirac equation might be preferred. Of course, Darwin, mass-velocity, and spin-orbit effects can be added to the nonrelativistic solution to provide a wealth of approximations lying between the Schrödinger equation and the four-component Dirac equation.

For modest-sized molecules of up to ~15 light atoms or ~100 electrons and small-molecule relativistic calculations, coupled-cluster theory (Coester, 1958; Coester and Kümmel, 1960; Čížek, 1966, 1969; Paldus *et al.*, 1972; Bartlett and Purvis, 1978, 1980; Bishop and Lührmann, 1978) has become the preeminent tool to introduce the instantaneous effects of electron correlation that are not included in a mean-field approximation (Urban *et al.*, 1987; Bartlett, 1989, 1995; Paldus, 1991; Lee and Scuseria, 1995; Gauss, 1998). There are many textbook and similar accounts, each with a different focus (Lindgren and Morrison, 1986; Harris *et al.*, 1992; Bartlett and Stanton, 1994; Bishop, 1998; Crawford and Schaefer, 2000; Helgaker *et al.*, 2000; Bishop *et al.*, 2002; Shavitt and Bartlett, 2006).

In short, from the viewpoint of a physicist, coupled-cluster theory offers a synthesis of cluster expansions, Brueckner's summation of ladder diagrams (Brueckner, 1955), the summation of ring diagrams (Gell-Mann and Brueckner, 1957), and an infinite-order generalization of many-body perturbation theory (MBPT) (Kelly, 1969; Bartlett and Silver, 1974a, 1976). Hence, it is a very powerful method for correlation in many-electron systems. Its principal rationale compared to other quantum chemical methods is its correct scaling with size, termed size extensivity (Bartlett and Purvis, 1978, 1980). This means it is a purely linked diagram theory that guarantees correct scaling with the number of particles or units in a system, and facilitates accurate relative energies along a potential-energy surface or between different electronic states. Only with this property are applications to polymers, solids, or the electron gas possible, and, even for small molecules, its effects are numerically quite significant. Configuration interaction methods, long the focus of the correlation problem in quantum chemistry (Shavitt, 1998), do not, in general, have this property which is responsible for the emphasis on CC theory and its MBPT approximations (Kelly, 1969; Bartlett and Silver, 1974a, 1974b; Pople *et al.*, 1976) in chemistry.

The CC theory was introduced in 1960 (Coester and Kümmel, 1960) for calculating nuclear binding energies in nuclei that could be treated in the first approximation by a single configuration of neutrons or protons. The detailed equations for electrons were first presented in 1966 (Čížek, 1966) and its initial applications to electronic structure were reported (Čížek, 1966; Paldus *et al.*, 1972). Starting in 1978 general purpose programs and applications of CC theory were developed (Bartlett and Purvis, 1978, 1980; Pople *et al.*, 1978; Purvis and Bartlett, 1982). Early in the history of the CC, it was shown to be remarkably accurate for describing the correlation energy of the electron gas compared to the random-phase approximation (RPA) (Freeman, 1977; Bishop and Lührmann, 1978).

For more details, the history of CC theory is best told from the viewpoint of some of its principal developers. In the proceedings from the workshop "Coupled Cluster Theory of Electron Correlation" papers of Kümmel (1991) and Čížek (1991) address this issue. More recently, papers on this topic (Bartlett, 2005; Paldus, 2005) are pertinent. For the physics viewpoint, in the previous proceedings see Arponen (1991) and Bishop (1991).

For larger molecules and solids, far more approximate but more easily applied methods such as density-functional theory (DFT) or from the wave-function world the simplest correlated model MBPT(2) (also sometimes known as MP2 when using a Hartree-Fock reference function) are preferred. There are CC solutions for some simple polymers (Hirata, Grabowski, *et al.*, 2001; Hirata, Podeszwa, *et al.*, 2004). For nuclei, after an appropriate regularization of the strong interaction, CC theory can be applied almost as it is for molecules (Coester and Kümmel, 1960; Kümmel *et al.*, 1978; Guardiola *et al.*, 1996; Bishop *et al.*, 1998; Heisenberg and Mihaila, 1999; Mihaila and Heisenberg, 2000; Kowalski *et al.*, 2004; Włoch *et al.*, 2005).

Heavy-atom relativistic CC theory is also widely applied in several variants. These range from simply using relativistic pseudopotentials to describe the passive (Darwin and mass-velocity) relativistic effects (Perera and Bartlett, 1993; Sari *et al.*, 2001), to generalized pseudopotentials that also address spin-orbit effects (Mosyagin *et al.*, 2001), to one- and two-component Douglas-Kroll-Hess methods (Kaldor and Hess, 1994; Hess and Kaldor, 2000), and to a full four-component method (Eliav and Kaldor, 1996; Visscher *et al.*, 1996; Eliav *et al.*, 1998).

An essential element to understand when quantum chemists and electronic-structure physicists attempt to communicate (to paraphrase George Bernard Shaw, "one discipline divided by a common language") is that chemists are typically interested in molecules whose wave functions satisfy square-integrable boundary conditions, instead of infinite systems whose wave functions satisfy periodic boundary conditions. Since wave functions for individual molecules go to zero at infinity, this suits the Gaussian basis-set expansions used for molecules. For periodic boundary conditions, Gaussians are still often used, but there is also the prospect of using plane waves that are not tied to specific atoms, yet these have not yet found a role in the wave-function correlation treatment of individual molecules (see, however, Chawla and Voth, 1998; Sorouri *et al.*, 2006). Also purely numerical solutions can be considered and are for atomic (Lindgren and Salomonsen, 2002) and some diatomic applications of CC theory (Adamowicz *et al.*, 1985), but because of the multicenter nature of molecules, and the need for explicit consideration of two-particle effects in CC and related methods (as opposed to DFT), such grid-based solutions have not been shown to be as feasible.

On the other hand, finite Gaussian basis sets introduce an inherent error in any solution of the Schrödinger equation that has to be considered in its applications. High-level calculations will typically use a converging series of Gaussian basis functions such as the cc-pVXZ sets (Dunning, 1989; Kendall *et al.*, 1992; Woon and Dunning, 1993) or atomic natural orbital sets (Almlöf and Taylor, 1987), where cc means "correlation consistent," the pV indicates "polarized valence," meaning that the basis will have higher angular momentum orbitals than those required to describe an atom's ground state, and X will range from D for double zeta, meaning two linear combinations of Gaussian atomic orbitals per electron, to T, Q, 5, 6, etc. For the N atom, for example, there are 14 contracted Gaussian functions in the DZ form, 30 for TZ, 55 for QZ, 91 for the 5Z, and 140 for 6Z. Calculations followed by extrapolation can then be argued to approach the basis-set limit. A better but more complicated solution for the basis set is the inclusion of explicit r_{12} interactions with coupled-cluster methods (R12-CC) (Noga *et al.*, 1992). However, most molecular applications make little attempt to achieve the true basis-set limit, but instead depend upon the approximate cancellations known for the relative energies in spectroscopy, or along a reaction path, or breaking a bond into its fragments, causing much of the common basis-set correlation error to cancel from the computation. In fact, without this effect there would scarely be a computational chemistry.

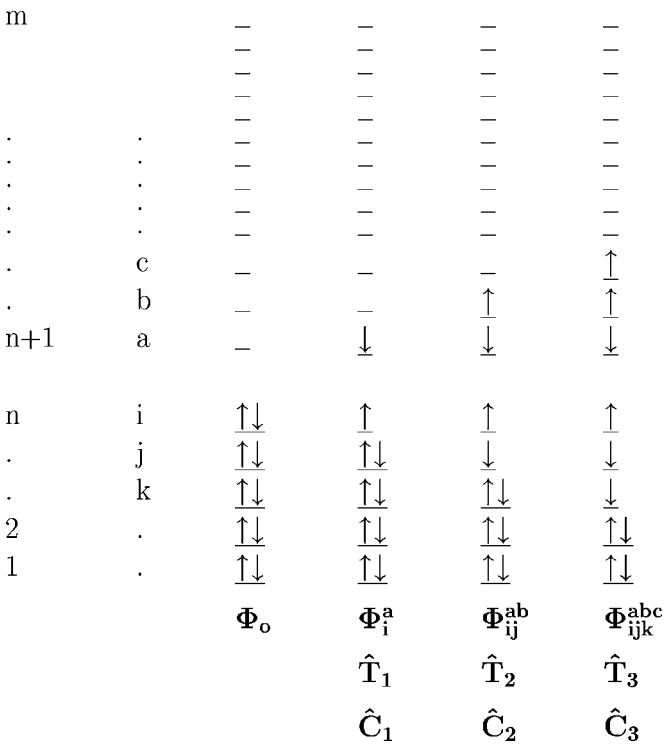

FIG. 2. Graphical examples of the selected single (Φ_i^a), double (Φ_{ij}^{ab}), and triple (Φ_{ijk}^{abc}) excitations due to the T_1 (C_1), T_2 (C_2), and T_3 (C_3) operators, respectively. Electrons from all possible occupied orbitals can be excited to all possible unoccupied orbitals, so $T_3\Phi_0=\sum_{\substack{i<j<k\\a<b<c}} t_{ijk}^{abc}\Phi_{ijk}^{abc}$.

II. PLAN FOR REVIEW

The intent of this review is to systematically develop the ideas that have enabled CC theory to become the predictive method for electron correlation in molecules, as supported by its numerical results. In Sec. III, we present an overview of solutions to the correlation problem, using elementary configuration space concepts to discuss its description using configuration interaction (CI). Configuration interaction is exact in the full CI limit, but lacks size extensivity with any truncation of the configuration space, such as to single and double excitation $\hat{C}_1$ and $\hat{C}_2$. This is the wave function $\Psi_{\mathrm{CISD}}=(1+\hat{C}_1+\hat{C}_2)\Phi_0$, with Φ_0 an independent particle (mean-field) reference function. See Fig. 2 for the definition of such excitations.

We then relate CI to Rayleigh-Schrödinger perturbation theory (RSPT) as a way to extract the CI eigenvalue. Rayleigh-Schrödinger perturbation theory has the same failings as truncated CI, but once all configurations that can contribute in a given order are considered, RSPT becomes many-body perturbation theory (MBPT), which as a fully linked method has to be size

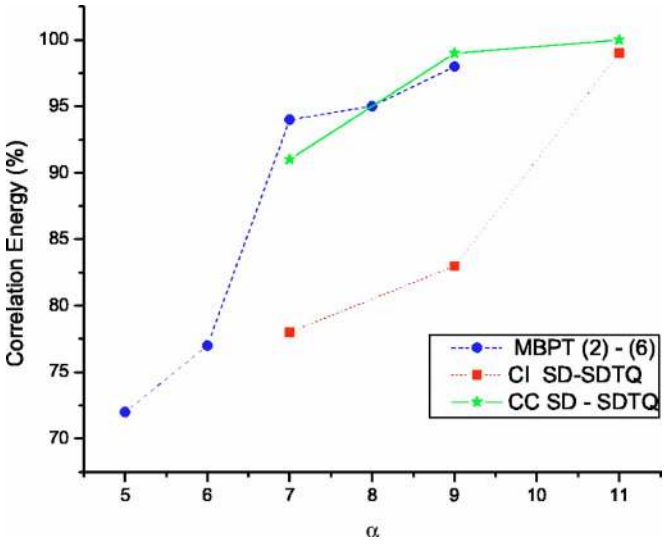

FIG. 3. (Color online) Performance of theories for the correlation energy in small molecules. Graphed is the percentage of the full correlation energy achieved by the CI, CC, and MBPT theories, as a function of the level of approximation. To facilitate comparisons, the ordinate gives the size-scaling parameter of the approximation $\alpha=\alpha_n+\alpha_N+\alpha_{it}$ in the computational cost function $n^{\alpha_n}N^{\alpha_N}N_{it}^{\alpha_{it}}$. Shown are MBPT (solid circles), approximations (2)–(6); CI (solid squares), approximations SD-SDTQ; and CC (stars), approximations SD-SDTQ. The correlation energy is defined with respect to the Hartree-Fock energy for the given basis set, and the full correlation energies are obtained from the FCI calculations quoted in Table I.

extensive. In practice, MBPT mostly offers a finite-order approximation to the correlation problem, with the inherent failings of such expansions.

On the contrary, coupled-cluster theory offers a very convenient and powerful resummation of MBPT diagrams, providing an infinite-order approximation in selected cluster operators. In particular, $\Psi_{\mathrm{MBPT}}=\exp(T)\Phi_0=\Psi_{\mathrm{CC}}$ for $T=T_1+T_2+\cdots+T_n$, where T_p is a connected cluster operator that corresponds to p-fold excitations (Fig. 2). Correct scaling with the number of particles (extensivity) is ensured due to the exponential form with the condition that T be connected. Limiting the resummations to all terms that arise from single and double excitation cluster operators T_1 and T_2, e.g., defines $\Psi_{\mathrm{CCSD}}=\exp(T_1+T_2)\Phi_0$, which adds all the products like $T_2^2/2$ and T_1T_2 to the CI wave function. As shown in Fig. 3, numerical results of CI with higher excitation operators compared to orders of MBPT and CC with higher excitation clusters clearly demonstrate the numerical superiority of CC theory.

In Secs. IV and V, we introduce the unambiguous easily applied diagrammatic approach that has been developed to derive the detailed form of the CC equations including T_2, coupled-cluster doubles (CCD), T_1 and T_2 (CCSD), and with triples (CCSDT) and connected quadruple excitations (CCSDTQ). The computational difficulty and the expense of the latter necessitate some simplified approximations, and these can be iterative like CCSDT-1, or noniterative like CCSD(T). Section VI defines and documents how well all these approximations work for real world applications in comparison with experiment.

Section VII introduces the Λ deexcitation operator, which allows the treatment of energy derivatives on potential-energy surfaces $\nabla E(\mathbf{R})=\langle 0|(1+\Lambda)\exp(-T)\times\nabla H(\mathbf{R})\exp(T)|0\rangle$ and for the density matrices $\gamma_{pq}=\langle\Phi_0|(1+\Lambda)\exp(-T)\hat{c}_p^\dagger\hat{c}_q\exp(T)|\Phi_0\rangle$ and $\Gamma_{pqrs}=\langle\Phi_0|(1+\Lambda)\exp(-T)\hat{c}_p^\dagger\hat{c}_q^\dagger\hat{c}_s\hat{c}_r\exp(T)|\Phi_0\rangle$, where $\hat{c}_p^\dagger\hat{c}_q$ are occupation number operators described in Sec. V. Λ and $\exp(T)$ are dual. Together they define the CC functional $E=\langle 0|(1+\Lambda)e^{-T}He^T|0\rangle$. Numerical results for molecular structures and vibrational frequencies are pertinent here.

In the next section, we consider excited, ionized, and electron attached states by using the ansatz $\hat{R}_k\Psi_{\mathrm{CC}}=\Psi_k$, where $\hat{R}_k=R_0^{(k)}+R_1^{(k)}+R_2^{(k)}+\cdots$ is another excitation operator which after a constant creates single, double, etc. excitations from the CC reference solution. Inserting this ansatz into the Schrödinger equation for the kth excited state and subtracting the ground state leads to the EOM-CC method $[\bar{H},\hat{R}_k]|0\rangle=\omega_k\hat{R}_k|0\rangle$, with $\omega_k=E_k-E_0$, and $\hat{R}_k$ is a right-hand eigenvector. The left-hand eigenvector ($\hat{L}_k$ is a deexcitation operator) $\hat{L}_k\bar{H}=\hat{L}_k\omega_k$, $\langle 0|\hat{L}_k\hat{R}_l|0\rangle=\delta_{kl}$; $L_0=(1+\Lambda)$ and $R_0=1$, making the connection with the ground-state functional. Excited states have the associated density matrices, $\gamma_{pq}^{kl}=\langle 0|\hat{L}_k\exp(-T)\hat{c}_p^\dagger\hat{c}_q(T)\hat{R}_l|0\rangle$. The spectrum of eigenvectors also defines second- and higher-order response properties. Many numerical results are presented.

The final section considers the generalization of the reference function $|\Phi_0\rangle$ to multireference form by replacing it with a linear combination of important determinants $\{\Phi_1,\Phi_2,\ldots,\Phi_m\}$, and redefines the cluster expansion operator accordingly to define two different multireference (MRCC) methods. These are pertinent when there are quasidegeneracies as would occur in open-shell atoms, or as bonds are broken in dissociation. One then obtains an effective Hamiltonian matrix and associated eigenvector equations that can treat several states at once, or be reduced to a multireference, state-specific form. Numerical illustrations of Hilbert-space and Fock-space MRCC applications are discussed, including the application of an intermediate Hamiltonian to eliminate intruder states.

III. SOME ESSENTIAL PRELIMINARIES

The Hamiltonian in the Born-Oppenheimer approximation is

$$H(\mathbf{R})=-\tfrac{1}{2}\sum_{i=1}^{n}\nabla^2(\mathbf{r}_i)-\sum_{\alpha}Z_\alpha/(\mathbf{r}_i-\mathbf{R}_\alpha)+\tfrac{1}{2}\sum_{i,j=1}^{n}1/(\mathbf{r}_i-\mathbf{r}_j)+\tfrac{1}{2}\sum_{\alpha,\beta}Z_\alpha Z_\beta/(\mathbf{R}_\alpha-\mathbf{R}_\beta)\qquad(1)$$

$$= \sum_i h(\mathbf{r}_i) + \tfrac{1}{2}\sum_{i,j} \hat{g}(\mathbf{r}_i,\mathbf{r}_j) + E_{\mathrm{NN}}, \tag{2}$$

where $\{\mathbf{r}_i\}$ locates the electrons and $\{\mathbf{R}_\alpha\}$ the nuclei. Z_α is the atomic number of the nucleus α. E_{NN} is a constant at any geometry, so it needs no further consideration within the clamped nuclei approximation.

Choosing to use expressions in terms of spin orbitals $x_1=1=\vec{r}_1\eta_1$ with η_1 the spin coordinate for electron 1, the independent particle wave function is $\mathcal{A}(\phi_1(1)\phi_2(2)\cdots\phi_n(n))$, where $\mathcal{A}=(1/\sqrt{n!})\Sigma_P(-1)^pP$, with P providing the permutation and $(-1)^p$ its parity.

Separating the electronic Hamiltonian that is parametrically dependent on $\mathbf{R}$ into an unperturbed and perturbed part,

$$H(\mathbf{r};\mathbf{R}) = H_0 + V, \tag{3}$$

$$H_0 = \sum_i [\hat{h} + \hat{u}](i) = \sum_i \hat{h}^{\mathrm{eff}}(i), \tag{4}$$

$$V = \tfrac{1}{2}\sum_{ij} \hat{g}(ij) - \sum_i \hat{u}(i), \tag{5}$$

where $\hat{u}(i)$ represents an average (mean) field potential as in the Hartree-Fock case, where $\hat{u}(1)=\hat{J}(1)-\hat{K}(1) = \int d\tau_2 \Sigma_j^n \phi_j^*(2)\phi_j(2)/|\mathbf{r}_1-\mathbf{r}_2| - \int d\tau_2 \Sigma_j^n \phi_j^*(2)P_{12}\phi_j(2)/|\mathbf{r}_1-\mathbf{r}_2|$, and $\hat{h}^{\mathrm{eff}}(1)=\hat{f}(1)$ is the Fock operator. $\mathbf{x}$ and $\mathbf{R}$ represent positions of all electrons and nuclei, respectively. The space-spin volume element is $d_{\tau 2}$, and P_{12} indicates the permutation of electrons 1 and 2. Unless stated otherwise, throughout this review we will assume the spin-orbital form of the one-particle equations. This is the simplest for formal manipulations and means all equations will be equally applicable to closed-shell and high-spin (i.e., maximum unpaired spin) open-shell atoms and molecules. In the simplest case, η will reduce to either α for spin $S_z=+1/2$ or β for spin $-1/2$. For generalized spin orbitals $\eta_1=N(\alpha_1+c\beta_1)$, which would sacrifice the S_z quantum number.

With the solution to the one-particle equation $\hat{h}^{\mathrm{eff}}(1)\phi_p(1)=\epsilon_p\phi_p(1)$, the solution of the unperturbed Schrödinger equation is given by $H_0\Phi_0=E_0\Phi_0$, where $E_0=\Sigma_i\epsilon_i$. Φ_0 is the single-determinant approximation to the electronic wave function $E_{\mathrm{ref}}=\langle\Phi_0|H|\Phi_0\rangle=E_0+E^{(1)}$.

In addition, in any finite basis-set solution of the one-particle equation, the spatial part of the orbitals $\boldsymbol{\phi}=\boldsymbol{\chi}\mathbf{c}$, where $\boldsymbol{\chi}$ is the underlying, typically Gaussian atomic-orbital basis set of dimension, M, and $\mathbf{c}$ is a vector of the coefficients. These functions are determined for different elements and are located on all atoms in a molecule. This leads to the equation $\mathbf{h}^{\mathrm{eff}}\mathbf{c}=\mathbf{Sc}\boldsymbol{\epsilon}$, where $\mathbf{S}$ is an overlap matrix $\mathbf{S}_{ij}=\langle\boldsymbol{\chi}_i|\boldsymbol{\chi}_j\rangle$. There are M solutions to this equation, so for $p\leqslant n$, we have occupied orbitals (those below a Fermi level), and for $p>n$, $M-n=N$ unoccupied orbitals, sometimes called virtual since they are a by-product of the finite basis calculation and have no role in defining h^{eff}.

A. Configuration interaction

The essence of the electron correlation problem in a one-particle basis set is to give the n-particle wave function the flexibility to keep electrons apart by the admixture of the higher excitations. The traditional route in quantum chemistry that goes back to Slater (1929), Parr (Parr and Crawford, 1948), and Boys (1950) has been configuration interaction (CI). That is, build an n-particle wave function from the singly excited, doubly excited, etc., determinants, $\{\Phi_i^a\},\{\Phi_{ij}^{ab}\},\ldots$, where each such excitation means a determinant where some of the n occupied orbitals, $i,j,k,l,\ldots,n$ are replaced by the $M-n=N$ virtual orbitals, $a,b,c,d,\ldots,N$ when the orbitals have the same spin. We use the indices p,q,r,s when the orbitals are unspecified. We choose intermediate normalization $\langle\Phi_0|\Psi_{\mathrm{CI}}\rangle=1$. The exact wave function in a finite basis set is the full CI (FCI), which means include all same-spin excitations up to n-tuple ones for n electrons,

$$\Psi_{\mathrm{CI}} = \Phi_0 + \sum_{a,i} C_i^a\Phi_i^a + \sum_{i>k,a>b} C_{ij}^{ab}\Phi_{ij}^{ab} + \cdots + \sum_{\substack{i>j>k>\cdots \\ a>b>c>\cdots}} C_{ijk\cdots n}^{abc\cdots M}\Phi_{ij\cdots n}^{ab\cdots N} \tag{6}$$

$$= \left(1 + \sum_p^n \hat{C}_p\right)\Phi_0, \tag{7}$$

where the coefficients $\{C_{ij\cdots}^{ab\cdots}\}$, of which there are $\sim(nN)^m$, where m indicates the excitation level, are normally determined variationally. The full CI is an impossibility for any but quite small molecules in small basis sets since the number of determinants is $\sim(nN)^n\sim M^n$ for M basis functions. However, the full CI is an unambiguous reference model for the correlation problem as it is the best possible solution in any finite basis set. It is variational $E_{\mathrm{CI}}>E_{\mathrm{exact}}$, invariant to all orbital rotations, and is size extensive. In a complete basis, the full CI, then termed the complete CI, gives the exact solution to the Schrödinger equation. When one refers to a truncated CI, one means that one is limited to some subset of the possible excitations, like all single and double excitations, or CISD. It is variational, invariant to orbital transformations among just the occupied or unoccupied orbitals, but it is not size extensive.

Paying a little more attention to the eigenvalue problem for a truncated CI like CISD, we have the equations

$$\langle\Phi_i^a|(H-\Delta E)\hat{C}_1 + H\hat{C}_2|0\rangle = 0, \tag{8}$$

$$\langle\Phi_{ij}^{ab}|H\hat{C}_1 + (H-\Delta E)\hat{C}_2|0\rangle = 0, \tag{9}$$

$$E_{\mathrm{CISD}} = \langle\Phi_0|H|\Phi_0\rangle + \Delta E, \tag{10}$$

$$\Delta E = \langle \Phi_0 | H(\hat{C}_1 + \hat{C}_2) | \Phi_0 \rangle. \tag{11}$$

The size-extensivity problem in CI arises from the $-\Delta E C_n$ terms, which will remain in any less than full CI calculation. These, of course, contribute unlinked diagrams (discussed in the next section) into the CISD energy, since ΔE is represented by closed diagrams, causing its product with C_n to be unlinked. Such unlinked terms can only be removed from the CI equations by formal consideration of some kinds of contributions from higher excitations beyond those in the particular truncated CI. The proper inclusion of such contributions is accomplished in MBPT and coupled-cluster theory.

B. Perturbation theory

The connection between CI and perturbation theory is readily apparent when perturbation theory (PT) is used to extract the CI eigenvalue. Using the CISD matrix problem for the ground-state energy as an example,

$$\begin{bmatrix} \langle \Phi_0|H|\Phi_0\rangle & \langle \Phi_0|H|\mathbf{h}\rangle \\ \langle \mathbf{h}|H|\Phi_0\rangle & \langle \mathbf{h}|H|\mathbf{h}\rangle \end{bmatrix} \begin{bmatrix} 1 \\ \mathbf{C} \end{bmatrix} = \begin{bmatrix} 1 \\ \mathbf{C} \end{bmatrix} E,$$

where $|\mathbf{h}\rangle$ indicates the single $|\Phi_i^a\rangle$ and double $|\Phi_{ij}^{ab}\rangle$ excitations in configuration space. Solving for $\mathbf{C}$ in the matrix equation, a little manipulation gives the ground-state eigenvalue

$$E = \langle \Phi_0|H|\Phi_0\rangle + \langle \Phi_0|H|\mathbf{h}\rangle\langle h|E - H|\mathbf{h}\rangle^{-1}\langle \mathbf{h}|H|\Phi_0\rangle. \tag{12}$$

From this expression, Rayleigh-Schrödinger PT emerges from a separation of $H = H_0 + V$, where $H_0 = \Sigma_i h^{\text{eff}}(i)$, $V = H - H_0$, and a recognition that $E = E_0 + E^{(1)} + E^{(2)} + \cdots$. Then, $\mathbf{R} = \langle \mathbf{h}|E_0 - H_0 + V - \Delta E|\mathbf{h}\rangle^{-1} = \mathbf{R}_0 + \mathbf{R}_0(V - \Delta E)\mathbf{R}$. This leads to the energy $E = \langle \Phi_0|H|\Psi_{\text{RSPT}}\rangle$, and wave-function corrections $\Psi_{\text{RSPT}} = \Phi_0 + \Psi^{(1)} + \Psi^{(2)} + \cdots$ (Löwdin, 1968). Within the configuration space $|\mathbf{h}\rangle$,

$$E_0 = \sum_{i=1}^{n} \epsilon_i, \tag{13}$$

$$E^{(1)} = \langle \Phi_0|V|\Phi_0\rangle, \tag{14}$$

$$E^{(2)} = \langle \Phi_0|H|\mathbf{h}\rangle\langle \mathbf{h}|\mathbf{E}_0 - \mathbf{H}_0|\mathbf{h}\rangle^{-1}\langle \mathbf{h}|H|\Phi_0\rangle = \langle \Phi_0|VR_0V|\Phi_0\rangle = \langle \Phi_0|V|\Psi^{(1)}\rangle, \tag{15}$$

$$E^{(3)} = \langle \Phi_0|VR_0(V - E^{(1)})R_0V|\Phi_0\rangle \tag{16}$$

$$= \langle \Phi_0|V|\Psi^{(2)}\rangle = \langle \Psi^{(1)}|V - E^{(1)}|\Psi^{(1)}\rangle, \tag{17}$$

$$E^{(4)} = \langle \Phi_0|V|\Psi^{(3)}\rangle = \langle \Phi_0|VR_0(V - E^{(1)})|\Psi^{(2)}\rangle - E^{(2)}\langle \Psi^{(1)}|\Psi^{(1)}\rangle \tag{18}$$

$$= \langle \Psi^{(2)}|E_0 - H_0|\Psi^{(2)}\rangle - E^{(2)}\langle \Psi^{(1)}|\Psi^{(1)}\ldots,$$

$$\ldots . \tag{19}$$

The resolvent operator $\hat{R}_0 = |\mathbf{h}\rangle\langle \mathbf{h}|E_0 - H_0|\mathbf{h}\rangle^{-1}\langle \mathbf{h}| = |\mathbf{h}\rangle\mathbf{R}_0\langle \mathbf{h}|$. We also have $(E_0 - H_0)|\Phi_{ij\ldots}^{ab\cdots}\rangle = (\epsilon_i + \epsilon_j + \cdots - \epsilon_a - \epsilon_b - \cdots)|\Phi_{ij}^{ab}\rangle$, which makes the resolvent matrix diagonal. With a Hartree-Fock (HF) reference, only double excitations contribute to $E^{(2)}$ and $E^{(3)}$.

Note that as long as the configuration space is restricted to a subset of possible excitations, like single and double excitations, renomalization terms like $-E^{(2)}\langle \Psi^{(1)}|\Psi^{(1)}\rangle$ remain. Since $E^{(2)}$ has to scale linearly with the number of particles, and it may be shown that $\langle \Psi^{(1)}|\Psi^{(1)}\rangle$ does likewise, such renormalization terms have the potential [except for exclusion principle violating (EPV) terms, discussed later] to scale as $\sim n^2$ with those in higher orders of PT scaling with higher powers of n. So any truncated CI eigenvalue will retain such terms. However, in the full CI they would not. Their elimination is achieved in a given order when all higher excitations are included in the space of configurations $|\mathbf{h}\rangle$ that can contribute to that order. That is, in fourth order we have to consider $|\mathbf{h}\rangle = |\mathbf{h}_1\mathbf{h}_2\mathbf{h}_3\mathbf{h}_4\rangle$ where we also have triple and quadruple excitations. Once we include the latter, with some algebra (Bartlett and Silver, 1975) it can be shown that $-E^{(2)}\langle \Psi^{(1)}|\Psi^{(1)}\rangle$ is solely determined by double excitations and is removed from $E^{(4)}$ by the role of quadruple excitations in the lead term of $E^{(4)}$. This cancellation between different categories of excitations was first shown by Brueckner (1955). This is the substance of the linked-diagram theorem, as proved to all orders by Goldstone (1957) using time-dependent, diagrammatic techniques. It may also be proven in a time-independent way (Paldus and Čížek, 1975; Manne, 1977; Shavitt and Bartlett, 2006). Hence, if we do not restrict our configuration space but allow all excitations that can contribute in a given order (that is always less than the full CI space), we make the transition from RSPT to MBPT and dispense with any renormalization or unlinked terms. In MBPT, we can then write

$$|\Psi_{\text{MBPT}}\rangle = |\Phi_0\rangle + \sum_{k=1}^{n} [\hat{R}_0(V - E^{(1)})]^k|\Phi_0\rangle_L, \tag{20}$$

$$E^{(n+1)} = \langle \Phi_0|V|\Phi^{(n)}\rangle_L, \tag{21}$$

$$E^{(2n+1)} = \langle \Phi^{(n)}|V - E^{(1)}|\Phi^{(n)}\rangle_L, \tag{22}$$

$$E^{(2n)} = \langle \Phi^{(n)}|E_0 - H_0|\Phi^{(n)}\rangle_L, \tag{23}$$

where L indicates the restriction to linked diagrams. In this form, MBPT assumes the formal simplicity of Brillouin-Wigner perturbation theory (Löwdin, 1968), but without the dependence on an unknown energy.

This simple example leads to several important consequences. (i) Rayleigh-Schrödinger perturbation theory when allowing all categories of excitations that can occur in a given order of perturbation theory becomes many-body perturbation theory (MBPT), where the many-body terminology emphasizes that the theory has to provide correct scaling with the number of particles or size-extensive results for the energy, wave function, and density matrices (i.e., there are no unlinked diagrams). (ii) The converse is if we restrict the excitations in RSPT to subsets like single and double excitations, as

in CISD, infinite-order RSPT=CISD, and any such truncated CI is not size extensive. Only the full CI is.

An important benefit of the linked-cluster factorization is that the contribution of $|\mathbf{h}_4\rangle$ into $E^{(4)}$ might appear to require eight-index denominators since $\mathbf{R}_0$ would contain $|\mathbf{h}_4\rangle\langle\mathbf{h}_4|E_0-H_0|\mathbf{h}_4\rangle^{-1}\langle\mathbf{h}_4|\subset|\Phi^{abcd}_{ijkl}\rangle(\epsilon_i+\epsilon_j+\epsilon_k+\epsilon_l-\epsilon_a-\epsilon_b-\epsilon_c-\epsilon_d)^{-1}\langle\Phi^{abcd}_{ijkl}|$, but all such terms are replaced by a product of two four-index denominators $(\epsilon_i+\epsilon_j-\epsilon_a-\epsilon_b)(\epsilon_k+\epsilon_l-\epsilon_c-\epsilon_d)$ by simply putting two terms over a common denominator (Bartlett and Silver, 1975), a simple application of the Frantz-Mills factorization theorem (Frantz and Mills, 1960). The effect of such a factorization is important numerically, since an eight-index denominator would require an $\sim n^4N^6$ computational procedure, while four-index denominators, even as products, never require more than an $\sim n^2N^4$ procedure. This is the same as CISD, but now the effects of essential quadruple excitations are included.

One final lesson in this simple example is that for two electrons (i,j) we have no quadruple excitations, so rather than canceling the renomalization term, the exact result would have to retain it. However, we can still allow the formal quadruple excitations like $|\mathbf{h}_4\rangle$ to be included in the equations, even though we know that these determinants violate the exclusion principle for two electrons making their contribution zero. However, after the cancellation of the renormalization term, we are left with nonvanishing contributions of those determinants that appear as part of the quadruple excitation linked diagrams that remain, even for two electrons. For two electrons their value is equal to that of the renormalization term, thereby accounting for it. These residual terms are somewhat misleadingly called EPV for exclusion principle violating (Kelly, 1962), though, of course, there is no violation. It is just a different way of counting (Szalay and Bartlett, 1992). This will also be the reason why all equations in MBPT and CC theory will have unrestricted summation indices, which is very different from CI, where the exclusion principle is enforced for every determinant in the wave function. This, too, offers a distinct computational advantage.

C. Coupled-cluster theory

The basic equations of coupled-cluster theory are deceptively simple. We start from the fact that the exact, linked-diagram wave function above (as will be shown in the next section) can be written as

$$\Psi_{\mathrm{MBPT}}=\Psi_{\mathrm{CC}}=\exp(T)\Phi_0=\Omega\Phi_0, \tag{24}$$

$$\Psi_{\mathrm{CC}}=(1+T+T^2/2+T^3/3!+\cdots)\Phi_0, \tag{25}$$

where Ω is often called the wave operator as it takes an unperturbed solution into the exact solution. The cluster operator T is composed of a series of connected operators that can be expanded in terms of its components that introduce single Φ^a_i, double Φ^{ab}_{ij}, triple Φ^{abc}_{ijk}, etc. excitations into the wave function as in Fig. 2,

$$T=T_1+T_2+T_3+\cdots+T_n, \tag{26}$$

$$T_n=(n!)^{-2}\sum_{\substack{i,j,\ldots\\a,b,\ldots}} t^{ab\cdots}_{ij\cdots}\hat{c}^\dagger_a\hat{c}^\dagger_b\cdots\hat{c}_j\hat{c}_i, \tag{27}$$

$$T_1\Phi_0=\sum_{i,a} t^a_i\Phi^a_i, \tag{28}$$

$$T_2\Phi_0=\sum_{i>j,a>b} t^{ab}_{ij}\Phi^{ab}_{ij}, \tag{29}$$

$$T_3\Phi_0=\sum_{i>j>k,a>b>c} t^{abc}_{ijk}\Phi^{abc}_{ijk}, \tag{30}$$

$$T_4\Phi_0=\sum_{i>j>k>l,a>b>c>d} t^{abcd}_{ijkl}\Phi^{abcd}_{ijkl}, \tag{31}$$

$\cdots$.

These T_n contributions are referred to as connected since they cannot be reduced further. However, by virtue of the nonlinear terms in the exponential expansion, we have, in addition, the disconnected (but linked) components of the exact wave function,

$$\tfrac{1}{2}T_2^2\Phi_0=\sum_{\substack{i>j,a>b\\k>l,c>d}} t^{ab}_{ij}t^{cd}_{kl}\Phi^{abcd}_{ijkl}, \tag{32}$$

$$\tfrac{1}{2}T_1^2\Phi_0=\sum_{\substack{i,a\\j,b}} t^a_it^b_j\Phi^{ab}_{ij}, \tag{33}$$

$$T_1T_2\Phi_0=\sum_{\substack{ia\\k>l,c>d}} t^a_it^{cd}_{kl}\Phi^{abc}_{ijk}, \tag{34}$$

$\cdots$.

Note that even though these terms such as $T_2^2/2$ introduce quadruple excitations into the wave function, they are greatly simplified as their coefficients are composed of products of just double excitation coefficients, or $\sim n^2N^2$ coefficients instead of the $\sim n^4N^4$ associated with T_4.

The equations for the CC amplitudes $\{t^{ab\cdots}_{ij\cdots}\}$ are obtained by insertion into the Schrödinger equation, followed by projection onto a sufficient number of excitations,

$$\exp(-T)H\exp(T)\Phi_0=\bar{H}\Phi_0=E\Phi_0, \tag{35}$$

$$\langle\Phi^{ab\cdots}_{ij\cdots}|\bar{H}|\Phi_0\rangle=Q\bar{H}P=0, \tag{36}$$

$$E=\langle\Phi_0|\exp(-T)H\exp(T)|\Phi_0\rangle=\langle\Phi_0|\bar{H}|\Phi_0\rangle. \tag{37}$$

From the well-known Hausdorff expansion,

$$\bar{H} = H + [H,T] + \frac{1}{2}[[H,T]T] + \frac{1}{3!}[[[H,T]T]T] + \frac{1}{4!}[[[[H,T]T]T]T], \quad (38)$$

which has to terminate after fourfold commutators when H has no more than two-electron operators in it. Hence, the CC equations (36) are connected, as any terms that would not have indices in common between H and T would be eliminated. This makes the CC wave function $\Psi_{CC}=\exp(T)|\Phi_0\rangle$ linked, and consequently the energy in Eq. (37) is too. This requires that the energy be size extensive (Bartlett and Purvis, 1978), which is an essential requirement of the theory. Note that Eq. (36) is of the general form $T_p=f(T_1,T_2,\ldots,T_{p-1})+g(T_p,T_{p+1},T_{p+2})$. The contribution of the first term is always $\leqslant n^p N^{p+1}$, while T_p into T_p is always one N higher, with T_{p+1} being nN^2 and T_{p+2} being n^2N^3 higher. Hence, for CCSD where $T_3=T_4=0$, we have a computational scaling of $\sim n^2N^4$; CCSDT is $\sim n^3N^5$, and CCSDTQ is $\sim n^4N^6$.

Comparing the exact CC solution with the full CI, we see that

$$C_1 = T_1, \quad (39)$$

$$C_2 = T_2 + \tfrac{1}{2}T_1^2, \quad (40)$$

$$C_3 = T_3 + T_1T_2 + T_1^3/3!, \quad (41)$$

$$C_4 = T_4 + T_2^2/2 + T_1T_3 + T_1^2T_2/2 + T_1^4/4!, \quad (42)$$

$$\vdots,$$

which demonstrates the cluster decomposition of the wave function. As the Hamiltonian has at most two-particle interactions in it, logically one might expect that the simultaneous correlation of two electrons in different parts of a molecule, as represented by $T_2^2/2$, is more important in the wave function than the true, connected four-particle cluster interactions associated with T_4, and for electronic structure this is indeed the case. Hence, a coupled-cluster wave function limited to connected double excitations (CCD) $\Psi_{CCD}=\exp(T_2)\Phi_0$, the simplest CC approximation, already includes the disconnected parts of quadruples, hextuples, and higher even-ordered excitations. Such disconnected products are responsible for the size-extensivity property of the method. That is, it is appropriate for many electrons. Without this, CC theory, like truncated CI, could not be applied to infinite systems such as crystalline solids or the electron gas.

Besides the obvious application to infinite systems, a manifestation of size extensivity in chemistry is the energy released (or absorbed) in a reaction, called the heat of the reaction. For example, for the reaction $A+B \rightarrow C+D$, $\Delta E_{rxn}=\Delta E(C)+\Delta E(D)-\Delta E(A)-\Delta E(B)$. When these energies are obtained from CC theory, it is appropriate to add them as above since (assume closed shells for simplicity) $H_{A+B}\Psi_{CC}(A+B)=H_A\Psi_{CC}(A)H_B\Psi_{CC}(B)$ and $E_{AB}=E_A+E_B$, but for a nonextensive method such as CI, separate calculations have to be made for $A+B$ and $C+D$ far apart, to get meaningful energy differences, since $H_{A+B}\Psi_{CI}(A+B)\neq H_A\Psi_{CI}(A)H_B\Psi_{CI}(B)$. Hence, there cannot be any such thing as a table of energies computed by truncated CI for a variety of molecules, which can then be added to evaluate energies (heats) of chemical reactions.

Another manifestation is obtaining consistent, relative energies along a PES. That is, the theory should give meaningful energy differences for activation barriers where bonds are being formed and broken, or even for the detailed vibrational frequencies for a molecule in its equilibrium geometry. Size extensivity is absolutely essential in today's quantum chemistry, and that has led to the emphasis on CC and its MBPT approximations.

Since the full CI has to be the exact result in a basis set, it provides an unambiguous measure of how well a given approximation does for electron correlation. In Table I and Fig. 3, we illustrate results from CI subject to higher excitation operators and finite-order MBPT and CC theory with higher connected operators. The plot shows convergence to 100% of the correlation energy with an excitation level or order of perturbation theory. All methods first require an integral transformation from atomic to molecular orbitals. For $M=n+N$ basis functions, this scales as $\sim M^5$. In terms of computational scaling, the CI and CC methods without further restrictions scale as $\sim n^l N^{l+2} N_{it}$ with the level of excitation l, where n means the number of occupied orbitals and N is the number of unoccupied ones, and N_{it} indicates the number of iterations required to converge. In other words, to do CISD requires $\sim n^2N^2$ coefficients in $\hat{C}_2$ and at least one summation of N^2 in the evaluation of $\langle\Phi_{ij}^{ab}|H\hat{C}_2|\Phi_0\rangle$. Adding quadruple excitations into CI requires $\sim n^2N^2$ more time and computational resources. As even in a small calculation, $n=10$, $N=100$, the extension to quadruple excitations is $\sim 10^6$ times as difficult. The most important parts of the quadruple excitations in CI are those that account for the unlinked diagrams. Hence, the transition to MBPT has already eliminated such terms to all orders, making even the low-order results better in some cases. The MBPT(2) approximation is limited by the integral transformation unlike the other methods, as it has a very quick $\sim n^2N^2$ evaluation. The MBPT(3) approximation scales the same as CISD, but it is noniterative as are all the MBPT approximations. The power of CC theory is shown when considering the scaling of CCSD which is the same as CISD, but unlike the latter CCSD already benefits from the elimination of unlinked quadruple excitation diagrams, and the largest part of the remainder of the linked ones is conveniently introduced by the disconnected term $T_2^2/2$. But the scaling of this term is only $\sim n^2N^4$, compared to $\sim n^4N^6$ for the quadruples in CISDTQ, which would include connected, disconnected, and unlinked terms. This is obviously an enormous savings. Full MBPT(4) scales as $\sim n^3N^4$, since the rate-determining step is for connected

TABLE I. Correlation corrections (in mH) with various CC methods relative to FCI[a] values.

Molecule		CCSD[b]	CCSDT[b]	CCSDTQ[b]	CCSDTQP[c]
BH	R_e	1.79	0.068	0.001	0.000
	$1.5R_e$	2.64	0.026	0.000	0.000
	$2.0R_e$	5.05	−0.091	0.001	0.000
HF	R_e	3.006	0.266	0.018	0.000
	$1.5R_e$	5.099	0.646	0.041	0.000
	$2.0R_e$	10.181	1.125	0.062	0.001
H_2O	R_e	4.122	0.531	0.023	0.002
	$1.5R_e$	10.158	1.784	0.139	0.025
	$2.0R_e$	21.404	−2.472	−0.015	0.026
SiH_2	R_e	2.843	0.100	0.002	0.001
	$1.5R_e$	6.685	0.058	−0.015	0.001
	$2.0R_e$	14.869	−3.689	−0.346	0.001
CH_2	R_e	3.544	0.206	0.007	0.000
	$1.5R_e$	6.961	0.310	0.026	0.000
	$2.0R_e$	14.648	−1.900	−0.050	0.000
N_2	R_e	13.465	1.626	0.192	0.016
C_2	R_e	29.597	3.273	0.622	0.103
mean abs. err.		9.17	1.069	0.092	0.010

[a]Bauschlicher and Taylor, 1986, 1987a, 1987b; Bauschlicher *et al.*, 1986; Kucharski and Bartlett 1993; Christiansen *et al.*, 1996.
[b]Kucharski and Bartlett, 1998a.
[c]Musiał *et al.*, 2002b.

triple excitations. If they are eliminated leaving SDQ-MBPT(4), then we have the noniterative ($\sim n^2N^4$) approximation to CCSD. The noniterative approximation MBPT(4) to CCSDT has one N higher in scaling instead of two because there is no $T_3 \rightarrow T_3$ coupling in MBPT(4). Those terms would arise in fifth order, along with the first contribution from connected quadruple excitations T_4. The $T_4 \rightarrow T_4$ part of connected quadruples first arises in sixth order. By combining MBPT and CC theory, noniterative approximations such as CCSD(T) are derived. These are discussed in Sec. V. Because of this combination, CCSD(T) scales as $\sim n^2N^4N_{\rm it}+n^3N^4$, which is a significant savings on CCSDT, and there is no storage of the $\sim n^3N^3t_{ijk}^{abc}$ amplitudes. An iterative method such as CCSDT-3 (Sec. V.D) scales as $\sim n^3N^4N_{\rm it}$, and also does not require storage of triple excitation amplitudes.

IV. NORMAL-ORDERED HAMILTONIAN

The CC equations can be developed systematically using the unifying and compact diagrammatic development that has evolved over several years (Čížek, 1969; Paldus *et al.*, 1972; Kucharski and Bartlett, 1986). Diagrammatic methods begin with the second-quantized form of the electronic Hamiltonian in Eq. (1). In the following, we have no time or frequency dependence so creation operators $\hat{p}^\dagger, \hat{a}_p^\dagger, \hat{X}_p^\dagger, \hat{c}_p^\dagger$ and annihilation operators $\hat{p}, \hat{a}_p, \hat{X}_p, \hat{c}_p$ work in occupation number space, such that

$$\hat{c}_b^\dagger|0\rangle = (-1)^{m_b}|\underset{ijk}{111\cdots}\,\underset{abc}{010\cdots}\rangle$$

with $|0\rangle$ the Fermi vacuum and

$$\hat{c}_k|0\rangle = (-1)^{m_k}|\underset{ijk}{110\cdots}\,\underset{abc}{000\cdots}\rangle.$$

The parity of the operation is determined by the number of occupied orbtials m_b (m_k) to the left of the b (k) location. The important part of these operators, regardless of chosen notation, is their indices, so the most compact notation is simply to use $\hat{p}^\dagger$ and $\hat{p}$ in the operators. Then the Hamiltonian can be written in terms of field operators, $\hat{\psi}^\dagger(x_1)=\Sigma_p\phi_p(x_1)\hat{p}^\dagger$,

$$H = \int \hat{\psi}^\dagger(x_1)\hat{h}\hat{\psi}(x_1)d\tau_1 + \frac{1}{2}\int d\tau_1 \int d\tau_2 \hat{\psi}^\dagger(x_1)\hat{\psi}^\dagger(x_2)\frac{1}{r_{12}}[\hat{\psi}(x_1)\hat{\psi}(x_2) - \hat{\psi}(x_2)\hat{\psi}(x_1)], \tag{43}$$

$$H = \sum_{pq}\langle p|h|q\rangle\hat{p}^\dagger\hat{q} + \tfrac{1}{4}\sum_{pqrs}\langle pq||rs\rangle\hat{p}^\dagger\hat{q}^\dagger\hat{s}\hat{r}. \tag{44}$$

Here $\langle pq\|rs\rangle$ represents an antisymmetrized integral defined as $\langle pq|rs\rangle-\langle pq|sr\rangle$, where $\langle pq|rs\rangle = \int\int \varphi_p^*(1)\varphi_q^*(2)1/r_{12}\varphi_r(1)\varphi_s(2)d\tau_1 d\tau_2$. See also definitions listed in Table II. From the definition of $\hat{p}^\dagger$ and $\hat{p}$, consider all the possibilities $\hat{p}^\dagger\hat{q}^\dagger=-\hat{q}^\dagger\hat{p}^\dagger$, $\hat{p}\hat{q}=-\hat{q}\hat{p}$, and $\hat{p}^\dagger\hat{q} = \delta_{pq}-\hat{q}\hat{p}^\dagger$, which give the standard anticommutation re-

TABLE II. The rules to interpret the diagram algebraically.

Each upgoing line is labeled with a "particle" label $a,b,c,d,\ldots$ and each downgoing line with a "hole" label $i,j,k,l,\ldots$. Open lines should be labeled in sequence as $a,i;b,j;c,k$, etc.

Each one-particle vertex in the diagrammatic equation should be interpreted as the integral

⟨left out |operator| right in⟩

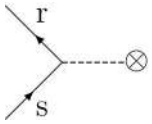

$$= \langle r|f|s\rangle$$

Each two-particle vertex corresponds to the antisymmetrized integral

⟨left out, right out ‖left in, right in⟩

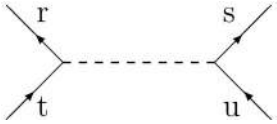

$$= \langle rs||tu\rangle = \langle rs|tu\rangle - \langle rs|ut\rangle$$

Similarly, the cluster vertices occurring in the diagrammatic equations correspond to

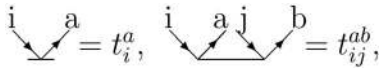

etc., and are antisymmetric as well; hence $t_{ij}^{ab}=-t_{ji}^{ab}=-t_{ij}^{ba}=t_{ji}^{ba}$ and similarly for t_{ijk}^{abc}.

All the orbital labels are summed over "internal" lines, i.e., lines terminating below the last H_N.

The sign of the diagram is obtained from (-1) raised to the power of the sum of hole lines and loops: $(-1)^{h+l}$. For the purpose of getting the sign, open lines are closed into fictitious loops by paring $i,a;j,b$; etc.

The weigh factor for the diagram is specified by $(\frac{1}{2})^m$, where m is the number of pairs of "equivalent" lines. A pair of equivalent lines is defined as being two lines originating at the same vertex and ending at another, but identical vertex, and going in the same direction.

To maintain full antisymmetry of an amplitude, the algebraic expression for a diagram should be preceded by a permutation operator permuting the open lines in all distinct ways, $\Sigma_P(-1)^P P$.

A factor of $\frac{1}{2}$ is also required for each pair of equivalent T_n vertices (a pair of T vertices is considered equivalent if they have the same number of line pairs and are connected in equivalent ways to the interaction vertex), i.e.,

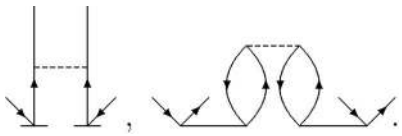

lation $\hat{p}^\dagger\hat{q}+\hat{q}\hat{p}^\dagger=\delta_{pq}$. Once $\hat{p}$ and $\hat{q}$ refer to occupied orbitals $i,j,k,\ldots$ and unoccupied ones $a,b,c,\ldots$, the normal order indicated by $\{\}$ is defined to have all hole $\hat{i}^\dagger$ and particle $\hat{a}$ operators moved to the right of the other operators, to facilitate $\hat{i}^\dagger|\Phi_0\rangle=\hat{i}^\dagger|0\rangle=0$ and $\hat{a}|0\rangle=0$. So $\{\hat{a}^\dagger\hat{i}\}=\hat{a}^\dagger\hat{i}$, $\{\hat{i}\hat{a}^\dagger\}=-\hat{a}^\dagger\hat{i}$. Now introducing the contraction definition

$$\hat{p}^\dagger\hat{q} = \{\hat{p}^\dagger\hat{q}\} + \{\overbrace{\hat{p}^\dagger\hat{q}}\}$$

and considering all the hole-hole, particle-particle, etc. forms, we immediately see that this contraction vanishes unless

$$\overbrace{\hat{p}^\dagger\hat{q}} = \delta_{pq=i},$$

where $\hat{p}^\dagger$ and $\hat{q}$ represent hole operators $\hat{i},\hat{j},\hat{k},\hat{l}$, while

$$\overbrace{\hat{q}\hat{p}^\dagger} = \delta_{pq=a},$$

similarly vanishes unless the operators correspond to particles $\hat{a},\hat{b},\hat{c},\hat{d}$. The form of the Hamiltonian above can be put into normal-ordered form by virtue of Wick's theorem (Wick, 1950; Čížek, 1966; Paldus and Čížek, 1975). The particular form used here, which is integral to the diagrammatic development that is the cornerstone of this review, is the time-independent mixed particle-hole operator form of the theorem (Bogoliubov and Shirkov, 1959). Wick's theorem says any product of second-quantized operators,

$$ABC\ldots = \{ABC\ldots\} + \sum_{\substack{\text{all}\\ \text{single}\\ \text{contractions}}} \overbrace{\{ABC\ldots\}} + \sum_{\substack{\text{all}\\ \text{double}\\ \text{contractions}}} \overbrace{\overbrace{\{ABC\ldots\}}} + \cdots + \sum_{\substack{\text{all}\\ \text{fully}\\ \text{contracted}\\ \text{prdts}}} \overbrace{\overbrace{\overbrace{\{ABC\ldots\}}}}. \tag{45}$$

Using this theorem (and now suppressing the ^ on the operators for simplicity) defines the normal-ordered operator

$$p^\dagger q = \{p^\dagger q\} + \{\overbrace{p^\dagger q}\} = \{p^\dagger q\} + \delta_{pq=i}. \tag{46}$$

For the two-particle part,

$$\begin{aligned} p^\dagger q^\dagger sr &= \{p^\dagger q^\dagger sr\} + \{\overbrace{p^\dagger q^\dagger sr}\} + \{p^\dagger \overbrace{q^\dagger sr}\} \\ &\quad + \{\overbrace{p^\dagger q^\dagger sr}\} + \{p^\dagger \overbrace{q^\dagger sr}\} \\ &\quad + \{\overbrace{p^\dagger q^\dagger sr}\} + \{p^\dagger \overbrace{q^\dagger sr}\} \\ &= \{p^\dagger q^\dagger sr\} + \overbrace{p^\dagger r}\{q^\dagger s\} + \overbrace{q^\dagger s}\{p^\dagger r\} \\ &\quad - \overbrace{p^\dagger s}\{q^\dagger r\} - \overbrace{q^\dagger r}\{p^\dagger s\} \\ &\quad + \overbrace{p^\dagger r}\overbrace{q^\dagger s} - \overbrace{p^\dagger s}\overbrace{q^\dagger r}. \end{aligned}$$

Hence, the normal-ordered Hamiltonian becomes

$$H = \sum_p f_{pp}\{p^\dagger p\} + \sum_{p\neq q} f_{pq}\{p^\dagger q\} + \tfrac{1}{4}\sum \langle pq||rs\rangle\{p^\dagger q^\dagger sr\} + \langle 0|H|0\rangle. \tag{47}$$

Choosing to subtract the constant $\langle 0|H|0\rangle = E_0 + E^{(1)} = E_{\text{ref}}$, we have a slight redefinition

$$H_N = H - \langle 0|H|0\rangle, \tag{48}$$

$$f_N = f - \langle 0|f|0\rangle, \tag{49}$$

$$W_N = W - \langle 0|W|0\rangle. \tag{50}$$

In this way, all internal contractions are removed from the operators themselves, making all subsequent derivations dependent upon contractions among products of normal-order operators. For purposes of perturbation expansions, in the most general case, the normal-ordered $H_N = H_0 + V_N$,

$$H_{0_N} = \sum_p f_{pp}\{p^\dagger p\} + \sum_{i\neq j} f_{ij}\{i^\dagger j\} + \sum_{a\neq b} f_{ab}\{a^\dagger b\}, \tag{51}$$

$$V_N = \sum_{a,i} f_{ai}\{a^\dagger i + i^\dagger a\} + \tfrac{1}{4}\sum \langle pq||rs\rangle\{p^\dagger q^\dagger sr\}, \tag{52}$$

$$V_N = f_{\text{ov}} + W_N, \tag{53}$$

where f_{ov} represents the occupied-virtual part of f_N and W_N is the two-electron operator.

Hence, the Schrödinger equation now becomes $H_N\Psi = \Delta E\Psi$, where $\Delta E = E - E_{\text{ref}}$, the correlation correction (Löwdin, 1959). This eliminates $E^{(1)}$ from expressions previously containing $V - E^{(1)}$ once we understand that V_N is normal ordered as above.

Note that the appearance of the Fock operator in the Hamiltonian is a consequence of normal ordering and does not presuppose HF orbitals or a HF reference function. The Hamiltonian is completely general. However, for the canonical HF case $f_{pq} = \epsilon_p\delta_{pq}$, giving the simple form $H_N = \Sigma_p \epsilon_p\{p^\dagger p\} + W_N$. For any other choice of orbitals and reference determinant, such as Kohn-Sham (where the density is given by a single determinant) (Kohn and Sham, 1965), natural (Löwdin, 1955) (where the first natural determinant gives the best single determinant approximation to the density matrix), and Brueckner (Brueckner, 1955) (where the Brueckner determinant has maximum overlap with the exact wave function), we retain the f_{ij} and f_{ab} parts in H_0 and f_{ai} in V_N. That is, we insist upon orbital invariance for any rotation of the occupied orbitals among themselves, or the virtual orbitals among themselves. For non-Hartree-Fock orbitals $f_{ai} \neq 0$, so those effects, which rotate the virtual space into the occupied space, will change the results (except for full CI) and are introduced in V_N. Many-body perturbation theory will be invariant to any rotations in the occupied or virtual space, as long as H_0 does not change. Hence, this choice of H_0 has this property and is the only one that does. Generalized MBPT presented elsewhere (Bartlett, 1995) assumes this H_0, and as a special case of CC theory it naturally allows MBPT to be done with any single determinant reference and associated orbitals. As an infinite-order method, the CC solutions are formally independent of H_0, except the choice of H_0 will suggest a natural iterative scheme for the solution of the nonlinear equations. Coupled-cluster theory will also be invariant to rotations in the occupied or virtual space, and at the CCSD level and beyond, noninvariant, but insensitive to orbital rotations that mix the two spaces, beginning to approach full CI's invariance. This feature (discussed later) gives CC theory a very high degree of flexibility for orbital choices not shared by MBPT or truncated CI.

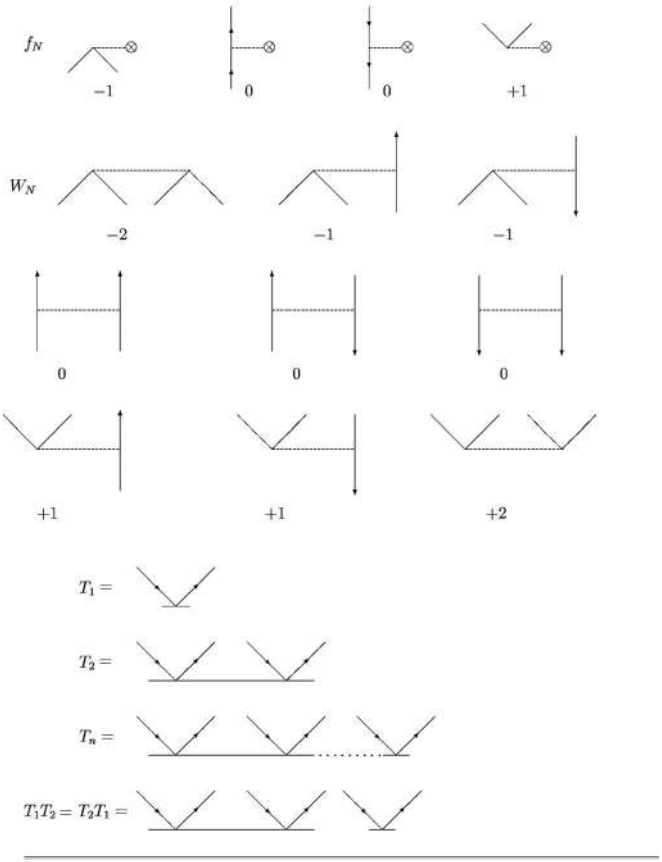

FIG. 4. Diagrammatic form of the f_N, W_N, and T_n operators. The labels at the bottom of the f_N and W_N operators refer to the changes in the excitation level caused by that form of the operator.

V. COUPLED-CLUSTER EQUATIONS

We choose the diagrammatic notation shown in Fig. 4 for the Hamiltonian H_N. Note that two (four) lines connected with the one- (two-) electron operator indicate two (four) creation-annihilation operators occurring in the definition of the Hamiltonian, Eq. (48). Our diagrams are based upon normal-ordered operators, spin orbitals, and use antisymmetrized two-electron integrals and cluster amplitudes, but are drawn in the Goldstone form with one antisymmetrized diagram representing several conventional Goldstone diagrams, as in the Hugenholtz convention. We also identify the various terms in the perturbation V_N by their excitation level, meaning that if it is 0, there is no change, but +1 increases the excitation, and −2 decreases it by that amount. The three particle-hole pairs in T_3 and higher cluster amplitudes have to also be understood to be treated equivalently, as there is no diagrammatic distinction between the center pair and the other two. Using these diagrams, we can immediately write the linked diagrams of the MBPT wave function,

$$\Psi_{\mathrm{MBPT}} = \Phi_0 + \sum_{k=1}^{\infty} (R_0V)^k|\Phi_0\rangle_L = \Phi_0 + \Phi^{(1)} + \Phi^{(2)} + \cdots$$

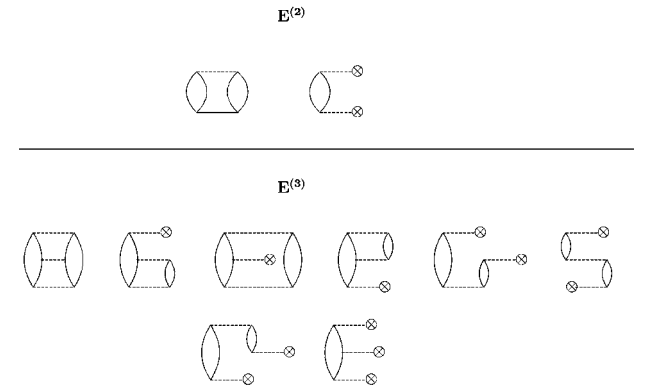

FIG. 5. Skeleton diagrams for the second- and third-order MBPT energies.

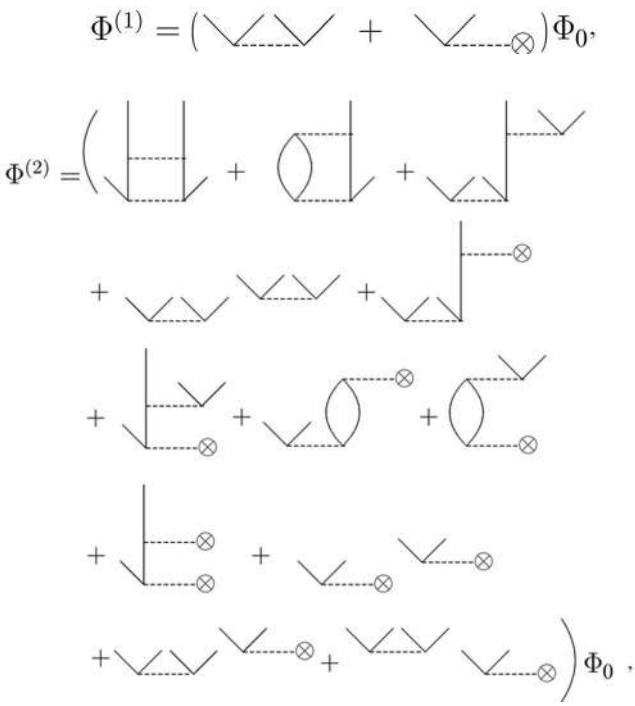

where we choose not to indicate the line directions. These skeleton diagrams are sufficient for our current formal manipulations, but the line directions would have to be introduced in a computational formula. The energy diagrams $E^{(n+1)}=\langle 0|V|\Phi^{(n)}\rangle$ are closed, with examples shown in Fig. 5. The wave functions are necessarily linked, meaning that there are no closed energy diagrams. But the remaining open linked diagrams have both connected and disconnected parts. Now cluster operators are introduced,

$$T_2 = \sum_{i>j,a>b} t_{ij}^{ab}\{a^\dagger i b^\dagger j\} =$$

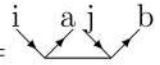

to sum all connected terms that result in a net double excitation and

$$T_1 = \sum_{i,a} t_i^a \{a^\dagger i\} =$$ 

to do the same for single excitations, and T_3, T_4, etc. for the higher connected terms. The linked, but disconnected terms like

arise from the higher terms in the exponential expansion once it is understood that the factorization theorem (Frantz and Mills, 1960) provides

$$\tfrac{1}{2}T_2^{(1)2} =$$ 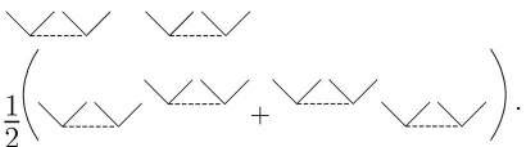

That is, we exploit the factorization theorem to remove the eight-index denominator that occurs via

in using all distinct time orders of the two-particle interactions in favor of a product of two four-index ones, and for each T_2 cluster operator. Generalization to any order can be established with mathematical induction (Shavitt and Bartlett, 2006) so that it is apparent that the linked-diagram MBPT wave function may be written as

$$\Psi_{\mathrm{MBPT}} = |0\rangle + \sum_{n=1}^{\infty} (\hat{R}_0 V)^n |0\rangle_L = \exp(T)|0\rangle, \tag{54}$$

where $\hat{R}_0$ is the resolvent defined in Sec. III.B. This was first stated by Hubbard (1957). This also tells us that the wave operator $\Omega = \exp(T)$ takes the approximation $|0\rangle$ into $|\Psi\rangle$.

We find the choice of spin-orbital, antisymmetrized two-electron integrals and amplitudes to be the most convenient for formal derivations, while at the same time accounting for closed- and (single determinant) open-shell molecules. The equations for the various special cases (discussed below) can be derived from the general form by adding line directions and carrying out the appropriate spin integrations. Also, based upon antisymmetrized spin-orbital forms, we present below and in Fig. 6 easily applied tools that enable an unambiguous generation of all the diagrams with no redundancy, eliminating the uncertainty often associated with diagrammatic derivations.

As discussed in Eqs. (21)–(23), the CC equations are

$$\langle 0|\bar{H}|0\rangle = E|0\rangle, \tag{55}$$

$$\langle {}^{ab\cdots}_{ij\cdots}|\bar{H}|0\rangle = 0. \tag{56}$$

Individual, normal-ordered excitations will be indicated by $\langle {}^{ab\cdots}_{ij\cdots}| = \langle 0|\{\hat{i}^\dagger \hat{a} \hat{j}^\dagger \hat{b} \cdots\}$. The quantity

$$\bar{H}_N = H_N + [H,T] + \frac{1}{2}[[H,T]T] + \frac{1}{3!}[[[H,T]T]T] + \frac{1}{4!}[[[[H,T]T]T]T], \tag{57}$$

$$\bar{H}_N = \exp(-T) H_N \exp(T) = [H_N \exp(T)]_C \tag{58}$$

obtained from H by a similarity transformation, Eq. (58), is a critical one in CC theory since it terminates after fourfold commutators. That is, because the Hamiltonian has only one- and two-particle operators, the maximum number of T operators that can lead to nonvanishing contributions to the CC amplitude equations is four, regardless of their excitation level. This feature will cause the CC equations to always have a finite number of terms, or be in closed form, despite the fact that the CC wave function remains an unterminated exponential in T. The commutators necessarily eliminate any terms in H and T that have no indices in common. Hence, the equations for the energy and amplitudes in CC are linked, and the amplitudes, themselves, necessarily connected. The concept of an exponential wave function for fermions was considered by Coester and Kümmel (1960), with the first workable equations presented by Čížek (1966) for the simplest model, coupled-cluster doubles (CCD), then called coupled-pair many-electron theory (CPMET).

Using the occupation number representation and recognizing that we can only have fully contracted operators in a vacuum matrix element of normal-ordered operators to be nonvanishing, we can derive the energy as a simple illustration,

$$E = \langle 0|\bar{H}|0\rangle, \tag{59}$$

$$E = \langle 0|H + (HT_1)_C + (HT_2)_C + (HT_1^2/2)_C|0\rangle = E_{\mathrm{ref}} + \langle 0|(f_{vo}T_1)_C + (WT_2)_C + (WT_1^2/2)|0\rangle, \tag{60}$$

$$\langle 0|(f_{vo}T_1)_C|0\rangle = \sum_{ai}\sum_{pq} f_{pq} t_i^a [\langle 0|\{p^\dagger q\}\{a^\dagger i\}|0\rangle] = \sum_{ai} f_{ia} t_i^a =$$  , (61)

$$\langle 0|(WT_2)_C|0\rangle = \frac{1}{4}\sum_{ijab}\frac{1}{4}\sum_{pqrs}\langle pq||rs\rangle t_{ij}^{ab}\langle 0|\{p^\dagger q^\dagger sr\}\{a^\dagger ib^\dagger j\}+\{p^\dagger q^\dagger sr\}\{a^\dagger ib^\dagger j\}$$
$$+\{p^\dagger q^\dagger sr\}\{a^\dagger ib^\dagger j\}+\{p^\dagger q^\dagger sr\}\{a^\dagger ib^\dagger j\}|0\rangle$$
$$=\frac{1}{4}\sum_{ai,bj}\langle ij||ab\rangle t_{ij}^{ab} =$$ 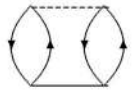 , (62)

$$\langle 0|(WT_1^2/2)_C|0\rangle = \frac{1}{8}\sum_{ijab}\sum_{pqrs}\langle pq||rs\rangle t_i^a t_j^b\langle 0|\{p^\dagger q^\dagger sr\}\{a^\dagger i\}\{b^\dagger j\}+\{p^\dagger q^\dagger sr\}\{a^\dagger i\}\{b^\dagger j\}$$
$$+\{p^\dagger q^\dagger sr\}\{a^\dagger i\}\{b^\dagger j\}+\{p^\dagger q^\dagger sr\}\{a^\dagger i\}\{b^\dagger j\}|0\rangle$$
$$=\frac{1}{2}\sum_{ai,bj}\langle ij||ab\rangle t_i^a t_j^b =$$ 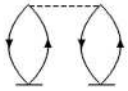 . (63)

Note the sign rule, which means if the number of lines crossed in the full contraction is even, the term is positive; if odd, it is negative. Though straightforward, the redundancy of contractions that lead to identical expressions makes such an exercise tedious. With the diagrams, however, we immediately have the answer.

A. Double excitations in CC theory

For the CCD wave function [$|\Psi_{\mathrm{CCD}}\rangle = \exp(T_2)|0\rangle$], we have

$$0 = \langle {}_{ij}^{ab}|H_N \exp(T_2)|0\rangle_C \quad \forall\, a,b,i,j \tag{64}$$
$$= \langle {}_{ij}^{ab}|H_N + H_N T_2 + H_N T_2^2/2|0\rangle_C \tag{65}$$
$$= \langle {}_{ij}^{ab}|W + H_0 T_2 + W T_2 + W T_2^2/2|0\rangle_C. \tag{66}$$

We used the fact that H_0 cannot couple a double excitation with the reference function $|0\rangle$, or a double with a quadruple that would derive from T_2^2. If we persist in using occupation number tools above to obtain the results, we would need to evaluate the several vacuum contractions,

$$\tfrac{1}{4}\sum_{pqrs}\langle pq||rs\rangle\langle 0|\{i^\dagger aj^\dagger b\}\{p^\dagger q^\dagger sr\}|0\rangle, \tag{67}$$

$$\sum_{pq} f_{pq}t_{kl}^{cd}\langle 0|\{i^\dagger aj^\dagger b\}\{p^\dagger q\}\{c^\dagger kd^\dagger l\}|0\rangle, \tag{68}$$

$$\tfrac{1}{4}\sum_{pqrs}\langle pq||rs\rangle t_{kl}^{cd}\langle 0|\{i^\dagger aj^\dagger b\}\{p^\dagger q^\dagger sr\}\{c^\dagger kd^\dagger l\}|0\rangle, \tag{69}$$

$$\tfrac{1}{16}\sum_{pqrs}\langle pq||rs\rangle t_{kl}^{cd}t_{mn}^{ef}\langle 0|\{i^\dagger aj^\dagger b\}\{p^\dagger q^\dagger sr\}\{c^\dagger kd^\dagger l\}\{e^\dagger mf^\dagger n\}|0\rangle. \tag{70}$$

However, the nonlinear term begins to challenge our patience [one might even go back to using determinants and Slater's rules, which can be done through CCD at least (Čížek and Paldus, 1971; Hurley, 1976)]. We prefer more powerful diagrammatic ways to derive the CC equations for higher than double excitations.

The diagrams introduced in Fig. 4 and shown in Fig. 6 immediately tell us what the CCD diagrams are, where we use the excitation and deexcitation level indicated under the f and W operators. The diagrams take advantage of the fact that (i) the particular double excitation projection need never be explicitly included, and (ii) the factor of $\frac{1}{4}$ in the antisymmetrized W operator will be subsummed into the diagrams' numerical factors, rather than having to be associated with four different contractions that amount to the same term, and (iii) the sign of the terms will be automatic. Furthermore, we follow the prescription shown in Fig. 6 where we identify the net excitation level, the excitation level of the products of T amplitudes, and the relevant part of the perturbation that will reduce or enhance the excitation level to that

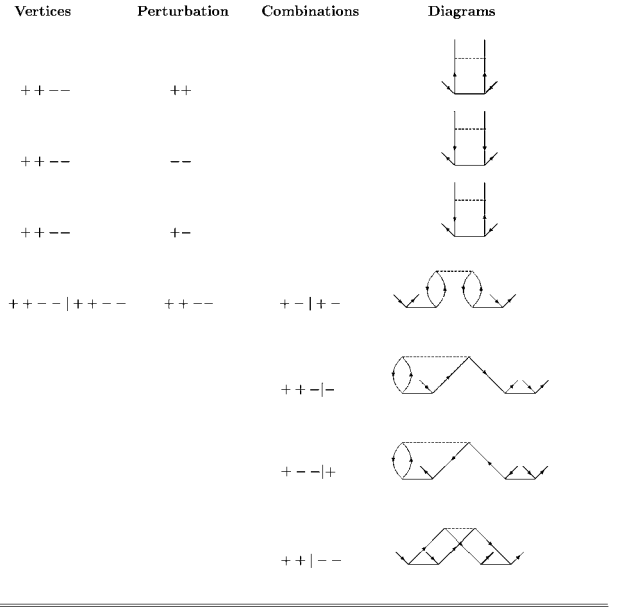

FIG. 6. Generation of the WT_2 and $WT_2^2/2$ contributions to the T_2 amplitude.

desired. Then we make all possible, simple combinations that will allow us to achieve the final, net excitation level. Since there are only a handful of combinations, and each leads uniquely to one and only one distinct antisymmetrized diagram (regardless of how it is drawn), anyone can follow this prescription confidently to derive unique diagrams. When the diagram is interpreted using the rules listed in Table II, we easily have the algebraic form in terms of spin-orbital, antisymmetrized integrals and antisymmetrized amplitudes, which are shown in Fig. 6.

B. Choice of single determinant reference function

From this point, the actual equations programmed depend upon the choices made for the spin-orbital form. The possibilities are shown in Fig. 7. If we are describing a closed-shell molecule with doubly occupied spatial orbitals as in Fig. 7(a), i.e., spin orbital $\phi_p = p = P\alpha$ and $\phi_{p+1} = q = P\beta$, we can go from antisymmetrized diagrams to the usual Goldstone form by drawing all the exchange

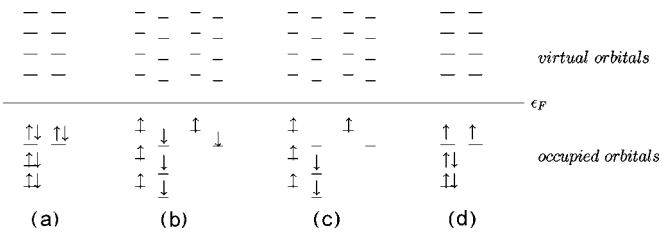

FIG. 7. The choices made for the spin-orbital form: (a) RHF (closed-shell molecule with doubly occupied spatial orbitals), (b) UHF (closed-shell spin polarized situation), (c) UHF open-shell triplet, and (d) ROHF (triplet maximum double occupancy).

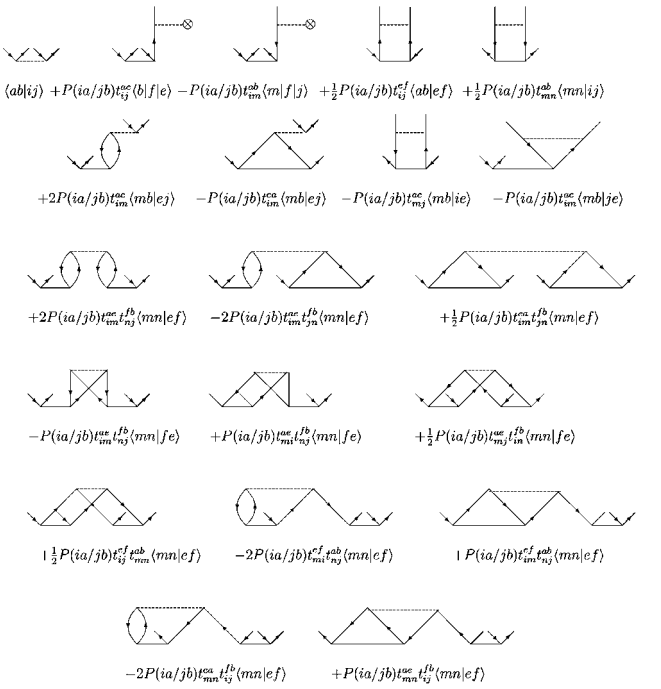

FIG. 8. Diagrammatic representation of the CCD method in the closed-shell spatial orbital form together with the corresponding algebraic expression. Summation over repeated upper and lower indices assumed. $P(ia/jb)$ implies a sum of two components differing by permutaion of ia and jb.

variants as shown in Fig. 8. This allows the immediate interpretation of the CC equations in terms of the spatial orbitals P as all closed loops now account for a factor of 2 in the equations, and there is a vertical symmetry $\frac{1}{2}$ rule but no equivalent line rule. The diagrams and the interpretation are shown in Fig. 8.

If we want to describe a closed-shell but spin-polarized system like Fig. 7(b), then we require different orbitals for different spins (DODS), $p = P_\alpha\alpha, p+1 = P_\beta\beta$, where $P_\alpha \neq P_\beta$. For the HF case, this is termed unrestricted Hartree-Fock (UHF). The diagrams and computational equations are shown in Fig. 9. We present the diagrams for $\alpha\beta$ and $\alpha\alpha$ spin blocks, since the $\beta\beta$ block can be easily obtained from Fig. 9(a). Note that all working equations take advantage of spin integration, since otherwise the spin-orbital calculations would be $\sim 2^6$ slower than the closed-shell calculation. Once the spin integration is made, the difference in time for DODS versus doubly occupied is ~ 3. Such a single UHF determinant is not an eigenfunction of spin, unlike the doubly occupied case. The more common use for a UHF reference is for open shells [Fig. 7(c)] when the number of α electrons exceeds those for β. Though also not an eigenfunction of spin, it will be much closer for high-spin cases. In contrast, for the closed-shell spin-polarized example, the UHF solution can be a 50-50 mixture of the singlet and triplet, like for H_2 at large R separation.

The intermediate situation is shown in Fig. 7(d). Here

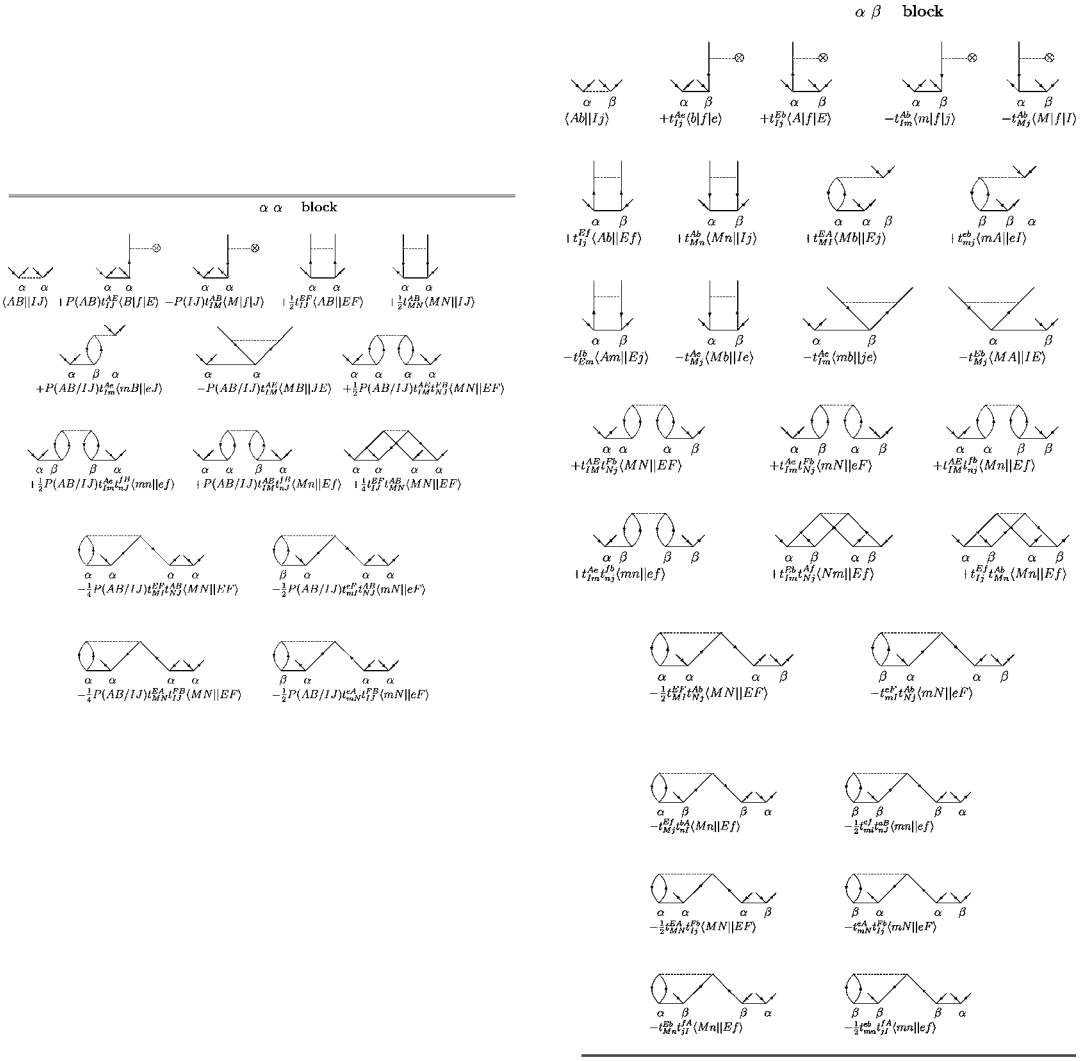

FIG. 9. Diagrammatic representation of the CCD method in the spin-expanded open-shell form together with corresponding algebraic expressions. Summation over repeated upper and lower indices assumed. The antisymmetrizer is defined as $P(pq/rs)=1+(qp)(sr)-(qp)(rs)-(pq)(sr)$. The capital letters A, B, I, J, etc. refer to α spin-orbitals, and lower case letters a, b, i, j, etc. denote β spin-orbitals.

we have maximum double occupancy up to open-shell orbitals. This kind of wave function is usually referred to as a restricted open-shell Hartree-Fock (ROHF) function. Here the single determinant approximation is a spin eigenfunction $\hat{S}^2|\mathrm{ROHF}\rangle=S(S+1)|\mathrm{ROHF}\rangle$. However, using that as the reference determinant does not mean that the corresponding CC method will provide a spin eigenfunction. The complication occurs due to the role of nonlinear terms. If T is spin adapted, then its direct product with a second spin-adapted T leads to a reducible representation that has to be properly reduced to give the spin eigenfunction. And in CC theory, unlike CI where there are no nonlinear terms, this is not easy. Our approach (Lauderdale *et al.*, 1992; Bartlett, 1995) to using ROHF is to build the Fock matrix **f** in terms of those orbitals, and then exploit the fact that any rotation of the occupied-occupied and virtual-virtual block is allowed, to semicanonicalize the matrix to the form

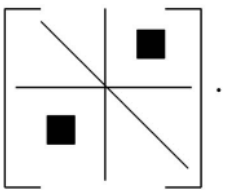

From this point, the calculation is like any other UHF calculation, except we have to have f_{ai} terms in the perturbation, V. In this way, any kind of reference determinant and orbitals can be used in CC theory. However, because of the essential role of f_{ai}, which now will arise in second-order perturbation theory like W (see Fig. 5), it is not meaningful to use such arbitrary orbitals without at least the CCSD approximation discussed below.

For completeness, consider a low-spin situation, like that for an open-shell singlet. Here we require that two determinants with the same $S_z=0$ value be coupled together to get a spin eigenfunction $\frac{1}{\sqrt{2}}[|A_\alpha B_\beta|\pm|A_\beta B_\alpha|]$.

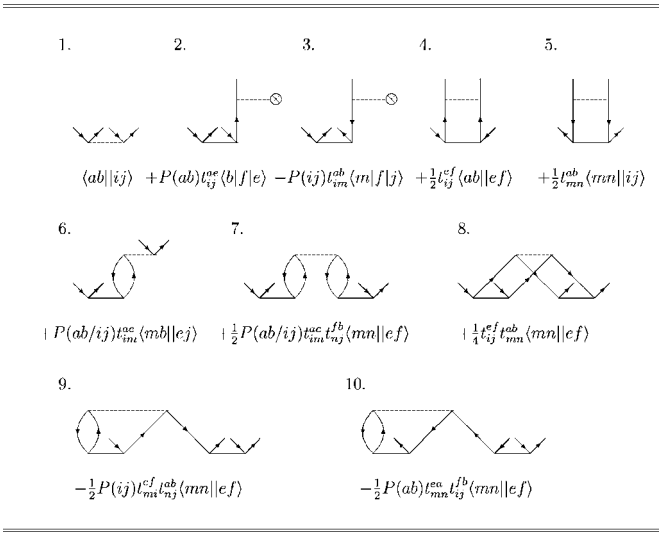

FIG. 10. Diagrammatic representation of the CCD method in the generic spin-orbital form together with the corresponding algebraic expression. Summation over repeated upper and lower indices is assumed. The antisymmetric permutation operator $P(pq/rs)$ is defined as $P(pq/rs)=P(pq)(rs)=1+(qp)(sr)-(qp)(rs)-(pq)(sr)$.

For the $S_z=0$ component of the triplet, we can describe equally well the state starting from a single determinant $|A_\alpha B_\alpha|, S_z=1$; but for the singlet, we are forced to use both determinants, which would require the equivalent treatment of two determinants. Single determinant reference CC cannot describe such states appropriately without modification (Balkova and Bartlett, 1992). In terms of configurations instead of determinants, where a configuration means a combination of determinants that are spin eigenfunctions, the open-shell singlet is a single configuration, and a proper orthogonal spin-adapted single reference CC theory is possible (Li and Paldus, 2004), but for more general cases it is formally and computationally much more difficult than might be expected, due to the complications introduced by the nonlinear terms discussed above. Consequently, the single determinant reference CC methods in ACES II (Stanton *et al.*, 1993; Bartlett and Watts, 1998) will allow for UHF, ROHF, RHF, or their equivalents with Kohn-Sham, natural, Brueckner, or quasi-Hartree-Fock (QRHF) orbital references. The latter means orbitals taken from some related system like using neutral orbitals to describe an N_2^+ state or F^- orbitals to describe the F atom. Such almost arbitrary orbital choices are possible in CCSD and beyond because of the theory's orbital insensitivity, as CCSD does not depend much upon a variationally optimum reference function (see below). For open-shell singlets a two-determinant CC method, which is the simplest realization of multideterminant CC, has been developed and is included in ACES II (Balkova and Bartlett, 1992; Szalay *et al.*, 1995).

The CCD equations in their most general and—at the same time—most compact form are shown in Fig. 10. Here we do not separate the spin part from the space part of the spin orbital, which means that we do not perform the spin integration. Each line is summed over the whole range of one-particle functions: the hole lines over all occupied spin orbitals and the particle lines over all virtual spin orbitals. Such a situation occurs when we treat nucleons with the CC approach (Kowalski *et al.*, 2004). Naturally, for that case we need a new Hamiltonian with properly defined one-nucleon and two-nucleon integrals transformed to the spin-orbital basis, but in other respects such calculations require us simply to evaluate the diagrams in Fig. 10. The algebraic expressions coresponding to the latter are given in Eq. (67) (Fig. 10.1), Eq. (68) (Fig. 10.2–3), Eq. (69) (Fig. 10.4–6), and Eq. (70) (Fig. 10.7–10).

The generic form of the CCD equations as given in Fig. 10 also has another important application, namely, in relativistic calculations. Solving, e.g., the full four-component Dirac equation (Pisani and Clementi, 1995; Visscher *et al.*, 1996) requires the general, i.e., non-spin-integrated formulas for CC equations. Also for other somewhat simpler calculations using the two-component Douglas-Kroll-Hess Hamiltonian (Kaldor and Hess, 1994), the spin integration cannot be performed since here j is the appropriate quantum number instead of s_z, which indicates that the generic form of the CC equation should be used, although some symmetry simplification is still possible (Visscher, 1996).

Hence, the generic CC equations enable the treatment of two- and four-component relativistic problems as well as nucleons in the same manner as electrons, as long as no inappropriate further simplifications of the generic formulas are made. This generality recommends using the underlying spin-orbital framework for both formal and computational aspects of CC theory.

C. Single excitations in CC theory

The role of single excitations in CCSD (Purvis and Bartlett, 1982) theory, $\Psi_{\mathrm{CCSD}}=\exp(T_1+T_2)|0\rangle$, is quite important. Whereas the contribution to the energy from single excitations subject to a RHF or UHF reference function first appears in the fourth-order energy, for a non-HF reference, singles appear in second order just like doubles, and can be quite large. Also, whereas CCD subject to HF is correct through the third-order energy of perturbation theory, the one-particle density matrix, and thus all properties, is already wrong in second order. CCSD fixes this.

Another important point is that we know that single determinant references can be related by $|0\rangle=\exp(T_1)|\Theta\rangle$ (Thouless, 1961; Flocke and Bartlett, 2003); so rather than trying to get some kind of optimum reference function for CC theory, it is frequently preferable to simply solve the CCSD equations and allow the $\exp(T_1)$ operator to account for orbital changes in the reference function, passively. As we go to even higher levels of CC theory, like $\Psi_{\mathrm{CCSDT}}=\exp(T_1+T_2+T_3)|0\rangle$, the additional coupling between T_1, T_2, and T_3 further enhances this effect, causing the CC result to begin to approach the complete orbital invariance of full CI.

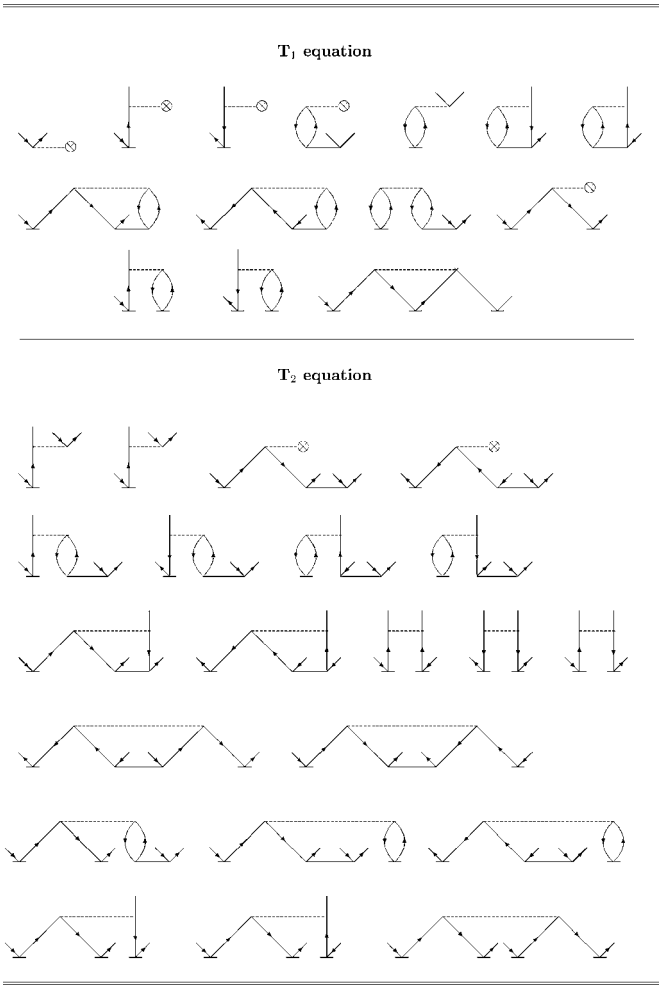

FIG. 11. Diagrams representing the single excitation and single contributions to the double-excitation CCSD equations. Diagrams occurring in the T_2 equation plus those present in the CCD model (Fig. 10) form the full T_2 equation in the CCSD method.

However, the CCSD equations have 45 diagrams compared to only 10 for CCD, and they would be difficult to derive without diagrammatic (or computer-aided) procedures (Hirata, 2003). Using the diagrams, we easily get expressions and additional diagrams shown in Fig. 11. We will not interpret these diagrams, but that could be easily done using the rules in Table II. All interpretations and diagrams through CCSDTQ have been presented (Shavitt and Bartlett, 2006). CCSD was first formulated and implemented in 1982 (Purvis and Bartlett, 1982). With this foundation, higher-connected-cluster operators could be introduced to rapidly approach the full CI solution.

Another way to get the benefit of $\exp(T_1)$ but limit the computation to just the few diagrams of CCD is to exploit the flexibility to make orbital rotations such that $T_1=0$. The orbitals that accomplish this are termed Brueckner orbitals. The determinant composed of these orbitals, Φ_B, is also guaranteed to have maximum overlap with the exact wave function,

$$|\langle\Psi|\Phi_B\rangle| = \max. \tag{71}$$

If a reference determinant $|\Phi_0\rangle$ is chosen, then a determinant different from $|\Phi_0\rangle$ is obtained by rotating virtual orbitals into occupied orbitals, represented by the operator $t_i^a\{a^\dagger i\}$, which leads to

$$\langle\Psi|\Phi_i^a\rangle = 0 \quad \forall\, i,a. \tag{72}$$

The condition of vanishing T_1 amplitudes partitions the orbital space into a new occupied and virtual space. Since they are obtained by rotating virtual orbitals into the occupied space, the T_1 equation, where all diagrams containing T_1 amplitudes are removed, defines the virtual-occupied block of an effective, Brueckner, Hamiltonian,

$$[H^{\text{eff}}]_{ai} = f_{ai} + \sum_{jb} f_{jb}t_{ij}^{ab} + \tfrac{1}{2}\sum_{jbc}\langle aj||bc\rangle t_{ij}^{bc} - \tfrac{1}{2}\sum_{jkb}\langle jk||ib\rangle t_{jk}^{ab}. \tag{73}$$

Diagonalization of the Brueckner effective Hamiltonian provides updates to t_i^a until at convergence $T_1=H_{ai}^{\text{eff}}=0$. Brueckner orbital-based CC theory and its extensions have been used in a variety of CC applications (Chiles and Dykstra, 1981; Adamowicz and Bartlett, 1985; Handy *et al.*, 1989; Stanton *et al.*, 1992; Krylov *et al.*, 2000) where the hope, particularly for properties other than the energy, is that higher-order products involving T_1 with T_3 and higher clusters that are implicitly set to zero will help for some classes of problems (Watts and Bartlett, 1994). It also offers an important link to a correlated effective one-particle theory that offers an exact, correlated analog to Hartree-Fock theory, including a Koopmans-type theorem that would give exact ionization potentials for its orbital energies (Lindgren and Salomonsen, 2002; Beste and Bartlett, 2004).

D. Triple and quadruple excitations in CC theory

Triple excitations in CC theory are also important, as they contribute to the fourth-order MBPT energy. At the CCD level, we already have the disconnected contributions of quadruple excitations in the wave function. Once we add singles, we have further disconnected contributions to the CI triples and quadruples, including all through fourth order in MBPT except for the connected triple excitations T_3. This is quite different from CI, because CI retains large contributions from unlinked diagrams whose initial contributions are not canceled until quadruple excitations are included in the CI. Hence, triple excitations are comparatively less important. This is shown in Fig. 3, where we illustrate the convergence of single reference CI, MBPT, and CC theory toward the full CI limit (see also Table I). Note the abrupt change when quadruple excitations are introduced in CI. Due to this cancellation of the fourth-order unlinked diagrams discussed in Sec. III.B, MBPT has the advantage that all the unlinked diagrams are removed from the beginning, but suffers from being finite-order approximations.

TABLE III. General formulas for the number of the diagrams in the CC equation for T_n amplitude (valid for $n>1$);[a] $N_a=1/24n^3+1\,5/8n^2+11\,1/12n+1$; $N_g=1/12n^3+3\,1/2n^2+24\,1/6n-9$.

	Diagrams in the T_n equation		Diagrams in the T_n equation	
Model	HF	non-HF	HF	NON-HF
		n even		
$CCT_1\cdots T_n$	N_a-n-2	N_a	N_g-n-2	N_g
$CCT_1\cdots T_{n+1}$	N_a-n+3	N_a+6	N_g-n+14	N_g+18
$CCT_1\cdots T_{n+2}$	N_a-n+4	N_a+7	N_g-n+19	N_g+23
		n odd		
$CCT_1\cdots T_n$	$N_a-\frac{9}{2}-\frac{9n+1}{8}$	$N_a-\frac{5}{2}-\frac{n+1}{8}$	$N_g-\frac{5n}{4}-5\frac{1}{2}$	$N_g-\frac{n}{4}-3\frac{1}{2}$
$CCT_1\cdots T_{n+1}$	$N_a+\frac{1}{2}-\frac{9n+1}{8}$	$N_a+\frac{7}{2}-\frac{n+1}{8}$	$N_g-\frac{5n}{4}+10\frac{1}{2}$	$N_g-\frac{n}{4}+14\frac{1}{2}$
$CCT_1\cdots T_{n+2}$	$N_a+\frac{3}{2}-\frac{9n+1}{8}$	$N_a+\frac{9}{2}-\frac{n+1}{8}$	$N_g-\frac{5n}{4}+15\frac{1}{2}$	$N_g-\frac{n}{4}+19\frac{1}{2}$

[a]Constant term in T_2 equation not included.

Coupled-cluster theory combines the linked-diagram advantages of MBPT with infinite-order summations, so it has to give the best convergence of these three examples.

Drawing all the 99 diagrams for CCSDT and 180 CCSDTQ tells us little (see Tables III and IV for these numbers). Instead we can summarize the equations for higher-level CC theory in terms of the quasilinearized form, Figs. 12 and 13, based upon the intermediates from $\bar{H}$ that are actually computed in such programs. These are shown diagrammatically in Fig. 14 and alge-

TABLE IV. Number of antisymmetrized and Goldstone diagrams in the T_n equation, $n=1$ to 6.

		Antisymmetrized diagrams		Goldstone diagrams	
T_n	Model	HF	non-HF	HF	non-HF
T_1	$CC\cdots T_1$	4	7[a]	8	11[a]
	$CC\cdots T_2$	9	13[a]	20	25[a]
	$CC\cdots T_3$	10	14[a]	24	29[a]
T_2[a]	$CC\cdots T_2$	26	30	50	54
	$CC\cdots T_3$	31	36	66	72
	$CC\cdots T_4$	32	37	71	77
T_3	$CC\cdots T_3$	42	47	88	93
	$CC\cdots T_4$	47	53	104	111
	$CC\cdots T_5$	48	54	109	116
T_4	$CC\cdots T_4$	68	74	143	149
	$CC\cdots T_5$	73	80	159	167
	$CC\cdots T_6$	74	81	164	172
T_5	$CC\cdots T_5$	92	99	198	205
	$CC\cdots T_6$	97	105	214	223
	$CC\cdots T_7$	98	106	219	228
T_6	$CC\cdots T_6$	127	135	272	280
	$CC\cdots T_7$	132	141	288	298
	$CC\cdots T_8$	133	142	293	303

[a]Constant term not included.

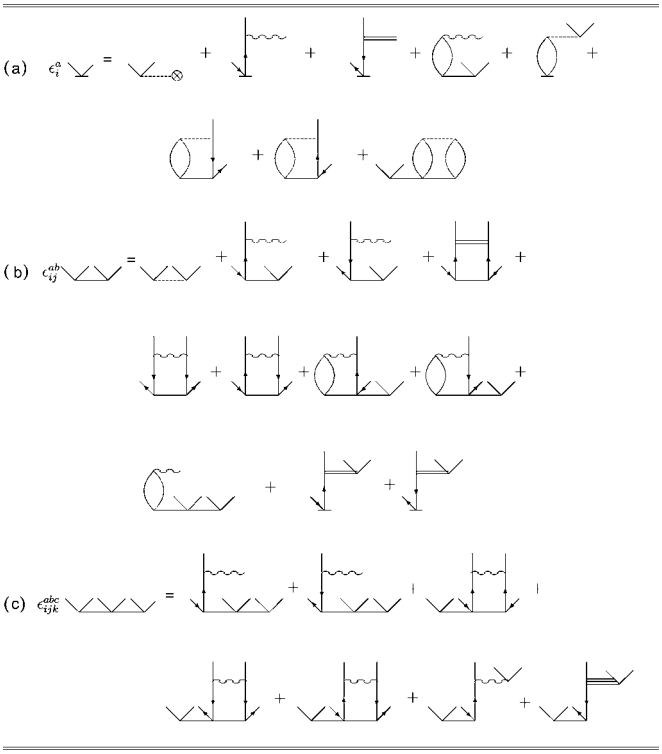

FIG. 12. Diagrammatic CCSDT equations with total factorization of nonlinear terms: (a), (b), and (c) represent the T_1, T_2, and T_3 equations, respectively.

braically in Table V. The quasilinearized form is obtained using the factorization procedure, which can be explained with the following example. Taking the intermediate

defined in Fig. 14.3a and applying it in the term

[third term in Fig. 12(a)], we obtain the following three diagrams:

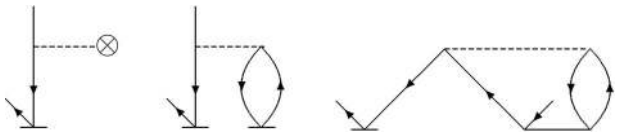

which can be identified easily as those contributing to the T_1 equation in Fig. 11. Taking other intermediates defined in Fig. 14 and applying them to the terms in the equation shown in Figs. 12(a)–12(c), we can reproduce all terms contributing to the T_1, T_2, and T_3 equations in the CCSDT model, respectively. For completness, we also present the quasilinearized form of the CCSD equations in Fig. 15 (cf. Figs. 10 and 11). Use of the recursively computed intermediates (Kucharski and Bartlett, 1991a) makes the concept of a high-order CC program

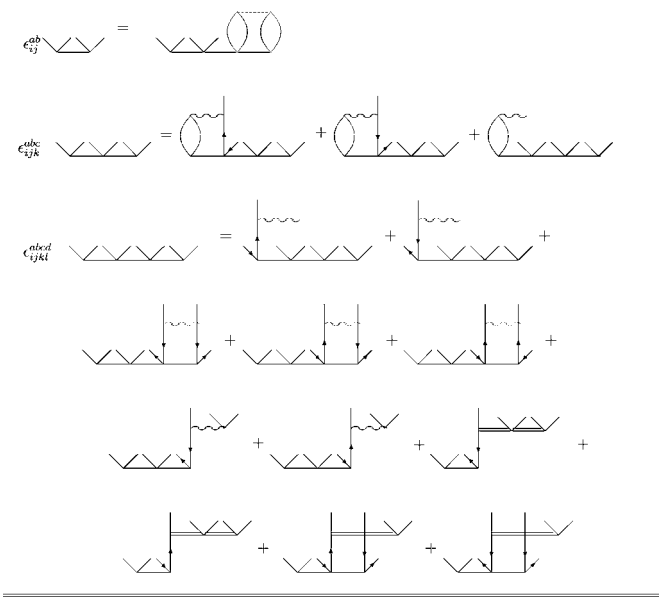

FIG. 13. Diagrams representing connected quadruple contributions to the double-, triple-, and quadruple-excitation equations in the CCSDTQ method.

quite straightforward, and that, plus using various automatic (Hirata, 2003) or other computer-generated programs (Olsen, 2000; Kallay and Surjan, 2001; Kallay and Gauss, 2004), has now made it possible to go to quite high levels of excitation through hextuples, i.e., CCSDTQPH, for example. Their application to chemically interesting problems, though, is limited by other factors.

As discussed briefly earlier, CCSD requires no more than $\sim n^2N^2t_{ij}^{ab}$ amplitudes, and the rate-determining step is the evaluation of the ladder diagram, $\sim n^2N^4$, the fourth diagram in Fig. 9, which already arises in CCD. Once we go to CCSDT, we have $\sim n^3N^3$ amplitudes and a computational dependence of $\sim n^3N^5$. In general, we have $\sim n^lN^l$ amplitudes and an $\sim n^lN^{l+2}$ computational dependence for the level of excitation l. For our modest-sized example from before $n=10$, $N=100$ functions, CCSDT would require storing some $\sim 10^9$ amplitudes. A lower bound to its time for the evaluation of a single iteration would be $\sim 10\times 10^{11}$ operations ($\sim$1 h for a 2 gigaflop processor). Doubling the size of molecule adds $\sim 2^{12}$ to the time attesting to the extreme nonlinear dependence of high-level CC calculations if no further simplification is made. Yet, today, CCSD (Purvis and Bartlett, 1982), CCSDT-1 (Lee *et al.*, 1984), CCSDT-3 (Noga *et al.*, 1987), CCSD[T] (Urban *et al.*, 1985), and CCSD(T) (Ragavachari *et al.*, 1989; Bartlett *et al.*, 1990) calculations are done with $\sim$300 basis functions and have used $\sim$600. The first two triples models include the principal effects of triple excitation iteratively, which requires only an $\sim n^3N^4$ step and is done without storing the t_{ijk}^{abc} amplitudes. The last two are further perturbative approximations of triples based upon CCSDT-1 that are

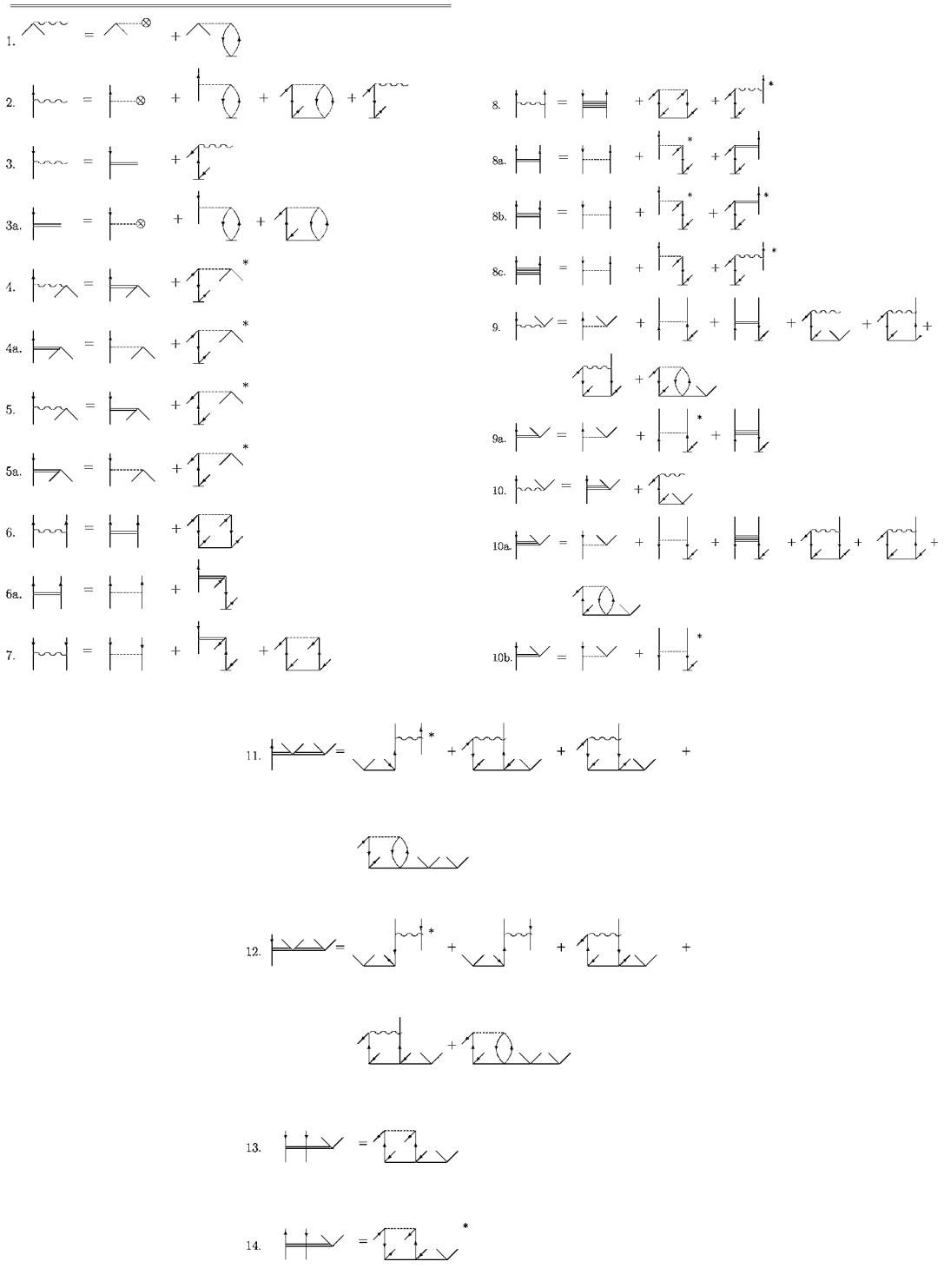

FIG. 14. Diagrammatic form of intermediates introduced in CCSDT and CCSDTQ models with total factorization of nonlinear terms. The * indicates that the intermediate is preceded by a 1/2 to avoid overcounting.

used to augment the CCSD solution (see Sec. V.E), but reduce the computational dependence down to a noniterative $\sim n^3N^4$ step augmenting an iterative $\sim n^2N^4$ CCSD calculation. At each level some accuracy is sacrificed for a broader range of applications.

In addition to the CCSD diagrams shown in Fig. 10, the additional diagrams that define CCSDT-1 (Lee *et al.*, 1984) are shown in Fig. 16, truncating the T_3 equation to its lead, second-order term and then adding the triple excitation contribution to the T_1 and T_2 equations. In this way, the T_3 amplitudes, which would appear on the right-hand side of the full CCSDT equations, are not allowed to contribute to T_3. However, the T_3 obtained does contribute to T_1 and T_2 and T_2 then updates the T_3 amplitudes, until reaching convergence. The $t_{ijk}^{abc[2]}$ (the

TABLE V. Algebraic expression for the intermediates used in the CCSDT and CCSDTQ equations.

Intermediate	Expression[a]
1. I_a^i	$f_a^i + t_n^f v_{af}^{in}$
2. I_b^a	$f_b^a + t_n^f v_{bf}^{an} - \frac{1}{2} t_{no}^{af} v_{bf}^{no} - t_n^a I_b^n$
3. I_j^i	$I_j'^i + t_j^f I_f^i$
3a. $I_j'^i$	$f_j^i + t_n^f v_{jf}^{in} + \frac{1}{2} t_{jn}^{fg} v_{fg}^{in}$
4. I_{bc}^{ai}	$\chi_{bc}^{ai} - \frac{1}{2} t_n^a v_{bc}^{ni}$
4a. χ_{bc}^{ai}	$v_{bc}^{ai} - \frac{1}{2} t_n^a v_{bc}^{ni}$
5. I_{ka}^{ij}	$\chi_{ka}^{ij} + \frac{1}{2} t_k^f v_{fa}^{ij}$
5a. χ_{ka}^{ij}	$v_{ka}^{ij} + \frac{1}{2} t_k^f v_{fa}^{ij}$
6. I_{cd}^{ab}	$I_{cd}'^{ab} + \frac{1}{2} t_{no}^{ab} v_{cd}^{no}$
6a. $I_{cd}'^{ab}$	$v_{cd}^{ab} - P(a/b) \chi_{cd}^{an} t_n^b$
7. I_{kl}^{ij}	$v_{kl}^{ij} + P(k/l) \chi_{kf}^{ij} t_l^f + \frac{1}{2} t_{kl}^{fg} v_{fg}^{ij}$
8. I_{bj}^{ia}	$\chi_{bj}'^{ia} + v_{bf}^{in} t_{jn}^{af} + \frac{1}{2} I_{bf}^{ia} t_j^f$
8a. χ_{bj}^{ia}	$v_{bj}^{ia} - \frac{1}{2} v_{bj}^{in} t_n^a + \chi_{bf}^{ia} t_j^f$
8b. $\chi_{bj}'^{ia}$	$v_{bj}^{ia} - \frac{1}{2} v_{bj}^{in} t_n^a + \frac{1}{2} \chi_{bf}^{ia} t_j^f$
8c. $\chi_{bj}'^{ia}$	$v_{bj}^{ia} - v_{bj}^{in} t_n^a + \frac{1}{2} I_{bf}^{ia} t_j^f$
9. I_{ci}^{ab}	$v_{ci}^{ab} + v_{cf}^{ab} t_i^f - P(a/b) t_n^a \chi_{ci}'^{nb} - I_c^n t_{ni}^{ab} + P(a/b) I_{cf}^{an} t_{in}^{bf} + \frac{1}{2} t_{no}^{ab} I_{ci}^{no} - \frac{1}{2} t_{noi}^{afb} v_{cf}^{no}$
9a. $I_{ci}'^{ab}$	$v_{ci}^{ab} + \frac{1}{2} v_{cf}^{ab} t_i^f - P(a/b) t_n^a \chi_{ci}'^{nb}$
10. I_{jk}^{ia}	$I_{jk}'^{ia} + I_f^i t_{jk}^{fa}$
10a. $I_{jk}'^{ia}$	$v_{jk}^{ia} - v_{jk}^{in} t_n^a + P(j/k) t_j^f \chi_{fk}'^{ia} + P(j/k) I_{jf}^{in} t_{kn}^{af} + \frac{1}{2} I_{fg}^{ia} t_{jk}^{fg} + \frac{1}{2} v_{fg}^{in} t_{jnk}^{fga}$
10b. $I_{jk}'^{ia}$	$v_{jk}^{ia} - \frac{1}{2} v_{jk}^{in} t_n^a$
11. $I_{dij}'^{abc}$	$\frac{1}{2} P(ab/c) I_{df}^{ab} t_{ij}^{fc} + P(a/bc) I_{df}^{an} t_{ijn}^{bcf} + \frac{1}{2} P(i/j) I_{di}^{no} t_{noj}^{abc} - \frac{1}{2} v_{df}^{no} t_{noij}^{afbc}$
12. $I_{jkl}'^{iab}$	$-\frac{1}{2} P(jk/l) I_{jk}^{in} t_{nl}^{ab} - P(a/b) P(kl/j) I_{fj}^{ia} t_{kl}^{fb} + P(j/kl) I_{jf}^{in} t_{k\,\mathrm{ln}}^{abf}$ $+ \frac{1}{2} P(a/b) I_{fg}^{ia} t_{jkl}^{fgb} + \frac{1}{2} v_{fg}^{in} t_{jnkl}^{fgab}$
13. $I_{klm}'^{ija}$	$\frac{1}{2} v_{fg}^{ij} t_{klm}^{fga}$
14. $I_{cjk}'^{iab}$	$\frac{1}{2} v_{cf}^{in} t_{jkn}^{abf}$

[a]Summation over repeated indices assumed. $P(i/j)$ or $P(a/b)$ implies the sum of two components differing by permutation of i, j and a, b indices, respectively. $P(ab\cdots/c\cdots)$ indicates that in addition to the identity permutation, the summation should include all possible permutations exchanging labels between subsets $(ab\cdots)$ and $(c\cdots)$. The same refers to $P(ij\cdots/k)$.

[2] instead of (2) indicates a generalized second order since the $\bar{T}_2$ amplitudes contain infinite-order terms) amplitudes are used on the fly to avoid any storage. Another convenience, if not a necessity in this evaluation, is that we are free to dismiss the off-diagonal part of the diagram

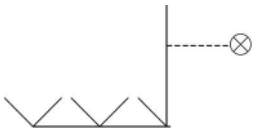

by exploiting the fact that CCSDT-1, like any other iterative CC approximation that always evaluates complete diagrams as opposed to using just selected parts of them, will be invariant to rotations in the occupied or virtual space. Hence, we are free to make the semicanonical transformation of the Fock matrix discussed in Sec. V.B to make the off-diagonal $f_{ij}=f_{ab}=0$. Without doing so, we could be left with an extra $\sim n^3N^4$ iterative step in the determination of the above diagram. For non-HF cases, in the equations below, we will assume that this transformation has already been made. As shown in Figs. 16 and 17, to make the transition from CCSDT-1 to CCSDT-3 (Noga *et al.*, 1987), which means that all possible contributions of T_2 and T_1 to T_3 are included instead of just their lead terms, it is apparent that this requires nothing but the replacement of the diagram units in CCSDT-1 by their corresponding $\bar{H}$ intermediates. Another way of saying this is

$$\epsilon_{ijk}^{abc} t_{ijk}^{abc}(T-3) = \langle {}_{ijk}^{abc}|[H_N \exp(T_1+T_2)]_C|0\rangle \tag{74}$$

instead of just using linear T_2 as is done in CCSDT-1. So this too is an iterative $\sim n^3N^4$ method, yet it has the enhanced orbital insensitivity that accrues due to the inclusion of higher-order terms in T_1 and T_2. This method still avoids the storage of the $\sim n^3N^3$ t_{ijk}^{abc} amplitudes and gains $\sim N$ in speed over the full CCSDT, making it a practical, yet highly accurate level of approximation for many molecular problems.

E. Noniterative approximations

Short circuiting the iterative procedure of CCSDT-1 and simply using converged $\bar{T}_2$ and $\bar{T}_1$ amplitudes from CCSD, and using the expectation value energy formula instead of that in Eqs. (59)–(63) (Urban *et al.*, 1985), gives

$$E = \langle 0|\exp(T^\dagger)H\exp(T)|0\rangle/\langle 0|\exp(T^\dagger)\exp(T)|0\rangle \tag{75}$$

$$= \langle 0|[\exp(T^\dagger)H\exp(T)]_C|0\rangle \tag{76}$$

$$= \langle 0|\exp(T^\dagger)[H\exp(T)]_C|0\rangle. \tag{77}$$

This formula recognizes that the H_N expectation value of the full CC wave function also gives the energy. By inserting the resolution of the identity, it is easy to see that

$$E = \langle 0|\exp(T^\dagger)\exp(T)\exp(-T)H_N\exp(T)|0\rangle/\langle 0|\exp(T^\dagger)\exp(T)|0\rangle \tag{78}$$

$$= \langle 0|\exp(T^\dagger)\exp(T)(P+Q)\exp(-T)H_N\exp(T)|0\rangle/\langle 0|\exp(T^\dagger)\exp(T)|0\rangle \tag{79}$$

$$= \langle 0|[H_N\exp(T)]_C|0\rangle, \tag{80}$$

which is the usual, sometimes called, transition formula. This formula follows from the fact that $Q\bar{H}|0\rangle=0$ as the CC equations would be satisfied for any excitation in Q. Whereas the transition formula is always in closed form, the expectation value form is not, either requiring division by the denominator in Eq. (75), or, as in Eq. (76), the division has already been incorporated by the restriction to the connected form in the numerator (Čížek, 1966) which similarly leads to an infinite series regardless of the number of electrons in the problem. For specific CC approximations like CCSD, the energy equivalence does not hold, and in fact it can be shown that important contributions from connected quadruple excitations will arise from the expectation value of CCSD (Bartlett and Noga, 1988). The third form, Eq. (80), is intermediate and particularly useful for the following analysis, as it imposes connectedness on the $(H_Ne^T)_c$ products.

Slightly generalizing the original derivation (Urban *et al.*, 1985) to the non-HF case (Watts *et al.*, 1993), we use the $t_{ijk}^{abc[2]}$ amplitude evaluated from the first iteration of CCSDT-1 to obtain the noniterative approximation CCSD[T] by computing the fourth-order terms that can arise from connected T_3,

$$E_T^{[4]} = \langle 0|T_3^{[2]\dagger}(H_0T_3^{[2]})_C + T_3^{[2]\dagger}(W\bar{T}_2)_C + \bar{T}_2^\dagger(WT_3^{[2]})_C + \bar{T}_1^\dagger(WT_3^{[2]})_C + \bar{T}_2^\dagger(f_{vo}T_3^{[2]})_C|0\rangle. \tag{81}$$

Using the $T_3^{[2]}$ equation, $\langle {}_{ijk}^{abc}|H_0T_3^{[2]}+W\bar{T}_2|0\rangle=0$, it is apparent that the first and second terms cancel, and the third term, the complex conjugate of the second, can be replaced by the negative of the first and the extra denominator indicated, to give the diagrams

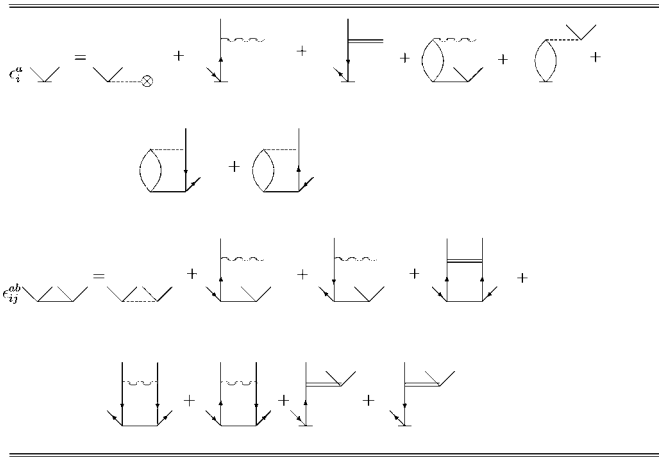

FIG. 15. Diagrammatic CCSD equations with total factorization of nonlinear terms.

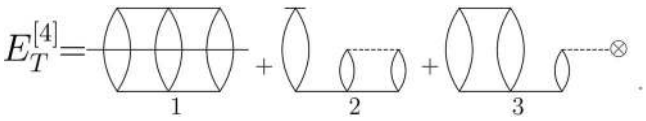

If we count orders relative to HF, then $\bar{T}_1$ would first arise in second order. So the appropriate purely fourth-order approximation is given by diagram 1, which is the original CCSD[T] (Urban *et al.*, 1985).

Once we consider non-HF cases, then the second diagram corresponds to a fourth-order term, and adding it we obtain CCSD(T) (Ragavachari *et al.*, 1989). Its evaluation is as follows:

$$\epsilon_i^a t_i^{a[3]}(T_3) = \langle {}^a_i|(WT_3)_C|0\rangle, \tag{82}$$

$$E_{ST}^{[5]} = \tfrac{1}{4}\sum_{i,a} \bar{t}_i^{a*} t_i^{a[3]}. \tag{83}$$

So when used for HF cases this selects only one of many fifth-order terms, yet the numerical results tend to improve since this diagram usually acts in an opposite direction to the first term, which is necessarily negative; so the second term can help to avoid overshooting the energy in difficult cases.

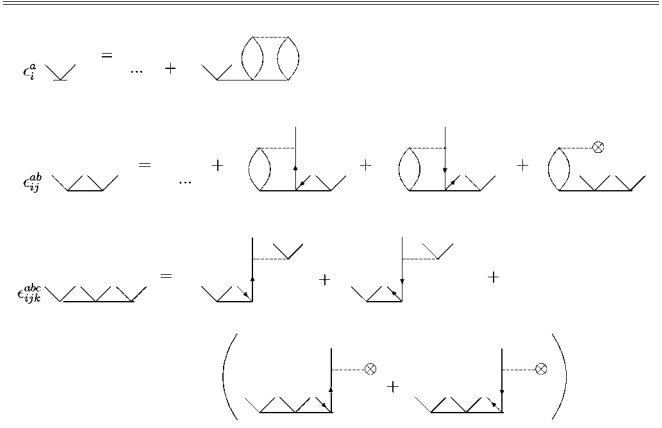

FIG. 16. Additional diagrams to the CCSD model that define the CCSDT-1 method.

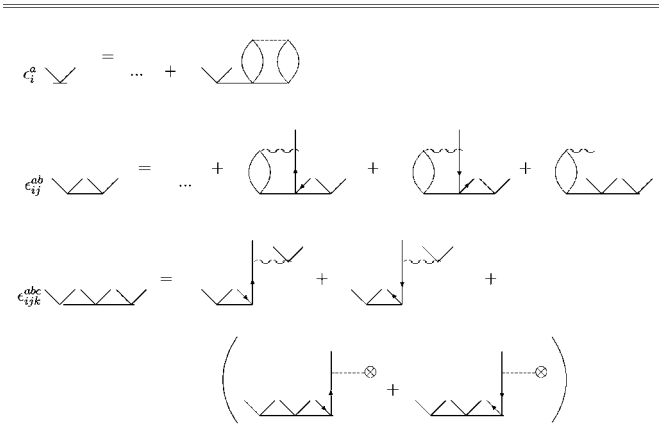

FIG. 17. Additional diagrams to the CCSD model that define the CCSDT-3 method.

Finally, the completely general form of Eq. (81) also adds diagram three (and presupposes the semicanonical transformation to avoid the off-diagonal diagram previously mentioned) (Watts *et al.*, 1993). This final, noniterative form has exactly the same invariance properties as iterative CC methods, as it is invariant to orbital rotations within the occupied or within the virtual space, a highly desirable benefit of the approximation. Among other properties, the invariance facilitates analytical derivatives of the energy as discussed in Sec. VII. The presence of the denominator in Eq. (75) can be exploited to derive renormalized approximations for noniterative corrections. This will be discussed in Sec. VI.C.

An even more general derivation of iterative and noniterative triple and quadruple excitation contributions can be made based upon the CC functional presented in Sec. VII, and derived there.

We can achieve even a lower dependence for some of the T_4 effects as follows. Assume we are improving upon an existing CCSDT solution, and for non-HF cases invoke the semicanonical transformation. Focusing on the lead term in the T_4 equations,

$$0 = \langle {}^{abcd}_{ijkl}|H_0 T_4|0\rangle + \langle {}^{abcd}_{ijkl}|(W\bar{T}_2^2/2)_C|0\rangle + \langle {}^{abcd}_{ijkl}|(W\bar{T}_3)_C|0\rangle \quad \forall\, a,b,c,d,i,j,k,l, \tag{84}$$

$$T_4^{[3]} = \hat{R}_4[(W\bar{T}_2^2/2)_C + (W\bar{T}_3)_C], \tag{85}$$

$$T_2^{[4]}(T_4) = \hat{R}_2 W T_4^{[3]}, \tag{86}$$

$$E^{[5]}(T_4) = \langle 0|WT_2^{[4]}(T_4)|0\rangle, \tag{87}$$

where the last term arises for the usual transition energy formula (R_2 means the double excitation part of the resolvent and R_4 the quadruples excitation part). Further manipulations of the energy expression give

$$E^{[5]}(T_4) = \langle 0|W\hat{R}_2\{WR_4[(W\bar{T}_2^2/2)_C + (W\bar{T}_3)_C]_C\}|0\rangle \tag{88}$$

$$= \tfrac{1}{2}\langle 0|T_2^{(1)\dagger}T_2^{(1)\dagger}WT_4^{[3]}|0\rangle. \quad (89)$$

We have identified WR_0 as the first approximation to $T_2^\dagger, T_2^{(1)\dagger}$. Then using the factorization theorem in the last line, $\frac{1}{2}(W\hat{R}_2W' + W\hat{R}_2'W') = \frac{1}{2}[W\epsilon_2^{-1}W' + W(\epsilon_2^{-1})'W'] = WW'(\epsilon_2+\epsilon_2')/\epsilon_2\epsilon_2'$ eliminates $\hat{R}_4(\epsilon_4)$ from the energy expression. As the eight-index ϵ_4 denominator would require in this case an $\sim n^4N^5$ computational step, its elimination reduces the computation to $\sim n^2N^5$ for the T_2^2 term and to $\sim n^3N^4$ for T_3.

Though this can be done rigorously in the fifth-order transition energy expression, it cannot be done in the amplitude expression. However, as we know that the $T_4^{[3]}$ amplitudes inserted into the T_2 equation will introduce this initial energy correction (Kucharski and Bartlett, 1998c), we can modify the T_2 equation by adding to it,

$$T_{2Q_f}^{[4]}(T_4) = \tfrac{1}{2}\hat{R}_2\{T_2^{(1)\dagger}[W(T_2^2/2 + T_3)_C]\}. \quad (90)$$

This can be incorporated into its iterative solution in the normal way, coupled to the T_1 and T_3 equations. Its energy contribution would then arise in the usual energy formula, Eq. (80). This factorization preserves the same computational simplicity of the factorized approximation into the amplitude equation as it only adds an $\sim n^3N^4$ and an $\sim n^2N^5$ step to an already $\sim n^3N^4$ CCSDT-n or $\sim n^3N^5$ full CCSDT method. It is also fundamentally different from the usual CC disconnected simplification as it approximately factorizes a connected T_4. In a series of comparisons for H_2O, HF, and BH molecules in their equilibrium geometry, the use of the $T_{2Q_f}^{[4]}$ amplitude approximation differs from using the regular quadruple contribution by <0.003 mH (Kucharski and Bartlett, 1998c).

Finally, using the expectation value energy expression as we did above for triples and isolating the contribution of quadruples, we have

$$E_{Q_f}^{[5]} = \tfrac{1}{2}\langle 0|\bar{T}_2^\dagger T_2^{(1)\dagger}[W(\bar{T}_2^2/2 + \bar{T}_3)_C]|0\rangle, \quad (91)$$

which defines a noniterative, fifth-order factorized quadruple contribution in analogy to that for T_3, called CCSDT(Q_f) (Kucharski and Bartlett, 1998c). One can also use a lower approximation than CCSDT with its $\sim n^3N^5$ step, by evaluating Q_f from an underlying CCSDT-n approximation, or go all the way to CCSD(TQ_f) where the usual T is combined with Q_f. The latter is the simplest possible initial approximation for connected T_3 and T_4. All such approximations, particularly the noniterative ones, make applications possible that could not be done otherwise. Several such noniterative approximations have been considered that are correct through fifth (Kucharski and Bartlett, 1998a) and sixth order (Kucharski and Bartlett, 1998b), using three different types of energy formulas: that from the expectation value, the normal expression, and the CC functional to be discussed in Sec. VII. Other such noniterative approximations that include quadruple excitations have been suggested (Gwaltney and Head-Gordon, 2001; Hirata, Nooijen, *et al.*, 2001; Hirata, Fan, *et al.*, 2004; Bomble *et al.*, 2005). The latter, termed CCSDT(Q), is correct to sixth order and the most complete to date. It is discussed in Sec. VII.

The above approximations have established the paradigm of converging, size-extensive approximations for electron correlation from

$$\begin{aligned}\text{MBPT(2)} < \text{CCSD} < \text{CCSD}(T) < \text{CCSDT} \\ < \text{CCSDT}(Q_f) < \text{CCSDT}(Q) \\ < \text{CCSDTQ} < \text{full CI}.\end{aligned}$$

Coupled with an adequate basis set for the phenomena of interest, this paradigm provides predictive results to within reasonable error bars.

One word about applications to nuclei. The abstract of Kowalski *et al.* (2004) says, "the quantum chemistry inspired coupled-cluster approximations provide an excellent description of ground and excited states of nuclei. The bulk of the correlation effects is obtained at the CCSD level. Triples, treated non-iteratively, provide virtually the exact description."

For those readers who prefer to continue with new theory developments, the next section focuses primarily on CC numerical results at equilibrium and some of the limitations in single reference CC (SR-CC) in breaking molecular bonds.

VI. SURVEY OF GROUND-STATE NUMERICAL RESULTS

A. Equilibrium properties

In the vicinity of the equilibrium geometry for molecules, single determinant CC theory is exceptionally accurate. However, all *ab initio* results depend upon the quality of the basis set as well as the correlation corrections. So we have three levels of meaningful numerical comparison for coupled-cluster theory with MBPT and CI: (a) comparison of CC with full CI; (b) comparison of CC with experiment as a function of basis set; and (c) comparison of CC with experiment at the extrapolated basis-set limit, or, alternatively, using CC-R12 where most of the basis-set dependence is removed due to explicit R12 inclusion.

Full CI comparisons are the least ambiguous, as one advantage of finite basis-set methods is that the exact results in the basis is given by the full CI that includes all excitations through n-fold for n electrons. The limitation, of course, is that the full CI itself cannot generally be obtained except for few electrons in small basis sets. Subject to this caveat, in Fig. 3 we demonstrate how the evaluation of the correlation energy converges with increasing CI excitation, with orders of MBPT diagrams, and with the addition of higher connected excitations in the infinite-order CC method. Whereas nonpolarized bases cannot be expected to offer meaningful measures of behavior, once polarization functions are included, the correlation effects for small molecules are indicative.

The next level of comparison is to experiment as a function of basis set. The most extensive set of results for CC theory has been presented by Helgaker and coworkers (Bak, Gauss, *et al.*, 2000; Bak, Jörgensen, *et al.*, 2000; Helgaker *et al.*, 2000; Coriani *et al.*, 2005). We replot some of their results for bond lengths for a selection of 31 molecules in Figs. 18(a) and 18(b). The structure of bound molecules is typically the easiest quantity to correctly describe in quantum chemistry, with even Hartree-Fock often being adequate. In each case the Hartree-Fock, MP2, CCSD, and CCSD(T) values with a triple-zeta (cc-pVTZ) basis and then a quadruple zeta basis are shown. In the triple-zeta basis, the HF distribution of errors centers at about −2 pm (−0.02 Å), and varies from −6 to +4 pm, while MP2 centers at about +2 pm and varies from −3 to +6. For the larger basis, the HF distribution is virtually the same, as the HF limit has likely been achieved already for this property, while the simplest correlated method MP2 is improved somewhat centering at +1 pm. CCSD further improves upon the MP2 distribution, with it being centered at exactly the experimental value in the QZ basis. CCSD(T) is not necessarily an improvement over CCSD for this example because of very small errors encountered and core correlation effects. The cc-pVXZ bases do not have functions explicitly chosen to correlate core electrons. The core effect is shown in Fig. 19 as a function of basis set where the cc-pCVQZ adds core correlation functions. Then the error in CCSD(T) is less than ±2 pm.

Energies are more difficult to obtain accurately. The worst energy for a basis-set-dependent quantum chemistry calculation is the heat of atomization for a polyatomic molecule, because separating a molecule into its atomic fragments maximizes the basis-set errors in the calculation. For 16 small molecules, the heat of atomization in a cc-pVQZ basis is shown in Fig. 20. CCSD(T) is a notable improvement over CCSD, which has a narrower distribution than MP2, but is not as well centered as the latter. The range of errors in CCSD(T) is about −13 to +6 kcal/mol (1 kcal/mol=4.184 kJ/mol =0.043 349 eV).

Bond dissociation energies are somewhat easier to describe accurately, because breaking one bond in a polyatomic molecule instead of all retains much of the basis-set error cancellation in the calculation, except for diatomic molecules. For a set of 13 molecules, the reaction enthalpies compared to experiment are illustrated in Fig. 21 for a core-corrected, cc-pCVQZ basis. The errors in CCSD range from −8 to +6 kcal/mol, and center just a little below experiment. CCSD(T) narrows the distribution somewhat (±6 kcal/mol) and is centered just slightly above experiment. There is substantial improvement from HF<MP2<CCSD<CCSD(T), as one would anticipate.

For a property other than the energy, CCSD(T) dipole moments in Debyes as a function of basis sets are compared to reference values for 11 polar molecules in Fig. 22. All such properties are evaluated analytically from the response density matrices discussed in the next section, which are the CC analogs (Bartlett, 1995) of the standard density matrices associated with variational wave functions. In good basis sets, the errors are less than ±0.2 D, compared to an even larger augmented QZ

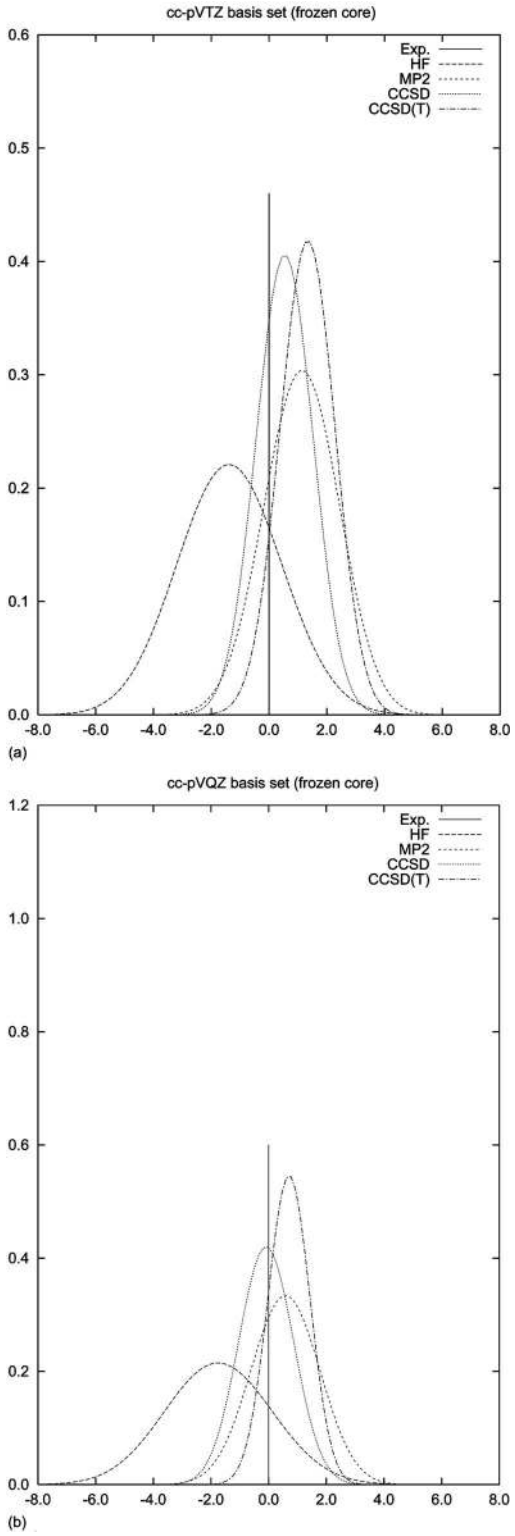

FIG. 18. Normal distribution functions of the deviations from experiment of the calculated bond distances (*pm*) for a set of 31 molecules in the (a) cc-pVTZ basis set and (b) cc-pVQZ basis set (Coriani *et al.*, 2005).

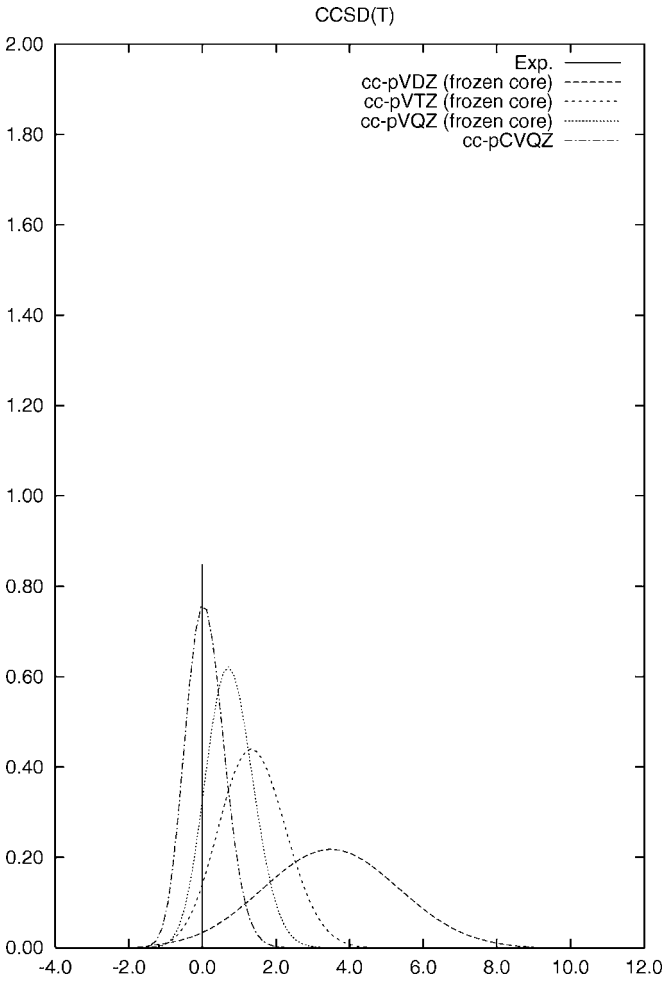

FIG. 19. Normal distribution functions of the deviations from experiment of the calculated bond distances (*pm*) for a set of 31 molecules for the CCSD(T) method in the cc-pVDZ, cc-pVTZ, cc-pVQZ, and cc-pCVQZ basis sets (Coriani *et al.*, 2005).

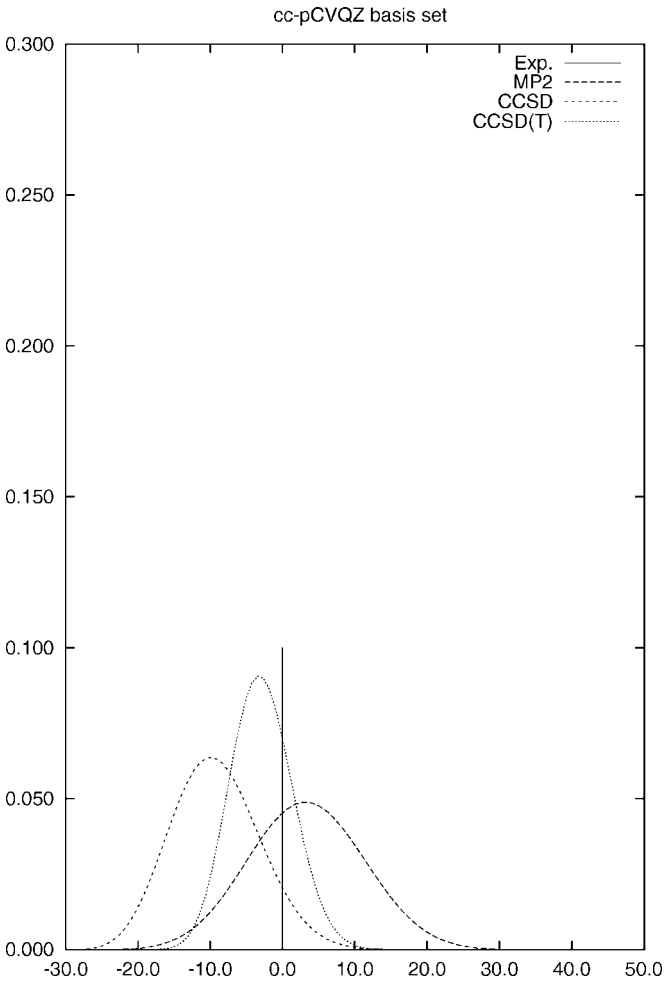

FIG. 20. Normal distribution of errors (kcal/mol) for calculated equilibrium atomization energies compared to experiment for a set of 16 molecules containing first-row atoms in the cc-pCVQZ basis set (Bak, Jörgensen, *et al.*, 2000).

basis. The augmentation adds several more diffuse basis functions than in the standard basis, and these functions will be important in accurately describing the dipole operator $\Sigma_i e_i \mathbf{r}_i$.

To summarize, with a triply polarized basis like cc-pVTZ, the CCSD(T) standard deviations are for structure (~0.0024 Å), dissociation energies for single bonds (~3.5 kcal/mol) (Helgaker *et al.*, 2000), and harmonic vibrational frequencies (~5–20 cm^{-1}) (Bartlett, 1995). Hence, this kind of accuracy for modest-sized molecules can be expected. To quote from the CI community, Thom Dunning has stated that "…of the methods in widespread use today, the CCSD(T) method is the only one that provides a consistently accurate description of molecular interactions for all interaction scales investigated, from more than 200 kcal/mol to 0.02 kcal/mol." Better basis sets, plus basis extrapolation, and better levels of CC theory like CCSDT-3 or CCSDT will typically (but not always) give even more accurate, but more expensive results. At the highest levels, we might also have to concern ourselves with achieving balance between T_4 and T_3, recommending a level like CCSDT-3(Q_f) (Kucharski and Bartlett, 1999) or CCSDT(Q) (Bomble *et al.*, 2005).

As illustrated in Tables VI and VII, if we want to obtain the harmonic vibrational frequency of a small molecule to an accuracy of ~1 cm^{-1}, we can only achieve that for N_2 (Kucharski *et al.*, 1999; Musiał *et al.*, 2001) and C_2 (Kucharski *et al.*, 2001) when using some consideration of pentuple excitations (P_f) on top of CCSDTQ, in a core-corrected, cc-pCV6Z basis. That basis set has 460 contracted Gaussian functions for N_2 and C_2. Note the convergence with basis set and the necessity of extrapolation to fill in the tables. In Table VIII we show results where further effects of basis sets as measured with explicit R12-CCSD (the best current approximation to removing the basis-set error in CC theory) and full CCSDTQP are used, plus adiabatic and relativistic corrections (Pawlowski *et al.*, 2003; Ruden *et al.*, 2004). The core-correlation effects are listed separately. Extremely high-accuracy CC extrapolated thermochemistry (HEAT) values have been presented by Tajti *et al.* (2004) to resolve discrepancies in the thermochemistry

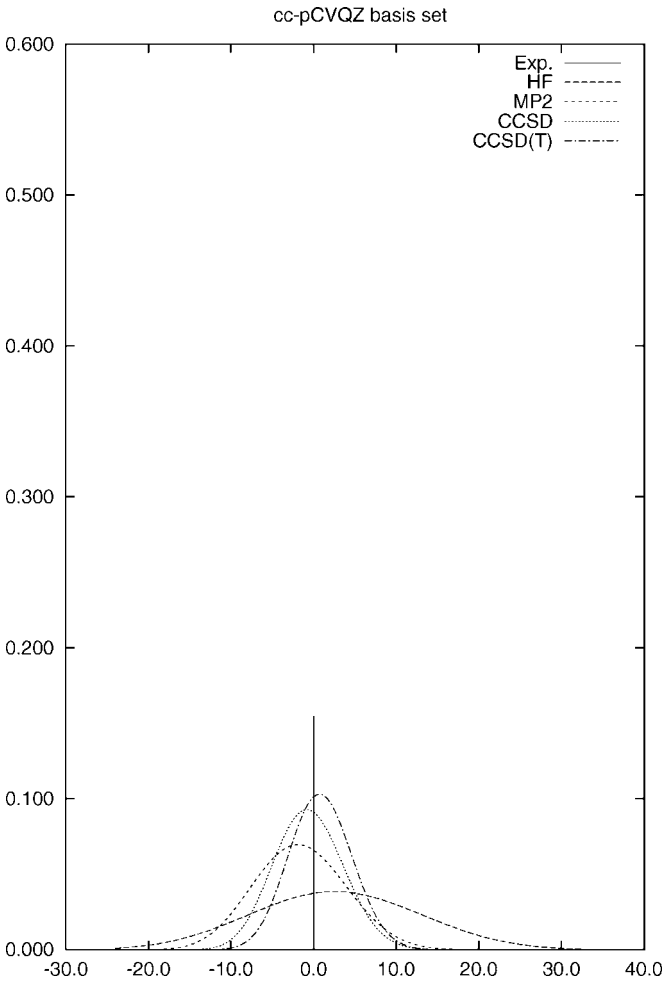

FIG. 21. Normal distribution of errors (kcal/mol) for calculated reaction enthalpies compared to experiment for a set of 13 reactions containing first-row atoms in the cc-pCVQZ basis set (Bak, Jörgensen, *et al.*, 2000).

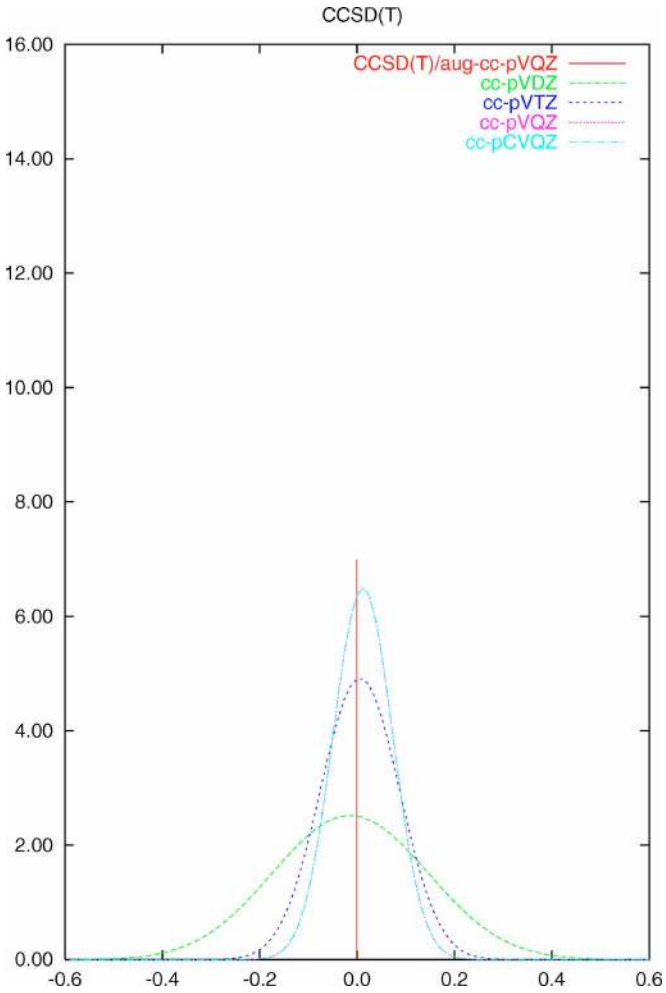

FIG. 22. (Color online) Normal distribution of dipole moment errors (D) related to the CCSD(T)/aug-cc-pVQZ reference numbers for a set of 11 polar closed-shell molecules for the CCSD(T) method in the cc-pVXZ ($X=D,T,Q$) and cc-pCVQZ basis sets (Bak, Gauss, *et al.*, 2000).

data bases for some small molecules and radicals. Other workers (Pawlowski *et al.*, 2003; Alexeev *et al.*, 2005) have provided similar ultimate accuracy CC results to answer questions that depend upon an accuracy of less than 1 kcal/mol. The fact that this can be done attests to the power of CC theory.

For a more demanding example for vibrational frequencies, consider the ozone molecule. Ozone has two nearly degenerate MO's (a_2 and b_1) of which only one $|a_2\bar{a}_2|$ is doubly occupied to define the Fermi vacuum. (The $\bar{a}_2$ means it has β spin.) This is an example of a problem with some multireference character, since a multireference approach would try to treat both orbitals equivalently. Instead, SR theory requires that the second be introduced via the double excitation operator in the cluster expansion, and since it will have a comparatively large weight in the final wave function compared to that for $|a_2\bar{a}_2|$, that can lead to slower convergence. More importantly, a proper wave function might be expected to include both determinants into a MR space from the beginning, which would then introduce excitations from both determinants equivalently, which the SR-CC theory does not do. As Figs. 23 and 24 show, for the symmetric A_1 vibrational frequencies the symmetric stretch and the bend CC theory still does very well, with the better methods showing some improvement over the lower ones. The first figure uses a DZP basis, while the second uses a cc-pVTZ basis. The effect of the larger basis set is pronounced, though the general behavior of the SR-CC methods is still quite good for symmetric vibrations. However, in all cases the antisymmetric vibration is not too well described.

This is an interesting feature of the O_3 problem discussed long ago (Stanton *et al.*, 1989). When the antisymmetric vibration is considered, two other determinants abruptly enter into the calculation, $|a_2\bar{b}_1|$ and $|\bar{a}_2 b_1|$, which together provide another singlet configuration that only contributes when the C_{2v} symmetry of O_3 is broken, allowing the formal a_2 and b_1 orbitals now to mix. This abrupt change causes some lack of balance in determining this antisymmetric vibrational frequency compared to the symmetric ones, which makes it a more demanding test for the theory. Both the effects of basis

TABLE VI. Computed and extrapolated harmonic frequencies with coupled-cluster methods for the N_2 molecule.

Basis set	No. basis functions	CC					Expt.
		SD(T)	SDT	SDT(Q_f)	SDTQ	SDTQ(P_f)	
				ω (cm^{-1})			
cc-pVDZ	28	2339[a]	2347[a]	2325[a]	2328[a]	2324[b]	
cc-pVTZ	60	2346[a]	2356[a]	2337[a]			
cc-pVQZ	110	2356[a]	2366[a]	2348[a]			
cc-pV5Z	182	2360[a]	2370[a]	2351[a]	2354[a,c]	2350	
cc-pCV5Z	290	2370[d]	2380[a,c]	2361[a,c]	2364[a,c]	2360	
cc-pV6Z	280	2361[a]	2371[a,c]	2352[a,c]	2355[a,c]	2351	
cc-pCV6Z	460	2371[d]	2381[a,c]	2362[a,c]	2365[a,c]	2361	2358.6[e]

[a]Kucharski *et al.*, 1999.
[b]Musiał *et al.*, 2001.
[c]Estimated value.
[d]Peterson *et al.*, 1997.
[e]Huber and Herzberg, 1979.

set and level of theory are important. The DIP-STEOM method (Nooijen and Bartlett, 1997c), which we have not yet defined but will in Sec. VIII, treats these determinants equivalently, and shows some improvement over other SR-CC methods. We will further consider this example using MR methods in Sec. IX.

A great deal of chemistry pertains to modest changes from equilibrium geometries like the vast majority of structure determinations, spectroscopic measurements, and heats of reaction. Transition states where bonds begin to break and form occur somewhat farther from equilibrium, and place some extra demands upon the theory. However, of all readily applicable quantum chemical and DFT methods, only CCSD(T) can reduce the error in the activation barrier for simple reactions to <1 kcal/mol (Lynch and Truhlar, 2003). Using a cc-pVTZ basis, the mean error for their benchmark examples is 0.91 kcal/mol, while with the augmented basis aug-cc-pVTZ the error is 0.24. All DFT methods currently applicable have errors more negative than -4 kcal/mol. In a rate constant, an error of ~ 1 kcal/mol in the barrier changes the rate by a factor of ~ 5.

B. Basis-set issue

The basis-set limitations in molecular applications are well known. For two-electron interactions, the solution of the correlation problem ultimately depends upon the MO product approximation $\sim\phi_p(1)\phi_q(2)$. Hence, the two-electron basis is much poorer than the one-electron basis set. It has been known since the time of Hylleraas

TABLE VII. Computed and extrapolated harmonic frequencies with coupled-cluster methods for the C_2 molecule.

Basis set	No. basis functions	CC					Expt.
		SD(T)	SDT	SDT(Q_f)	SDTQ	SDTQ(P_f)	
				ω (cm^{-1})			
cc-pVDZ	28	1828[a]	1829[a]	1821[a]	1816[a]	1814[b]	
cc-pVTZ	60	1845[a]	1847[a]	1838[a]	1833[a]		
cc-pVQZ	110	1856[a]	1859[a]	1849[a]			
cc-pV5Z	182	1859[a]	1861[a]	1852[a]	1847[a,c]	1845	
cc-pCV5Z	290	1870[d]	1872[a,c]	1862[a,c]	1857[a,c]	1855	
cc-pV6Z	280	1860[a]	1862[a,c]	1853[a,c]	1848[a,c]	1846	
cc-pCV6Z	460	1871[d]	1873[a,c]	1863[a,c]	1858[a,c]	1856	1854.7[e]

[a]Kucharski *et al.*, 2001.
[b]Musiał *et al.*, 2001.
[c]Estimated value.
[d]Peterson *et al.*, 1997.
[e]Huber and Herzberg, 1979.

TABLE VIII. Contributions to the best estimates of harmonic frequencies (in cm^{-1}).

	HF	N_2	F_2	CO
CCSD-R12[a]	4191.0	2443.2	1026.5	2238.5
CCSD(T)-CCSD[b]	−48.4	−80.6	−95.7	−71.5
CCSDTQ-CCSD(T)[b]	−4.5	−9.1	−12.2	−6.5
CCSDTQP-CCSDTQ[b]	−0.1	−3.9	−0.8	0.0
Core-correlation correction[b]	4.0	9.8	1.6	9.9
Total[b]	4142.0	2359.4	919.4	2170.4
Adiabatic correction[b]	0.4	0.0	0.0	
Relativistic correction[b]	−3.5	−1.4	−0.5	−1.3
Best estimate[b]	4138.9	2358.0	918.9	2169.1
Experiment[c]	4138.3	2358.6	916.6	2169.8

[a]Pawlowski *et al.*, 2003.
[b]Ruden *et al.*, 2004.
[c]Huber and Herzberg, 1979.

(1929) that wave functions that are constructed with explicit r_{12} dependence will be much more accurate. Such a wave function satisfies the so-called (singlet) electron cusp condition defined by Kato (1957),

$$\lim\left(\frac{\delta\Psi}{\delta r_{12}}\right) = \frac{1}{2}\Psi(r_{12}=0). \tag{92}$$

Kutzelnigg, Klopper, and Noga (Kutzelnigg, 1985; Noga *et al.*, 1992; Noga and Kutzelnigg, 1994) have developed such an explicit R12-dependent CC approach into a practical computational method, CC-R12. Within the CC-R12 ansatz, the exponential operator consists of the conventional, standard exponential T operator and a new R operator that takes care of the correlation cusp, and more importantly the short-range correlation. The final wave function ($|\Psi\rangle$) is expressed as

$$|\Psi\rangle = e^R e^T|\Phi\rangle = e^{(R+T)}|\Phi\rangle$$

and R is defined as

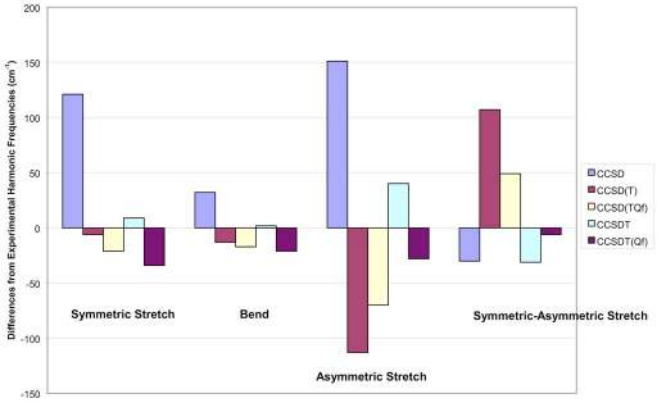

FIG. 23. (Color online) Vibrational frequencies of ozone (DZP basis set). Experimental values are 1135, 1089, and 716 cm^{-1} for symmetric stretch, asymmetric stretch, and bending modes, respectively (Tanaka and Morino, 1970; Barbe *et al.*, 1974).

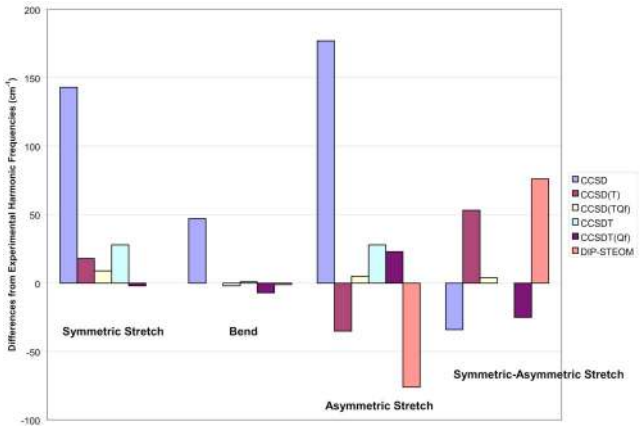

FIG. 24. (Color online) Vibrational frequencies of ozone (cc-pVTZ basis set). See Fig. 23 for the experimental values.

$$R = \tfrac{1}{4}c_{kl}^{ij}R_{ij}^{kl}, \tag{93}$$

$$R_{ij}^{kl} = \tfrac{1}{2}\bar{R}_{\alpha\beta}^{kl}\tilde{a}_{ij}^{\alpha\beta} = \tfrac{1}{2}(\bar{r}_{\alpha\beta}^{kl}\tilde{a}_{ij}^{\alpha\beta} - \bar{r}_{ab}^{kl}\tilde{a}_{ij}^{ab}), \tag{94}$$

$$\bar{r}_{pq}^{rs} = \langle rs|r_{12}|pq\rangle - \langle rs|r_{12}|qp\rangle, \tag{95}$$

where $\alpha,\beta,\ldots$ denote virtual orbitals within a complete basis; $\tilde{a}_{rs}^{pq} = \{p^\dagger q^\dagger sr\}$; c_{kl}^{ij} are a set of amplitudes defining the r_{12} contribution to the double excitation operator and r_{12} is an operator representing the interelectronic distance.

An R12 theory is most effective when applied to the coupled-cluster approach since it makes it possible to combine the fast convergence of the CC approach toward the full correlation limit with more robust saturation toward the complete basis-set limit (Noga *et al.*, 1992, 2001; Noga and Kutzelnigg, 1994; Noga and Valiron, 2000, 2002). From the computational point of view, the effort required to solve the additional set of equations connected with the R12 amplitudes is not much more demanding than normal CC, once the new three-electron integrals that arise in the theory are approximated by resolutions of the identity (ROI) approximations. However, ROI imposes a restriction to large basis sets. The performance of the CC-R12 approach has been summarized by Noga and Valiron (2002). The mean deviation from estimated complete basis-set limit CCSD(T) correlation energies for a number of ten-electron systems is equal to 16.14 mH, while the same quantity for the CCSD(T)-R12 method is reduced to 1.69 mH. A significant improvement due to the R12 ansatz is also observed for atomization energies and electrical properties (Franke *et al.*, 1995). Further improvments in the R12 theory arise from using it in an exponential form, $\exp(-\gamma r_{12}^2)$ (Hino *et al.*, 2002), that cuts off the inappropriate long-range effect of R12.

The advantage of the CC-R12 theory can be appreciated most fully for small molecular systems where very large basis sets can be used. Also, the extensions required for analytical gradients and EOM-CC excited states have not yet been made.

The other important issue refers to the use of the coupled-cluster method in calculations for large molecules. The construction of such computational schemes is guided by the idea of retaining the most essential subsets of CC amplitudes and neglecting the less important ones, which eventually leads to substantial reduction in the number of amplitudes. Such procedures are built upon either the singular value decomposition (SVD) approach (Kinoshita *et al.*, 2003; Hino *et al.*, 2004), the Cholesky decomposition (Beebe and Linderberg, 1977; Koch *et al.*, 2003), or they try to exploit localization arguments (Schuetz and Werner, 2000; Flocke and Bartlett, 2003). The singular value decomposition applies to any matrix, while Cholesky requires a positive-definite one. In the first case, we can replace the matrix by an expansion in vectors weighted by their singular values, which measures their importance. Then we can make a contraction of the usual MO indexed amplitudes $t_{ij\cdots}^{ab\cdots}$ by a contracted set t_X^Y as determined, in principle, by their singular values. [In practice, we have to obtain the weight factors from some simpler, related problem like MBPT(2).] Now the effective dimension of the CC problem is greatly reduced, again dramatically diminishing the high scaling of the unmodified calculation. This is called compressed coupled cluster. Very impressive localized orbital results for quite large molecules have been reported (Schuetz and Werner, 2000), some even with explicit R12 effects (Werner and Manby, 2006).

The coupled-cluster method CCSD has also been applied to polymers for its first numerical example for an infinite, translationally invariant system (Hirata, Grabowski, *et al.*, 2001; Hirata, Podeszwa, *et al.*, 2004). Prior CCD work was reported by Förner *et al.* (1997). Such correlated methods for periodic systems are difficult to do, primarily because of having to converge the lattice sums, even though long-range interaction terms can be effectively grouped together and the integral calculation limited to the symmetrically unique integrals that extend over several neighbor unit cells. The main new element in the cluster amplitudes is that in addition to the usual $i,j\cdots a,b\cdots$ orbital indices, one has to also add the wave vector $\mathbf{k}$ to the Bloch spin-orbitals. However, not all wave-vector indices are varied independently, because the t-excitation amplitudes will vanish when such excitations do not conserve momentum. In this respect, the polymer problem is closer to that described in standard physics texts on many-body theory than is the rest of this review. The CCSD equations then become

$$\langle 0|\bar{H}|0\rangle = KE_{\text{unit cell}}, \tag{96}$$

$$\langle \Phi_{ik_i}^{ak_a}|\bar{H}|0\rangle = 0 \quad \forall\, a,i,k_i, \tag{97}$$

$$\langle \Phi_{ik_ajk_b}^{ak_abk_b}|\bar{H}|0\rangle = 0 \quad \forall\, a,b,i,j,k_i,k_j,k_a, \tag{98}$$

where $(\mathbf{k}_a-\mathbf{k}_i)\cdot\mathbf{a}=2\pi m$ and $(\mathbf{k}_a+\mathbf{k}_b-\mathbf{k}_i-\mathbf{k}_j)\cdot\mathbf{a}=2\pi n$, with m and n integers and $\mathbf{a}$ the fundamental vector that defines the unit cell. K is the number of wave-vector sampling points. The detailed equations have been shown by Hirata, Grabowski, *et al.* (2001), and Hirata, Podeszwa, *et al.* (2004). Results have been presented for polyethylene, polyacetylene, polyyne $(C\equiv C)_\infty$, as well as prototypes $(LiH)_\infty$ and $(HF)_\infty$. In particular, the decay of the integrals and amplitudes as a function of the number of unit cells has been studied extensively.

If the CC paradigm of converging methods, MBPT(2) < CCSD < CCSD(T) < CCSDT < CCSDT(Q) < CCSDTQ < full CI, and its EOM-CC variants for excited, ionized, etc. states discussed in Sec. VIII could be effectively applied to 1D, 2D, and 3D systems, then CC theory would be able to offer significant insights into several interesting phenomena in solid-state physics, such as band gaps, phonon spectra, optical and magnetic properties, and superconductivity.

C. Bond breaking

When insisting upon correct separation all the way to the asymptotic dissociation limit for a molecule, there can be difficulties. This is not a problem with CC methods as such, but with the reference function used in the single determinant based CC. An RHF reference for a closed-shell molecule cannot separate correctly to open-shell fragments. So for even $H_2\rightarrow 2H$ it is well known that the RHF energy will go to an average of that for a proton H^+ and a hydride ion H^-. For the fragmentation of an open-shell molecule, ROHF will have similar problems to RHF. The unrestricted Hartree-Fock will usually correctly separate, but at the cost of breaking the symmetry of the wave function to permit an electron to localize on each H atom. Though the wave function is wrong, the energy is correct for such a solution at the dissociation limit. The density is also correct at separation. In the interest of developing CC methods that can even transcend the deficiencies of an incorrectly separating reference function, one often intentionally uses a RHF reference to test the CC approach. Obviously, CCSD, which is the full CI for H_2, would give the right answer for two electrons with any possible single determinant reference, including RHF and UHF.

Figure 25 shows the behavior of the F_2 potential-energy curve at various levels of CC theory (Musiał and Bartlett, 2005) with a RHF and a UHF reference. F_2 is an interesting case since, as shown in Fig. 26, the RHF curve is artificially bound because of its incorrect separation, while contrary to fact, the UHF curve shows no binding, as the two F atoms are lower in energy than the F_2 molecule. At the CCSDT level for RHF and CCSD for UHF, both curves are qualitatively correct as would be expected for a single bond, showing that CC theory has the capacity to overcome a misbehaving reference determinant. Closer inspection shows difficiences in that the CCSDT result slips below the asymptotic limit in the RHF reference case, while CCSD is too high. Adding the quadruple excitations CCSDTQ mostly corrects these features for the RHF reference. Results for the widely used CCSD(T) approximation are also shown.

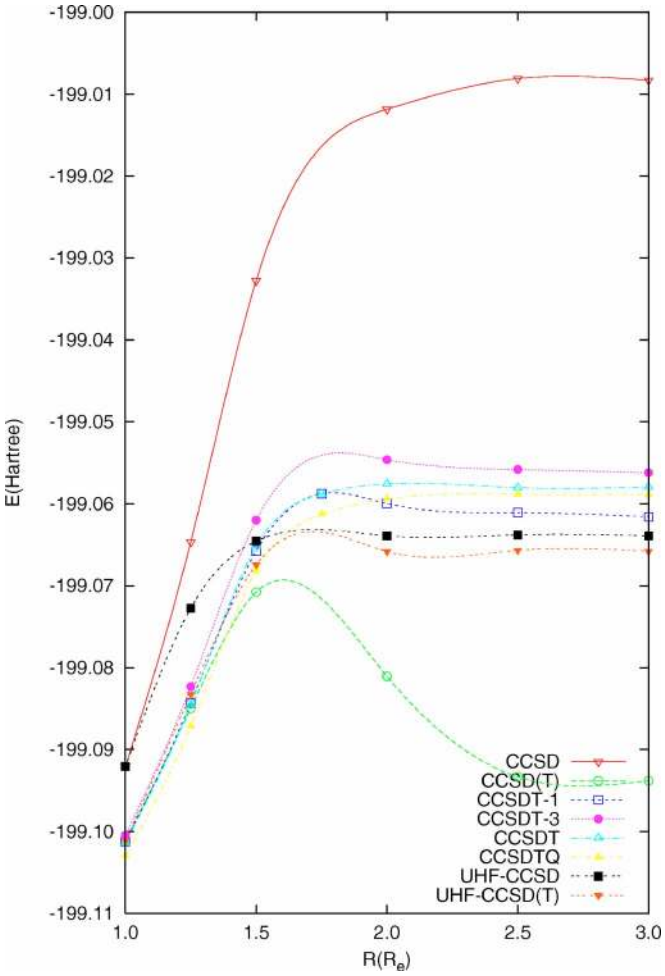

FIG. 25. (Color online) Potential-energy curves for the F_2 molecule obtained with various CC methods in a cc-pVDZ basis set.

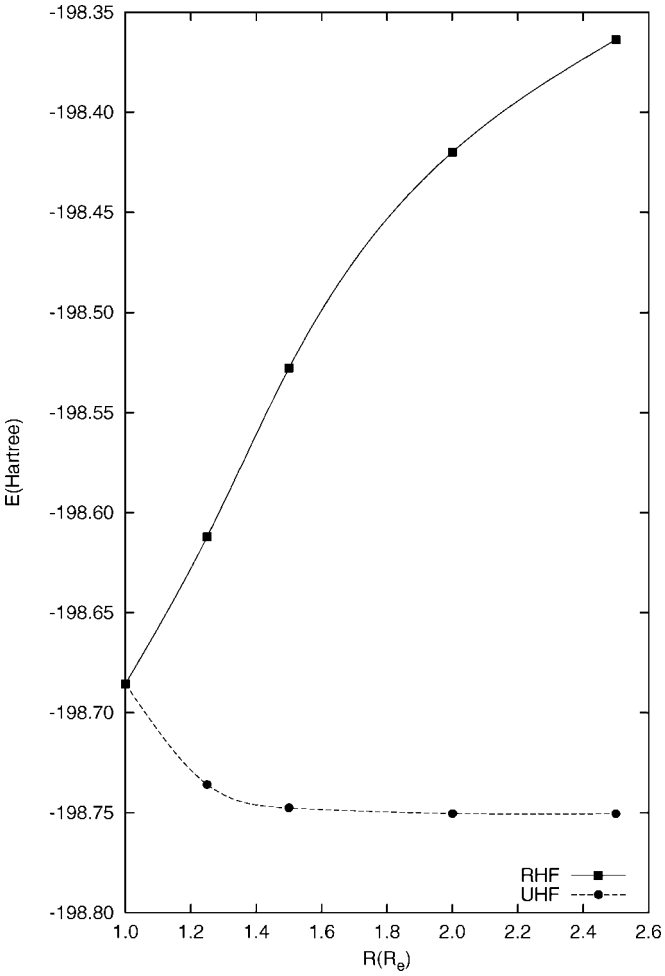

FIG. 26. The SCF potential curves for the F_2 molecule.

Obviously, any perturbative correction to the infinite-order CCSD for a RHF reference will invariably fail since as the bond breaks, the highest occupied MO (homo), ϵ_n, and the lowest unoccupied MO (lumo), ϵ_{n+1}, energies can become degenerate, causing the term to go to minus infinity. For the UHF reference, CCSD(T) has to behave better because the UHF function is separating correctly. Similarly, the differences between CCSD and CCSDT are less pronounced at separation, since the UHF is energetically correct there, but as the RHF solution is the correct, lowest-energy single-determinant solution at the equilibrium geometry, shortly beyond that the UHF becomes lower in energy than the RHF and there is a bifurcation. This region is sometimes called the spin recoupling region as the closed shell is beginning to take on the characteristics of two doublet open shells through the UHF localization, causing the spin-eigenfunction property of the RHF-CC method to be lost. However, insofar as we are converging onto the full CI solution for F_2, the actual eigenfunction would have to eventually become a spin eigenfunction even if we do not impose it *a priori*. However, we can monitor this behavior by evaluating $\langle \hat{S}^2 \rangle$.

We can compute $\langle \hat{S}^2 \rangle$ in two ways. (i) As a projected value in analogy to the transition formula for the energy, where $\langle 0|\hat{S}^2|\Psi\rangle = \bar{S}(\bar{S}+1)$, with an average multiplicity obtained from the approximate spin eigenvalue $\bar{S}$. This gives a quadratic equation where $2\bar{S}+1=\sqrt{1+4\langle 0|\hat{S}^2|\Psi\rangle}$ (Purvis *et al.*, 1988). (ii) As an expectation value $\langle \Psi|\hat{S}^2|\Psi\rangle = \bar{S}(\bar{S}+1)$, which is in general an infinite series in CC theory, but it will be shown in the next section that it can be written in closed form as $\langle 0|(1+\Lambda)\exp(-T)\hat{S}^2\exp(T)|0\rangle$ (Stanton, 1994). The former projected value is consistent with how the energy is determined in CC theory, and is a convenient index for UHF-based CC results, as $2\bar{S}+1$ will typically be a number like 3.0001 for a triplet state, attesting to the fact that there is little spin contamination. For a ROHF reference, however, it follows that $\langle 0|\hat{S}^2|0\rangle = S(S+1)$, which guarantees that the projected value would be exactly $2S+1$ regardless of $|\Psi\rangle$. So if we want to more definitively assess the residual spin contamination in the CC wave function, the second choice is preferred. Several numerical results for the spin multiplicity for open shells are shown elsewhere (Purvis *et al.*, 1988; Stanton, 1994; Bartlett, 1995).

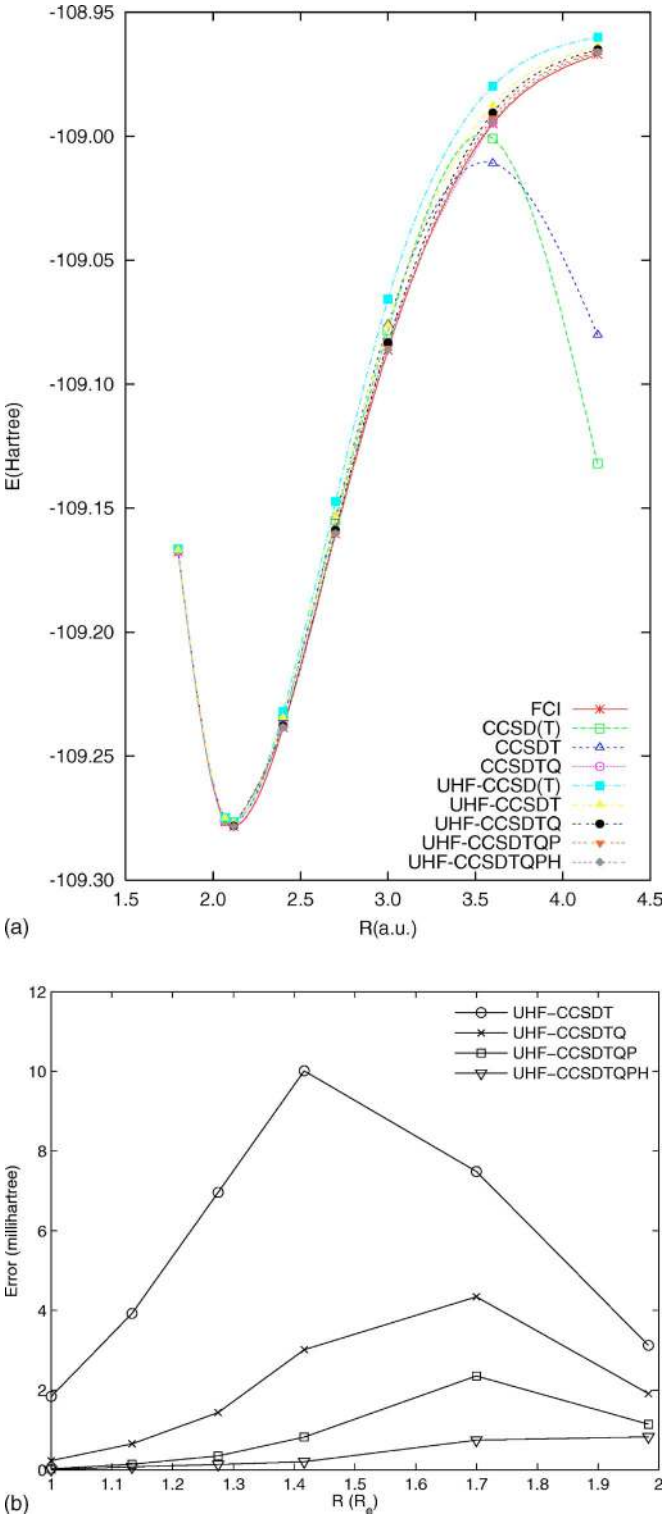

FIG. 27. (Color online) Potential-energy curves for the N_2 molecule. (a) CC results compared to full CI in a cc-pVDZ basis set (frozen core). (b) Errors compared to CI for UHF-CC methods as a function of R.

The more difficult example for bond breaking is offered by the triple bond in N_2. The curve needs to change from a normal closed-shell RHF-based solution at R_{eq} to two ^4S states for the N atoms, each with three unpaired electrons, whose multiplicity could be as high as a septet. Here, as shown in Fig. 27(a) (Chan *et al.*, 2004), the extreme change makes the RHF-based CCSD and CCSDT poorer in the large R region, with the latter falling beneath the asymptotic limit. Once again, the UHF-based CC curves are qualitatively correct. Closer inspection of the recoupling region shows the difficulties with the latter, however. This effect is nicely summarized in the paper of Chan, Kallay, and Gauss, see Fig. 27(b) (Chan *et al.*, 2004). Even though the UHF-CCSD(T) looks qualitatively right in Fig. 27(a), as shown in Fig. 27(b), between about 2 and 4 bohr it can be in error by up to about 19 mH, compared to UHF-CCSD's error of 26. As shown in Fig. 27(b), the maximum error is reduced to about 10 with UHF-CCSDT, while T_4 further reduces it to 4 mH. Pentuples (T_5) reduce that to 2.3 mH and hextuples (T_6) to 0.8 mH.

At the levels of CC theory that are available for serious molecular application, CCSD, CCSD(T), CCSDT-3, and maybe CCSDT-3 (Q_f) beyond some simple single bond-breaking examples, we cannot expect that that level of CC theory without further modification can overcome the deficiencies of an incorrectly separating single-determinant reference. And even if the UHF does separate correctly, there will still be regions of the PES that are less well described. Most would say that correct bond breaking requires a multireference treatment where more than one determinant is used in the reference function. As such, CI linear combinations can be built to ensure that all elements required for correct separation are present in the wave function. We discuss multireference CC in the last section of this review, but despite substantial effort (Lindgren, 1979; Jeziorski and Monkhorst, 1981; Lindgren and Mukherjee, 1987; Jeziorski and Paldus, 1989; Mukherjee and Pal, 1989; Kucharski and Bartlett, 1991b; Bartlett, 2002) and encouraging recent progress (Pittner, 2003; Li and Paldus, 2004) there is no generally applicable MR-CC for PES yet available. Instead, extensions of the more easily applied single reference methods are being pursued further. The essence of the problem, then, is how to get the critical effects of higher-order cluster contributions that facilitate bond breaking into a practical CC computational method with the accuracy and wide applicability that currently exists for molecules near their equilibrium geometries.

To illustrate the problem, consider the ansatz that the correct CC wave function for bond breaking should have a part that accounts for the so-called nondynamic correlation, which roughly means the quasidegeneracy encountered in bond breaking; and a second part that accounts for the dynamic correlation, which means to keep electrons apart. The full CI obviously has both, so this is an artificial separation but one found to be useful when discussing the problem, as the two effects are described somewhat differently. The nondynamic part typically requires a few or several highly weighted determinants to effect correct separation, while the dynamic part is composed of small contributions from very many determinants. The CC method does the latter extremely well, which is why such accurate, correlated results can

be obtained near a molecule's equilibrium geometry.

To illustrate this point we assume a CC ansatz (Piecuch *et al.*, 1993; Kinoshita *et al.*, 2005) that will force a solution to be composed of a nondynamic part, $\exp(T^{\text{ext}})|0\rangle$, and a dynamic part, $\exp(T^{\text{int}})$,

$$|\Psi\rangle = \exp(T^{\text{int}})\exp(T^{\text{ext}})|0\rangle, \tag{99}$$

$$[T^{\text{int}}, T^{\text{ext}}] = 0, \tag{100}$$

$$|\Theta\rangle = \exp(T^{\text{ext}})|0\rangle, \tag{101}$$

$$|\Psi\rangle = \exp(T^{\text{int}})|\Theta\rangle, \tag{102}$$

$$E_{\text{CAS-CI}} = E_{\text{ref}} = \langle 0|H|\Theta\rangle, \tag{103}$$

$$E_{\text{TCCSD}} = E_{\text{ref}} + \Delta E^{\text{int}}_{\text{CCSD}}, \tag{104}$$

where T^{ext} will be taken from a correct nondynamic solution, and T^{int} will be subsequently determined by the usual CC equations. Li and Paldus (1994) have used such an ansatz called externally corrected to add effects for quadruple and higher excitations into CCSD. Here we use a different variant that is limited to just single and double excitations that leads us to tailored CCSD (TCCSD). The simplest solution to bond breaking is to do the full CI in a small, active orbital space that has the essential elements for the bond breaking. For a single bond like the HF molecule, that means the occupied σ orbital and the unoccupied σ^*. Using two orbitals, a linear combination of the two determinants gives the correct, bond-breaking behavior shown in Fig. 28. Note how much higher the energy is than in the correlated results. However, this correct behavior is all that is required to enable the TCCSD result to show correct bond breaking. Extracting the external amplitudes from the full (sometimes called complete active space) CI in the two-orbital problem, by using the cluster decomposition, $T_1^{\text{ext}} = C_1$ and $T_2^{\text{ext}} = C_2 - (T_1^{\text{ext}})^2/2$. So by inserting the two $T_{1,2}^{\text{ext}}$ amplitudes involving the σ and σ^* orbitals, while all the rest ($T_{1,2}^{\text{int}}$) are obtained from the standard CCSD equations, in effect, the reference function in the ansatz becomes the two-determinant one. Usually that would require the tools of MR-CC, which would also have the advantage that the two functions would be treated completely equivalently, but by virtue of fixing the external amplitudes and determining the internal ones separately, some of the MR effect is introduced without operationally changing the vacuum from the single determinant. Tailored coupled-cluster TCCSD greatly improves the separation, yet the method only uses a single determinant reference and has much the same ease of application as the usual single reference CC theory. Once the coupling between T^{ext} and T^{int} is permitted, one moves toward the true MR-CC problem. One intermediate point is to add in the higher excitations into the single reference problem that would correspond to single and double excitations out of a second reference determinant (Oliphant and Adamowicz, 1992), which are triple and quadruple excitations out of the first. To make this

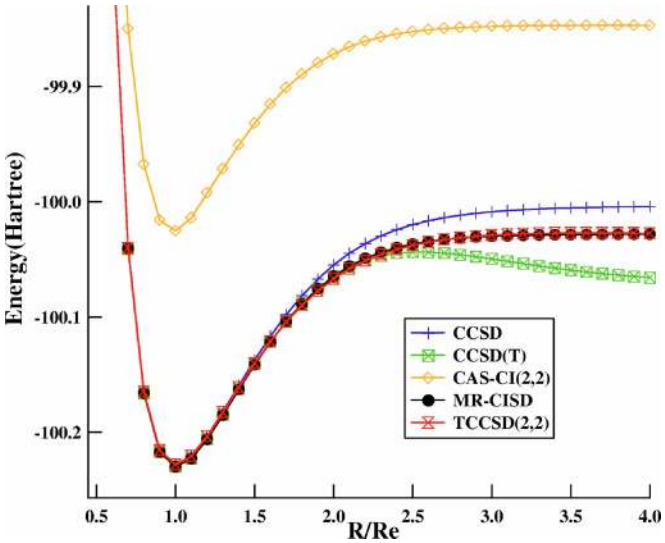

FIG. 28. (Color online) Potential-energy curves for the HF molecule in the cc-pVDZ basis set. The horizontal axis represents the internuclear distance normalized by the equilibrium bond length (R_e=1.733 a.u.) (Kinoshita *et al.*, 2005).

feasible also requires some kind of active orbital restriction to limit these excitations. Finally, if CC is built upon a generalized valence bond (GVB) reference, it would achieve the same bond-breaking behavior for a single bond, but now both components in the reference function would be treated equivalently (Balkova and Bartlett, 1995). Also, because of its fixed form, it is possible to do GVB-based CC (Van Voorhis and Head-Gordon, 2001) without all the complications of general MR-CC. Single bonds, however, are not really the problem.

Application to N_2 requires breaking a triple bond, so the active orbital space consists of the three valence occupied orbitals σ_g, π_u and the three corresponding unoccupied orbitals $\sigma_u(\sigma^*)$, $\pi_g(\pi^*)$. Figure 29 shows the correct behavior for this very small full CI. Here some of the effects of the higher-order excitations $\hat{C}_3$ through $\hat{C}_6$ are subsummed from cluster analysis into just the T_1 and T_2 external amplitudes, and once the remaining amplitudes are determined from the CCSD equations, there is again correct separation. The comparison here is to a very large (14-electron, 10-orbital) MR-CI result. The comparative timings for the two calculations are ~407 s for the MR-CI to ~1.25 s for the TCCSD. When increasing the basis from pVDZ to pVTZ, it is not practical to do the MR-CI but the TCCSD requires only ~36 s, which is essentially the same as for the ordinary CCSD itself. So in a calculation that is much faster than would be the case for even CCSDT, we achieve qualitatively correct bond breaking. The conclusion is that if we can hide into the T_1 and T_2 amplitudes in CCSD the essential effects required for the bond breaking, which are only known here from some consideration of the higher-order CI coefficients, it would give a viable approach. The down side is that if we allow the additional coupling between T^{ext} and T^{int}, we have to move to a MR-CC framework. Even the alternative of adding

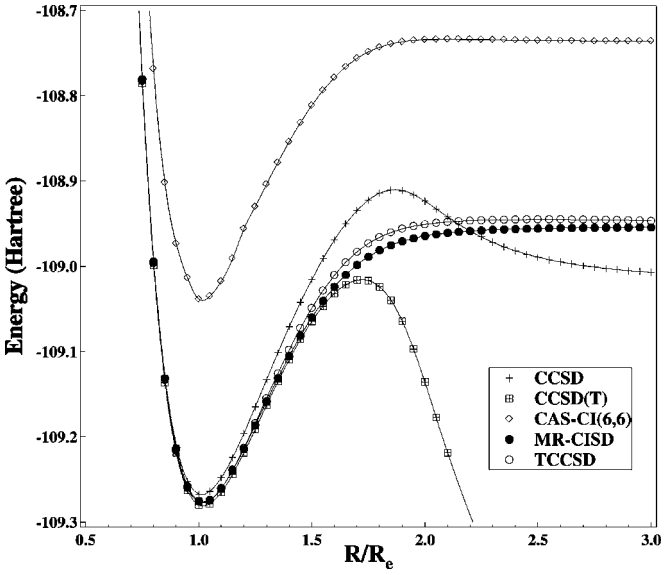

FIG. 29. Potential-energy curves for the N_2 molecule in the cc-pVDZ basis set. The horizontal axis represents the internuclear distance normalized by the equilibrium bond length (R_e =2.074 a.u.) (Kinoshita *et al.*, 2005).

some additional higher excitations in an augmented single reference approach is now quite limited, as there are 52 D_{2h} reference determinants in the six-orbital–six-electron CAS-CI for N_2.

It is clear that improvements on the basic single reference CC framework will have to arise from some kind of consideration of higher excitations, since $Q_n H \exp(T_1+T_2)P \neq 0$, $n>2$. This prohibits the equivalence shown in Eqs. (78)–(80). Of course, this is the basic idea of methods like CCSD(T), as discussed in Sec. V.E, but what other ways can this information be incorporated?

Another partial solution that has been suggested (Kowalski and Piecuch, 2000a) is to renormalize the SR-CC equations. The issue of renormalization might be approached from Eq. (75), where there is potentially a denominator. As shown in the derivation of CCSD(T) above, we used the connected expectation form for the energy without any denominator. However, we limited the numerator to just fourth-order terms. It might be argued that rather than cancelling the denominator completely from the equation, which leads to just connected terms in the numerator, we should retain the denominator to the same order as the numerator (Meissner and Bartlett, 2001). Once that is done, we have the general renormalized correction $\Delta E_R = \Delta E/(1+S)$ form, where S is an overlap and ΔE would be the triples correction, e.g., in CCSD(T). Expansion shows that $\Delta E_R = \Delta E - S\Delta E + S^2\Delta E - \cdots$. Clearly, except for the so-called EPV terms, which will arise as parts of linked diagrams, all such terms have unlinked character, just as $E^{(2)}\langle\Psi^{(1)}|\Psi^{(1)}\rangle$ did in our introductory fourth-order PT example in Sec. III. This violates size extensivity, the guiding principle of CC theory, which raises arguments about how far such methods should be pursued. However, in the limit of the full CC, the expression is exact. When quasidegeneracy is not present, $|S|<1$, but it grows rapidly as bonds are broken which offsets the fact that ΔE tends to go to minus infinity. This keeps the curve from turning over as in the N_2 and F_2 examples shown previously.

Many different kinds of approximations to this basic structure have been considered, termed renormalized and completely renormalized. To show just one, their CR-CCSD(T) correction (Kowalski and Piecuch, 2000b) is given by

$$\Delta E_{\text{CR-CCSD(T)}} = \frac{\langle 0|(\bar{T}_1+\bar{T}_2^\dagger)WR_3[W\exp(\bar{T}_1+\bar{T}_2)]_C|0\rangle}{\langle 0|[1+(\bar{T}_1^\dagger+\bar{T}_2^\dagger)(1+WR_3)]\exp(\bar{T}_1+\bar{T}_2)|0\rangle}, \quad (105)$$

where the denominator is composed of second- and third-order corrections (counting T_1 as first order) to accommodate the fourth-order terms in the numerator.

Although the details might be critical in finding the optimum way to renormalize, they all tend to have similar numerical behavior. For example, a different, but more easily evaluated one (Meissner and Bartlett, 2001) has

$$\Delta E_{R\text{-CCSD(T)}\{M\}} = \frac{\langle 0|(T_1^\dagger+\bar{T}_1^2/2+\bar{T}_2^\dagger)WR_3W\bar{T}_2|0\rangle}{\langle 0|[1+(\bar{T}_1^\dagger+\bar{T}_1^2/2+\bar{T}_2^\dagger)(1+WR_3)]\exp(\bar{T}_1+\bar{T}_2)|0\rangle}. \quad (106)$$

Results are shown for RHF reference N_2 compared to the full CI result in Fig. 30. Due to the denominator, the curve cannot turn over like the unmodified CCSD(T) did in Fig. 27(a). However, closer inspection of the two sets of curves shows that in the vicinity of the equilibrium geometry, the unmodified CC methods are superior to their renormalized versions. This is another manifestation of the size inextensivity of such models, which also guarantees that the vibrational frequencies obtained from some such model will not be nearly as good as the usual CC results. In fact, it can be argued that the size-extensive UHF-based CC results that can separate correctly are actually better for many applications.

If the denominator is limited to just provide EPV terms instead of more general denominators, then one can regain size extensivity. Some attempts at doing this have been considered (Kowalski and Piecuch, 2000b; Nooijen, 2005). The main objection to this approach is that when EPV parts of diagrams are retained, instead of the whole diagram that contains the EPV part (Bartlett and Musiał, 2006), the orbital invariance of CC methods is compromised. If localized orbitals are used,

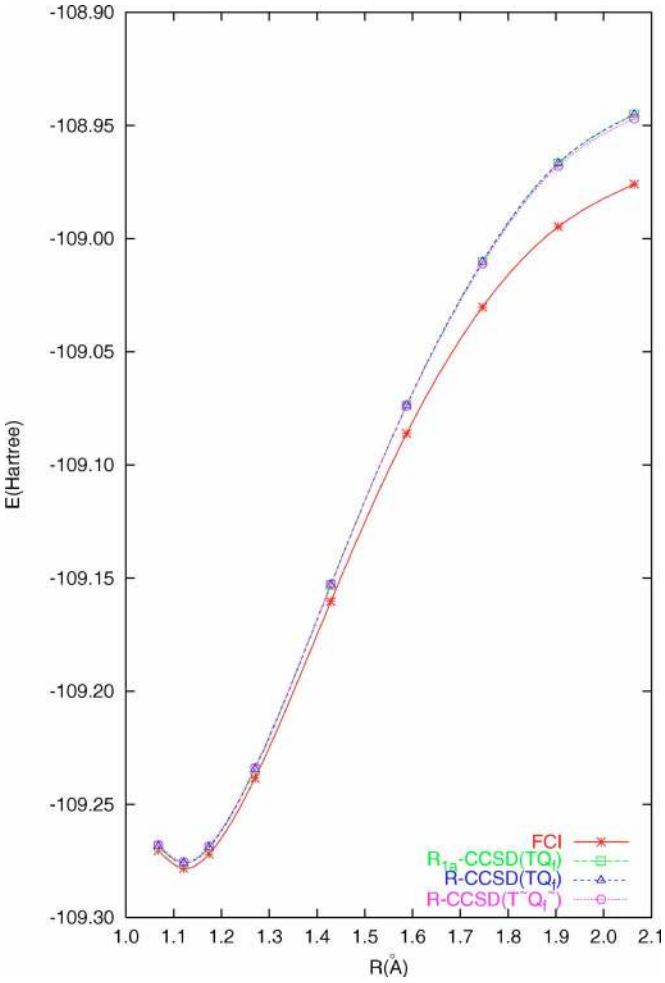

FIG. 30. (Color online) Potential-energy curves for the N_2 molecule in the cc-pVDZ basis set obtained with the FCI and R-CCSD(TQ_f) methods.

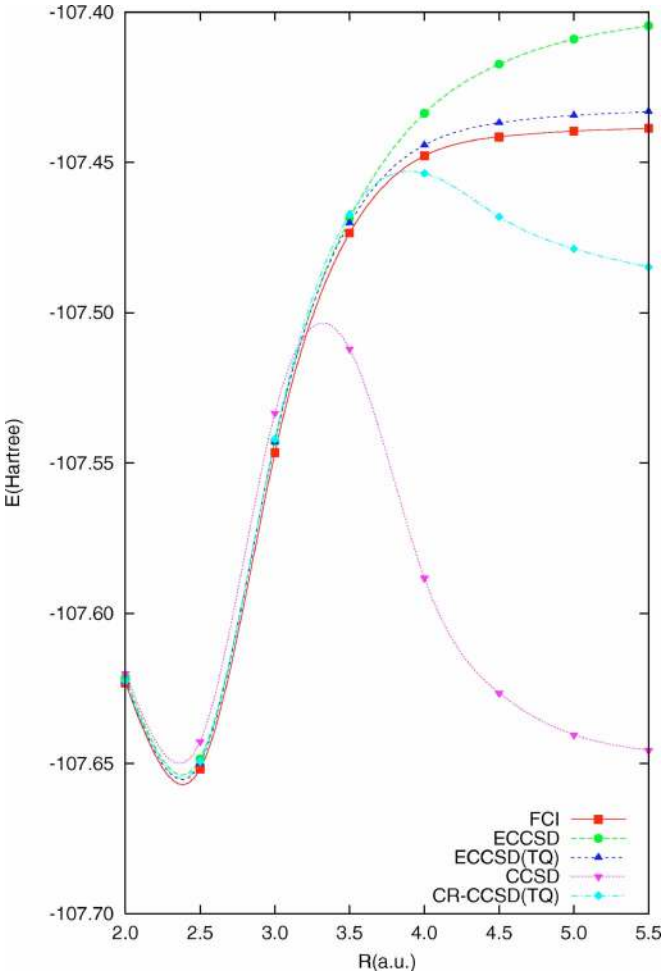

FIG. 31. (Color online) Potential-energy curves for the N_2 molecule in a STO-3G basis set obtained with the FCI, ECCSD, ECCSD(TQ), CCSD, and CR-CCSD(TQ) methods.

good virtually extensive results are obtained at separation, but a rotation of the orbitals destroys this behavior. Also, any particular choice of orbitals would have to apply at any R, and that further complicates the issue. So at this time, such renormalized CC approaches have significant formal limitations. There is also no denominator in iterative CC (like CCSDT-n) as opposed to noniterative CC approximations. So renormalization cannot be achieved by denominators, per se, but there is still room for other ways to exploit the higher $Q_n\bar{H}P$ equations such as by modification of the left-hand eigenvector of the CC functional (Moszyński *et al.*, 2005; Piecuch *et al.*, 2006).

Another possibility for a better description of bond breaking is offered by the so-called extended CC (ECC) method of Arponen and Bishop (Arponen, 1983; Arponen *et al.*, 1987a, 1987b). The main element of the ECC theory relies on using a double similarity transformation defined through two sets of amplitudes Σ and T. The ECC energy functional in the singles and doubles approximation (ECCSD) is expressed as

$$E(\mathrm{ECCSD}) = \langle 0|e^{\Sigma^\dagger} e^{-T} H e^{T} e^{-\Sigma^\dagger}|0\rangle, \tag{107}$$

where T is a standard cluster operator defined in Eqs. (26)–(29) and $\Sigma^\dagger$ is a deexcitation operator of the same cluster structure as $T^\dagger$,

$$\Sigma^\dagger = \Sigma_1^\dagger + \Sigma_2^\dagger \tag{108}$$

and

$$\Sigma_n^\dagger = \sum_{ij\cdots}^{ab\cdots} \sigma_{ab\cdots}^{ij\cdots} i^\dagger j^\dagger \cdots ba. \tag{109}$$

Taking advantage of the transformation (Arponen, 1983) and remembering that $\Sigma^\dagger|0\rangle = 0$, we may rewrite Eq. (107) as

$$E(\mathrm{ECCSD}) = \langle 0|[e^{\Sigma^\dagger}(He^{T})_c]_{\mathrm{dc}}|0\rangle, \tag{110}$$

where dc (doubly connected) indicates that the Σ operator is connected with H or at least two T operators. The double connectedness property ensures that the equations for Σ and T contain only connected contributions.

The usefulness of the ECCSD theory in the description of the bond-breaking situation has been considered

(Van Voorhis and Head-Gordon, 2000; Gwaltney *et al.*, 2002; Fan *et al.*, 2005). It can be observed from Fig. 31, taken from Fan *et al.* (2005), that the ECCSD curve shows correct behavior in the region of $2R_e$ unlike the standard variants such as CCSD or even renormalized versions with inclusion of the noniterative triples and quadruples CR-CCSD(TQ). Apparently the best curve is obtained by combining the so-called renormalized noniterative corrections with the ECCSD iterative solution (Fan *et al.*, 2005); see the ECCSD(TQ) curve in Fig. 31. It needs to be stressed, however, that the rigorous formulation of the ECC approach even in its simplest singles and doubles approximation is a complicated and costly method. One has to carry out simultaneous iterations of the two sets of the amplitude equations: Σ and T. The terms occurring in both equations are cumbersome and require a high-rank computational procedure. Some of the diagrams originating from the term $\langle\Phi_{ij}^{ab}|\Sigma_2^{\dagger 2}HT_2^4|0\rangle/48$ contributing to the T_2 amplitude after proper factorization scale as M^{10}, which is prohibitive for wider applications of the method. An inclusion of higher clusters, such as Σ_3 and T_3, which are necessary to obtain a method correct through fourth order of perturbation theory, is still more complex and only feasible in approximate versions.

VII. THE COUPLED-CLUSTER FUNCTIONAL AND THE TREATMENT OF PROPERTIES

A molecule has $3N-6$ vibrational degrees of freedom for N atoms, or, in terms of Cartesian forces that are most frequently obtained in calculations, $3N$ atomic derivatives. Absolutely essential to the wide range of CC applications that are made is the existence of analytical procedures to obtain the $3N$ forces, $\nabla E(\mathbf{R})=\mathbf{F}(\mathbf{R})$, to search a PES to determine the points where the forces vanish, which will give a molecule's structure and saddle points for transition states. Furthermore, to know that the molecule's geometry is indeed a minimum energy configuration requires the matrix of second derivatives, $\nabla\nabla E(\mathbf{R})$, the Hessian. This defines the harmonic force constants from which solution of the vibrational Schrödinger equation yields the vibrational frequencies. If at a point where $\mathbf{F}(\mathbf{R})=0$ all frequencies are real, then the geometry on the PES is a minimum, while if only one is imaginary, then we have a saddle point that corresponds to a transition state on a reaction coordinate. Without some procedure to evaluate the forces in about the same amount of time as the wave function and energy at a point, applications of theory to PES for polyatomic molecules would be hopeless. The fact that today this can be done for CC theory (Adamowicz *et al.*, 1984; Bartlett, 1986; Scuseria *et al.*, 1987; Salter *et al.*, 1989) is critical to its role as the reference method for most molecular applications.

The essential new idea required can be readily derived in a few steps. We know that the CC energy at each point of a PES is $E(\mathbf{R})P=P\bar{H}(\mathbf{R})P$. If we differentiate it with respect to $\mathbf{R}$, we obtain the forces. The key, then, is to arrange this expression for the forces into a computationally convenient form that can be evaluated in about the same amount of time as can the wave function itself. This is done through the following steps:

$$E(\mathbf{R})P = P\bar{H}(\mathbf{R})P, \tag{111}$$

$$\nabla E(\mathbf{R})P = P\nabla\bar{H}(\mathbf{R})P, \tag{112}$$

$$\nabla E(\mathbf{R})P = P\exp(-T)[\nabla H(\mathbf{R})]\exp(T)P + P[\bar{H},\nabla T(\mathbf{R})]P \tag{113}$$

$$= P\overline{\nabla H}(\mathbf{R})P + P\bar{H}(P+Q)\nabla T(\mathbf{R}) - \nabla T(\mathbf{R})(P+Q)\bar{H}P \tag{114}$$

$$= P\overline{\nabla H}(\mathbf{R})P + P\bar{H}Q\nabla T(\mathbf{R})P, \tag{115}$$

where after inserting the resolution of the identity $1=P+Q$, the last line uses the fact (i) that $\nabla T(\mathbf{R})$ has to correspond to an excitation from the reference determinant $|0\rangle$ or the P space, $P=|0\rangle\langle 0|$, to its orthogonal complement Q; and (ii) that $Q\bar{H}P=0$ by virtue of the CC equations being solved; the bar over the operator indicates its similarity transformed form $\bar{H}=e^{-T}He^{T}$, Eq. (58). We also need to consider the derivative of the amplitude equations $Q\bar{H}P=0$, which gives

$$Q\overline{\nabla H}(\mathbf{R})P + Q[\bar{H},\nabla T(\mathbf{R})]P = 0. \tag{116}$$

Again inserting the resolution, we can write

$$Q\overline{\nabla H}(\mathbf{R})P + Q[\bar{H}(P+Q)\nabla T(\mathbf{R}) - \nabla T(\mathbf{R})(P+Q)\bar{H}]P = 0, \tag{117}$$

$$Q\overline{\nabla H}(\mathbf{R})P + Q[\bar{H}Q\nabla T(\mathbf{R}) - \nabla T(\mathbf{R})P\bar{H}]P = 0. \tag{118}$$

The form of the last term can be recognized as that from first-order perturbation theory, since we have

$$(E - Q\bar{H}Q)\nabla T(\mathbf{R}) = Q\overline{\nabla H}(\mathbf{R})P, \tag{119}$$

$$\nabla T(\mathbf{R}) = (E - Q\bar{H}Q)^{-1}Q\overline{\nabla H}(\mathbf{R})P, \tag{120}$$

$$\nabla T(\mathbf{R}) = \mathcal{R}Q\overline{\nabla H}(\mathbf{R})P, \tag{121}$$

where we introduced the resolvent operators for $\bar{H}$, $\mathcal{R}$. Inserting this into the energy formula and defining $\Lambda=P\overline{\nabla H}\mathcal{R}Q$ leads to

$$\nabla E(\mathbf{R}) = \langle 0|(1+\Lambda)\overline{\nabla H}(\mathbf{R})|0\rangle. \tag{122}$$

The quantity Λ is independent of the $3N$ perturbations. Notice also that it is a deexcitation operator, as $\Lambda=P\Lambda Q=\Sigma_{i<j<\cdots<a<b<\ldots}\lambda_{ab\ldots}^{ij\cdots}\{i^{\dagger}aj^{\dagger}b\cdots\}$. It is also essential to recognize that $\overline{\nabla H}(\mathbf{R})=\exp(-T)\nabla H\exp(T)$ has removed any T dependence from the gradient, leaving

only the gradient of the Hamiltonian. Hence, combining these features we have a generalized Hellman-Feynman formula for the forces. If we specify to a single degree of freedom $\partial/\partial X_\alpha$, the formula becomes

$$E^\alpha(\mathbf{R}) = \langle 0|(1+\Lambda)\bar{H}^\alpha(\mathbf{R})|0\rangle. \tag{123}$$

This can be viewed as a generalization of the interchange theorem of double perturbation theory (Dalgarno and Stewart, 1958; Bartlett, 2004).

We can further generalize Eq. (123) using the integral Hellman-Feynman theorem, which simply means integrate the above expression to give the CC functional $E = \int_0^{\mathbf{R}} (\partial E/\partial \mathbf{R}) d\mathbf{R}$,

$$E(\mathbf{R}) = \langle 0|(1+\Lambda)\bar{H}|0\rangle. \tag{124}$$

The functional is a very important quantity in CC theory. As shown here, it arises as a natural consequence of simply asking for energy derivatives along with the energy (Adamowicz *et al.*, 1984; Bartlett, 1986; Salter *et al.*, 1989). From another viewpoint, it arises from a generalization of CC theory, where NCC (meaning normal CC in this designation) would be the usual CC equations and adding Λ is viewed as an extension (Arponen *et al.*, 1987a). A third way to obtain this formula is to introduce constraints via a Lagrangian multiplier when deriving the CC gradient equations (Koch *et al.*, 1990; Szalay *et al.*, 1993). The functional immediately shows that $\delta E/\delta\Lambda = 0$ gives the CC equations, $Q\bar{H}P = 0$, and variation with respect to T gives the Λ equations,

$$P\Lambda Q\bar{H}Q + P\bar{H}Q - EP\Lambda Q = 0, \tag{125}$$

$$P[\Lambda,\bar{H}]Q + P\bar{H}Q + P\bar{H}Q\Lambda Q = 0. \tag{126}$$

Note that Eq. (125) has E in it, as it is CI-like and linear in Λ. This leads to disconnected contributions to the Λ_2 equations, as shown in Fig. 32. The second form of the Λ equations formally eliminates E by introducing the commutator and facilitates its diagrammatic derivation. Figure 32 presents the skeleton (undirected diagrams) for Λ_1 and Λ_2 in the CCSD approximation. Through linear terms in T, $\Lambda = T^\dagger$.

The functional also allows the immediate definition of CC one-particle and two-particle response density matrices as

$$\gamma_{pq} = \langle 0|(1+\Lambda)e^{-T}\hat{p}^\dagger\hat{q}e^T|0\rangle, \tag{127}$$

$$\Gamma_{pqrs} = \langle 0|(1+\Lambda)e^{-T}\hat{p}^\dagger\hat{q}^\dagger\hat{s}\hat{r}e^T|0\rangle. \tag{128}$$

Notice that these density matrices apply equally well to methods like CCSD(T) that do not have associated wave functions. This is very different from that in ordinary quantum mechanics where the density matrix is defined as an expectation value of the wave function. It is true, however, that $\gamma_{pq} = \langle 0|e^{T^\dagger}\hat{p}^\dagger\hat{q}e^T|0\rangle/\langle 0|e^{T^\dagger}e^T|0\rangle$ in the limit

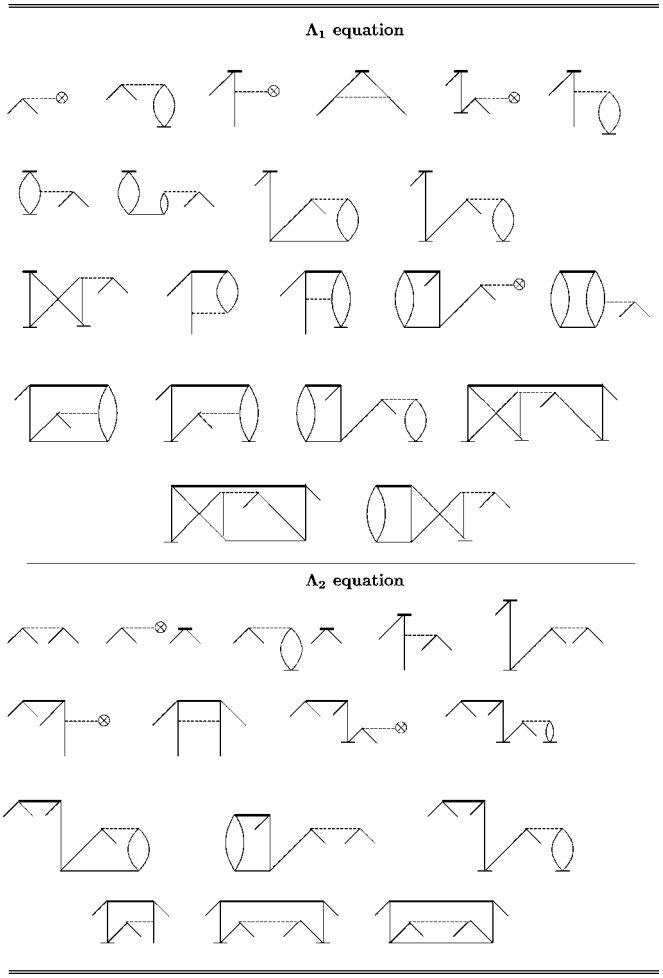

FIG. 32. Skeleton diagrams for the Λ_1 and Λ_2 equations for CCSD.

of all T_n, and similarly for the two matrix; but the expectation value is an infinite series and the Λ-based expression is always in closed form. In second-order perturbation theory, the two forms are equivalent. Detailed expressions for the particular blocks of the one-particle density matrix can be derived from the diagrams given in Fig. 33. For example, the particle-particle block can be expressed as [Fig. 33(a)] $\gamma_{ab} = \Sigma_m \lambda_a^m t_m^b + \frac{1}{2}\Sigma_{mne}\lambda_{ea}^{mn} t_{mn}^{eb} + \Sigma_{mne}\lambda_{ea}^{mn} t_m^e t_n^b$. Similar expressions correspond to the remaining blocks of γ. Using the same diagram rules, we can readily write down the response correlation corrections for the CC density matrices from just the normal ordered parts $\{\hat{p}^\dagger\hat{q}\}$, $\{\hat{p}^\dagger\hat{q}^\dagger\hat{s}\hat{r}\}$ of the density matrix operators. See Shavitt and Bartlett (2006) for the details. Most first-order properties, meaning those defined by first-order perturbation theory where a one-particle operator $\hat{h}^\alpha$ is added to the one-particle part of the Hamiltonian $\hat{h} + \hat{h}^\alpha$ (like moments, field gradients, etc.), arise from the generalized expectation value,

$$\bar{h}^\alpha = \langle 0|(1+\Lambda)e^{-T}\hat{h}^\alpha e^T|0\rangle, \tag{129}$$

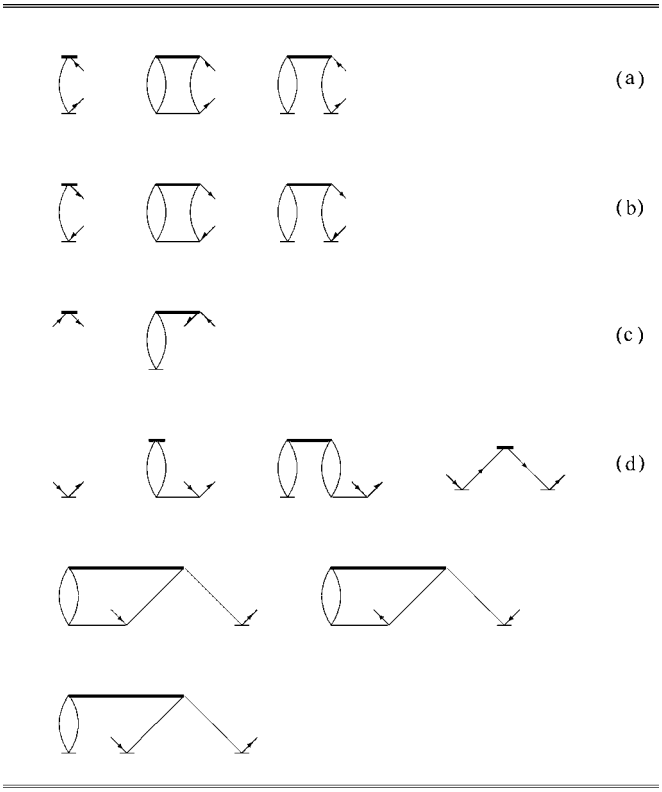

FIG. 33. Diagrams representing the one-particle reduced density matrix for CCSD: (a) particle-particle elements, (b) hole-hole elements, (c) hole-particle elements, and (d) particle-hole elements.

$$\bar{h}^{\alpha} = \sum_{p,q} \gamma_{pq} h^{\alpha}_{pq}, \tag{130}$$

and can be readily evaluated to quite high accuracy by CCSD and its modifications due to triples (Bartlett, 1995).

However, though any CCSD and higher approximation benefits from the fact that $|0\rangle = \exp(T_1)|\Theta\rangle$ relates two determinants and introduces substantial orbital insensitivity, the response density matrices do not explicitly contain the effects of orbital relaxation that occur for the reference determinant problem, which by virtue of changing the orbitals propagates through the correlation calculation. That is, it allows the occupied and virtual orbitals in the reference function to change to accommodate a perturbation due to h^{α}. For example, if $h^{\alpha} = \Sigma_{p,q}\langle p|z|q\rangle p^{\dagger}q$, which would be the z component of a perturbation due to a static electric field, the orbitals that define the Fermi vacuum would be changed by this perturbation. Such changes are normally introduced into the theory by orbital perturbation theory. That is, assuming a HF reference determinant one seeks the solution of the coupled-perturbed Hartree-Fock equations to define $\boldsymbol{\phi}^{\alpha} = \boldsymbol{\phi}\mathbf{d}^{\alpha}$, subject to $\langle \phi^{\alpha}|\phi\rangle + \langle \phi|\phi^{\alpha}\rangle = 0$. Each orbital equation written in terms of the unperturbed and perturbed Fock operators is

$$(\epsilon_p^{(0)} - \hat{f}^{(0)})\phi^{\alpha} = (\hat{f}^{\alpha} - \epsilon_p^{\alpha})\phi^{(0)}. \tag{131}$$

Expanding out the Fock operators and isolating the particular coefficient, the CPHF equations can be written in terms of the familiar **A** and **B** matrices from RPA (TDHF) theory,

$$(\mathbf{A} + \mathbf{B})\mathbf{d}^{\alpha} = -\mathbf{h}^{\alpha}, \tag{132}$$

$$A_{ai,bj} = (\epsilon_a - \epsilon_i)\delta_{ij}\delta_{ab} - \langle aj||bi\rangle, \tag{133}$$

$$B_{ai,bj} = \langle ab||ij\rangle. \tag{134}$$

Note that here too, we run into the problem of computing every $\mathbf{d}^{\alpha}$ unless we once again use the interchange theorem (Dalgarno and Stewart, 1958) by formally taking the inverse of $(\mathbf{A}+\mathbf{B})^{-1}$, the resolvent operator in CPHF theory, to isolate $\mathbf{d}^{\alpha}$ (Handy and Schaefer, 1984). Then putting this together with Eq. (123), we can isolate all effects of the true operator to define a MO relaxed density matrix D_{pq} such that we evaluate a property as

$$\bar{h}^{\alpha} = \sum_{p,q} h^{\alpha}_{pq} D_{pq}. \tag{135}$$

This density matrix obviously accounts for the appropriate orbital relaxation regardless of what the actual $\hat{h}^{\alpha}$ might be.

The most general kind of first-order property is the analytical gradient problem, which adds a third element that arises from the changes in the finite AO basis for the problem. For such a property, the first-quantized operator $h^{\alpha} = \partial h/\partial X^{\alpha}$ and the second-quantized form will add, in addition to the changes in the MO coefficients that introduce orbital relaxation, changes in the AO basis functions, as they follow the atoms in the molecule. That is, H_N^{α} is

$$H^{\alpha}(\mathbf{R}_0) = \sum_{p,q} \partial/\partial X_{\alpha}\langle p|f|q\rangle_{\mathbf{R}_0}\{p^{\dagger}q\} + \tfrac{1}{4}\sum_{pqrs} \partial/\partial X_{\alpha}\langle pq||rs\rangle\rangle_{\mathbf{R}_0}\{p^{\dagger}q^{\dagger}sr\} \tag{136}$$

and then

$$(\partial/\partial X_{\alpha})\phi_p(\mathbf{R}) = \sum_{\mu} (\partial/\partial X_{\alpha})\chi_{\mu}(\mathbf{R})\rangle_{\mathbf{R}_0} c_{\mu p}(\mathbf{R}_0) + \sum_{\mu} \chi_{\mu}(\mathbf{R}_0)(\partial/\partial X_{\alpha})c_{\mu p}(\mathbf{R})\rangle_{\mathbf{R}_0} \tag{137}$$

$$= \sum_{\mu} (\partial/\partial X_{\alpha})\chi_{\mu}(\mathbf{R})\rangle_{\mathbf{R}_0} c_{\mu p}(\mathbf{R}_0) + \sum_{q\neq p} \phi_q(\mathbf{R}_0)(\partial/\partial X_{\alpha})d_{qp}(\mathbf{R})\rangle_{\mathbf{R}_0}, \tag{138}$$

$$\phi^{\alpha} = \sum_{\mu} \chi_{\mu}^{\alpha}(\mathbf{R})]_{\mathbf{R}_0} c_{\mu p}(\mathbf{R}_0) + \sum_{q} \phi_q(\mathbf{R}_0) d_{qp}^{\alpha}(\mathbf{R})]_{\mathbf{R}_0}. \tag{139}$$

In any analytical gradient calculation where we choose to use a basis set of atomic orbital functions attached to the atoms, we have to compute all the one- and two-electron atomic orbital integrals at each $\mathbf{R}$ to account for the AO derivative term. This, however, is simply an $\sim M^4$ calculation, which is much faster than the CC calculation itself. The CPHF problem now has to be slightly modified to accommodate the new terms that arise from the AO derivatives, and those also affect the HF (reference) part of the analytical gradient calculation. Incorporated within the most general D_{pq} are the two interchange theorems, one to avoid T^{α} and the other to avoid $\mathbf{d}^{\alpha}$. Only with both does the analytical gradient formula assume a form that permits a computationally convenient evaluation of all $3N$ gradients for a CC wave function in about the same amount of time as the CC calculation itself. The evaluation of Λ, as a linear equation, is somewhat faster than that for T, while the additional evaluation of the derivative integrals adds overhead and, if they are stored rather than recomputed for a displacement, substantial disk space requirements. The rather involved analysis that leads to these final CC derivative equations is presented in detail elsewhere (Salter *et al.*, 1989; Shavitt and Bartlett, 2006). Analytical second derivatives were formulated some years ago (Salter and Bartlett, 1989), with an implementation by Gauss and Stanton (2002). Stanton and Gauss have also implemented analytical derivatives for excited states (Stanton and Gauss, 1995), as discussed in Sec. VIII.

Before we finish this section, we reconsider noniterative triple and quadruple excitation corrections to CC based upon the CC functional (Kucharski and Bartlett, 1998a; Crawford and Stanton, 1998) instead of the CC expectation value. First we assume an underlying CCSD solution and then isolate all terms that would depend upon T_3 or Λ_3,

$$E_T^{[4]} = \langle 0|\Lambda_3(H_0 T_3^{[2]})_C + \Lambda_3(W T_2^{[2]})_C + \Lambda_2(W T_3^{[2]})_C + \Lambda_1(W T_3^{[2]})_C + \Lambda_2(f_{vo} T_3^{[2]})_C|0\rangle.$$

Then using the fact that the $T_3^{[2]}$ amplitudes are defined by $\Lambda_3[(H_0 T_3^{[2]})_C + (W\bar{T}_2)_C]|0\rangle = 0$, we are left with

$$E_T^{[4]} = \langle 0|\Lambda_2(W T_3^{[2]})_C + \Lambda_1(W T_3^{[2]})_C + \Lambda_2(f_{vo} T_3^{[2]})_C|0\rangle.$$

The Λ-based diagrams are basically the same as those for CCSD(T) except that the top vertex represents Λ and because of the different symmetry we cannot further simplify the first term. So finally the diagrammatic terms are

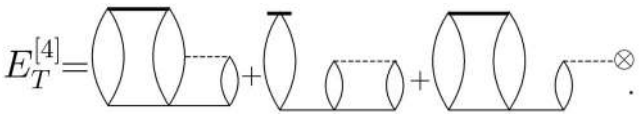

This ΛCCSD(T) modification has been proposed (Crawford and Stanton, 1998; Kucharski and Bartlett, 1998a) and shown to have prospects of being a better approximation than CCSD(T).

Starting from CCSDT and doing precisely the same thing for Λ_4 and $T_4^{[3]}$, and recognizing that $\Lambda_4[(H_0 T_4^{[3]})_C + (W\bar{T}_2^2/2)_C + (W\bar{T}_3)_C]|0\rangle = 0$, we have

$$E_Q = \langle 0|\Lambda_3(W T_4^{[3]})_C + \Lambda_2(W T_4^{[3]})_C + \Lambda_3(f_{\mathrm{vo}} T_4^{[3]})_C|0\rangle$$

or in diagrammatic form as

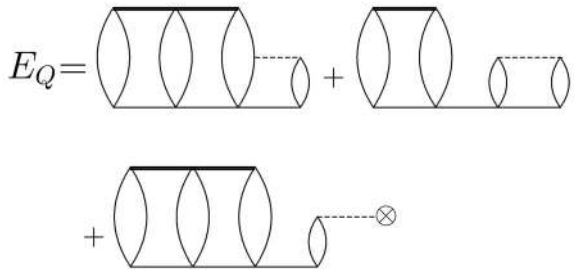

to define ΛCCSDT(Q). Unlike ΛCCSD(T), which only contains (generalized) fourth-order corrections, ΛCCSDT(Q) has both fifth- and sixth-order terms. This makes the rate-determining step $\sim n^4 N^5$ compared to $\sim n^3 N^4$ for the triple variant. If the (second diagram) fifth-order term itself is separated ΛCCSDT(Q_f), then as shown in Sec. VI it can be factorized into an $\sim n^2 N^5$ term for Q_f. Odd-order contributions, however, tend to be less stable than those based on even orders of perturbation theory. See Hirata, Fan, *et al.* (2004a) for a nonfactorized fifth-order approximation and Bomble *et al.* (2005) for a sixth-order approximation. The latter replaces Λ in the above diagrams by $T^{\dagger}$.

VIII. EQUATION-OF-MOTION COUPLED-CLUSTER METHOD FOR EXCITED, IONIZED, AND ELECTRON ATTACHED STATES

A convenient approach to excited states in CC theory is offered by the equation-of-motion (EOM-CC) method, whose basic ideas were presented in *Reviews of Modern Physics* (Rowe, 1968). The general idea was used in various quantum chemical contexts (Dunning and McKoy, 1967; Simons and Smith, 1973; McCurdy *et al.*, 1982).

It derives from simultaneously considering two Schrödinger equations, one for an excited state k and one for a ground or reference state,

$$H\Psi_k = E_k \Psi_k, \tag{140}$$

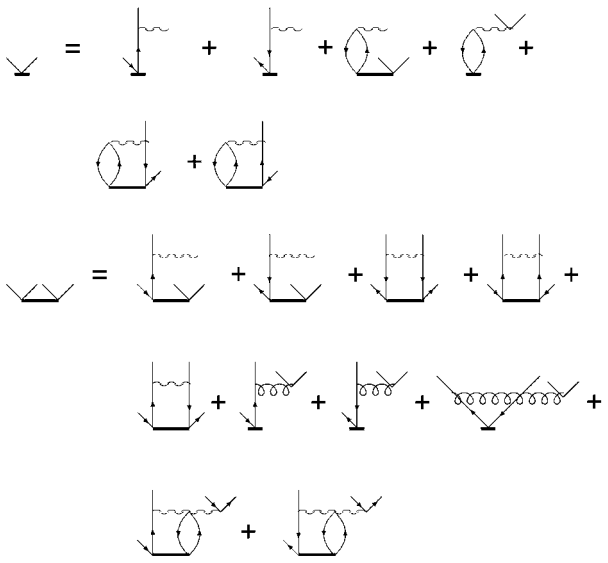

FIG. 34. Diagrammatic form of the EE-EOM-CCSD equations.

$$H\Psi_0 = E_0\Psi_0. \tag{141}$$

We introduce an operator Ω_k, such that it will create the excited state from the reference state,

$$\Psi_k = \Omega_k\Psi_0, \tag{142}$$

and after subtracting one equation from the other, and left multiplying by Ω, we obtain

$$[H,\Omega_k]\Psi_0 = \omega_k\Omega_k\Psi_0, \tag{143}$$

$$\omega_k = E_k - E_0. \tag{144}$$

At this point there are two decisions to make: what to choose for Ω_k and what to choose for Ψ_0. Answering the second question first, we want Ψ_0 to be a CC wave function $\Psi_0=\exp(T)|0\rangle$ (Emrich, 1981). The simplest option for Ω_k, if we want to create an electronic excited state, is to make it an excitation operator,

$$\Omega_k = \hat{R}_k = r_0(k) + \sum_{a,i} r_i^a(k)\{ai\} + \sum_{a>b,i>j} r_{ij}^{ab}(k)\{a^\dagger ib^\dagger j\} + \cdots \tag{145}$$

as we know that has to give the exact excited-state wave function. Also as an excitation operator, $[\Omega,T]=0$. Hence, using the CC wave function for the reference state, the EOM Eq. (143) becomes (Sekino and Bartlett, 1984; Geertsen *et al.*, 1989)

$$[\bar{H},R_k]|0\rangle = \omega_k R_k|0\rangle, \tag{146}$$

$$(\bar{H}R_k)_C|0\rangle = \omega_k R_k|0\rangle, \tag{147}$$

$$(\bar{\mathbf{H}}\mathbf{R}_k) = \mathbf{R}_k\omega_k, \tag{148}$$

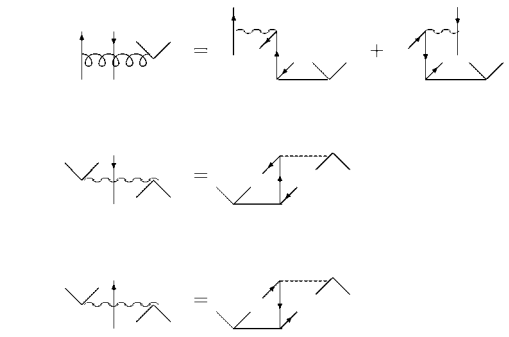

FIG. 35. Diagrammatic form of the three-body elements of $\bar{H}$ used in the EE-EOM-CCSD equations.

$$(\bar{\mathbf{H}}\mathbf{R})_C = \mathbf{R}\omega. \tag{149}$$

We use the symbol R_k for the operator (not to be confused with the resolvents from earlier) to indicate that it is a right-hand eigenvector because the matrix $\bar{\mathbf{H}} = \langle\mathbf{h}|e^{-T}He^T|\mathbf{h}\rangle$, where $|\mathbf{h}\rangle$ is the excitation manifold, is non-Hermitian. Limiting R_k to single and double excitations, $|\mathbf{h}\rangle=|\mathbf{h}_1\mathbf{h}_2\rangle$, defines EOM-CCSD (Comeau and Bartlett, 1993; Stanton and Bartlett, 1993b; Geertsen *et al.*, 1989) (see Figs. 34 and 35).

For the $\bar{\mathbf{H}}\mathbf{R}$ product diagrams, the EOM-CCSD matrix will have a rank of $\sim n^2N^2+nN$. For the $n=10$, $N=100$ example from earlier, we would have to extract eigenvalues and vectors for a matrix with a rank of a million. Adding triples to define EOM-CCSDT, it becomes a billion. In a typical problem, about 20 or so roots are obtained using large-scale non-Hermitian generalizations of Lanczos-type methods (Davidson, 1975; Hirao and Nakatsuji, 1982).

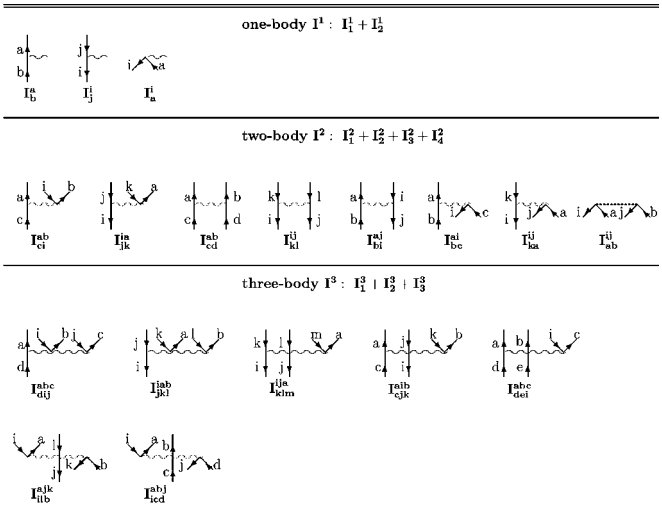

FIG. 36. The diagrammatic representation of the one-, two-, and three-body elements of $\bar{H}$.

The diagrammatic form of the $\bar{H}$ elements is composed of 1, 2, 3, 4, and higher particle number operators, $\bar{H}=\Sigma_{k=0}^{2}I_k^1+\Sigma_{k=0}^{4}I_k^2+\Sigma_{k=0}^{3}I_k^3+\Sigma_{k=0}^{3}I_k^4+\cdots$. The quantity I_k^n means an n-body element, while subscript k indicates that there are k annihilation lines (or k second-quantized annihilation operators). Due to the two-body nature of the electronic interaction, we have the relation that $k\leqslant 3$. Formally we can consider $k=4$, but in this case the intermediate I_4^2 is reduced to the two-electron integral. All are shown in Fig. 36. The $\bar{H}$ elements that represent a complete set of diagrammatic contributions are indicated by a wiggly line. Elsewhere we present the general formulas for the number of the diagrams contributing to the $\bar{H}$ elements (Musiał *et al.*, 2002a) and the number of diagrammatic terms occurring in the complete form of the I_k^n element for $n=1$, 2, 3, and 4.

In EOM-CC we can also consider excited states as those that correspond to an ionization into orbital a, where a is considered to be in the continuum. In the sudden approximation an electron in a continuum plane-wave orbital has no interaction with those in the bound, square-integrable orbitals. This makes the operator that ionizes the electron from the mth orbital become

$$\hat{R}_k=\sum_m r_m(k)\{m\}+\sum_{b,m>i} r_{im}^a(k)\{b^\dagger im\}+\cdots, \tag{150}$$

where we have one-hole and two-hole one-particle operators in the equivalent, IP-EOM-CCSD, approximation. We can equally well do an electron attachment, i.e., bring in an electron from the continuum,

$$\sum_a r^a(k)\{a^\dagger\}+\sum_{a>b,i} r_i^{ab}(k)\{a^\dagger b^\dagger i\}+\cdots, \tag{151}$$

to define an EA-EOM-CCSD approximation. Triple excitation operators introduce three-hole, two-particle and three-particle, two-hole operators (Musiał and Bartlett, 2003; Musiał *et al.*, 2003), respectively. We can consider double ionization, electron attachment (Nooijen and Bartlett, 1997c), etc., processes as we are simply exploiting the Fock space structure of the theory to obtain eigenvectors and eigenvalues for any sector of Fock space.

Since the matrix $\bar{\mathbf{H}}$ is not Hermitian, it also has left-hand eigenvectors, $\langle 0|\hat{L}_k$, with the same eigenvalue. That is,

$$\langle 0|\hat{L}_k\bar{\mathbf{H}}=\langle 0|\hat{L}_k\omega_k, \tag{152}$$

$$\mathbf{L}\bar{\mathbf{H}}=\boldsymbol{\omega}\mathbf{L}. \tag{153}$$

These are chosen to be normalized such that $\langle 0|\hat{L}_k\hat{R}_l|0\rangle=\delta_{kl}$. Unlike the right-hand eigenvector, the left-hand one is not necessarily connected to $\bar{H}$. We now should realize that the ground-state CC functional is simply a special case of the EOM-CC problem for excited states, as $L_0=(1+\Lambda)$ and $R_0=1$. So EOM-CC simply extends the concept into any stationary state.

To complete the specification of the excited state k, we require the corresponding density matrix, which in the EOM-CC framework is

$$\gamma_{pq}^k=\langle 0|\hat{L}_k e^{-T}p^\dagger q e^T\hat{R}_k|0\rangle \tag{154}$$

just as was used for the ground state. For oscillator strengths, we also require the transition density matrix

$$\gamma_{pq}^{kl}=\langle 0|\hat{L}_k e^{-T}p^\dagger q e^T\hat{R}_l|0\rangle, \tag{155}$$

which provides the dipole strength,

$$|\mu_{pq}^{kl}|^2=\langle 0|\hat{L}_k e^{-T}r_{pq}p^\dagger q e^T\hat{R}_l|0\rangle\langle 0|\hat{L}_l e^{-T}r_{pq}p^\dagger q e^T\hat{R}_k|0\rangle, \tag{156}$$

that gives the intensity of the transition. This is preferred since the individual transition density matrices are not self-adjoint in EOM-CC.

An alternative development of the excited-state problem is offered by the time-dependent linear-response CC method (Monkhorst, 1977), sometimes called CCLR (Sekino and Bartlett, 1984; Koch and Jörgensen, 1990). From this viewpoint, instead of dealing with stationary states, which are a characteristic of EOM-CC, one starts with the time-dependent Schrödinger equation and seeks the frequency-dependent polarizability. From its poles, one obtains the same EOM-CC excitation energies. The residue at the pole provides the dipole strength. However, there are some differences between the treatment of properties like dipole strengths in the CCLR compared to the EOM treatment outlined above. A discussion with applications of EOM-CC to the dynamic polarizability addresses these, formally and numerically (Rozyczko *et al.*, 1997; Sekino and Bartlett, 1999). A related approach to EOM-CC and CCLR is the SAC-CI method (Nakatsuji, 1978) whose differences are discussed elsewhere (Bartlett, 2005).

When any EOM-CC state is determined from a closed-shell reference CC calculation, whether singlet, doublet, or triplet, it too will be a spin eigenstate. When EOM-CC is used relative to an open-shell reference, that is not necessarily the case, but a measure of $\langle 0|\hat{L}_k\exp(-T)\hat{S}^2\exp(T)\hat{R}_k|0\rangle$ will typically show that the spin contamination is minor except for pathological cases. For ROHF-based EOM-CC calculations of excitation energies starting from the open-shell reference determinant, the approach of Szalay and Gauss (2000), though computationally based upon spin-orbital equations, returns an exact spin target state. This procedure thereby maintains the attractive generality of the underlying spin-orbital framework of CC theory presented in this review.

Other properties of interest that are amenable to EOM-CC are second-order properties, which means that they arise from second-order perturbation theory instead of first-order properties discussed in the last section that come from the generalized expectation value. For second-order properties, we require the first-order perturbed wave function and cannot make the simplifications made for first derivatives. Consequentially, for

some perturbation $\Sigma_\alpha \mu h^\alpha + \frac{1}{2}\Sigma_{\alpha,\beta}\mu^2 h^{\alpha\beta}$, we have from second-order perturbation theory that ($\Psi_{CC}=\Psi_{CC}^{(0)}$)

$$E^{\alpha\beta} = \langle \Psi_{CC}|h^{\alpha\beta}|\Psi_{CC}\rangle + \langle \Psi_{CC}|h^\alpha - E^\alpha|\Psi^\beta\rangle + \langle \Psi_{CC}|h^\beta - E^\beta|\Psi^\alpha\rangle, \tag{157}$$

$$|\Psi^\alpha\rangle = \mathcal{R}e^{-T}h^\alpha e^T|0\rangle = \mathcal{R}\bar{h}^\alpha|0\rangle, \tag{158}$$

$$E^{\alpha\beta} = \langle 0|(1+\Lambda)\bar{h}^{\alpha\beta}|0\rangle + \langle 0|(1+\Lambda)(\bar{h}^\alpha - E^\alpha)\mathcal{R}\bar{h}^\beta|0\rangle + \langle 0|(1+\Lambda)(\bar{h}^\beta - E^\beta)\mathcal{R}\bar{h}^\alpha|0\rangle = \langle 0|(1+\Lambda)\bar{h}^{\alpha\beta}|0\rangle + \Delta E^{\alpha\beta}. \tag{159}$$

Use was made that the left-hand eigenvector $\langle \Psi_{CC}| = \langle 0|(1+\Lambda)e^{-T}$. Note the contribution of the second-order $h^{\alpha\beta}$ perturbation is a generalized expectation value. For the other two terms, we use the resolvent $\mathcal{R}$, introduced in Sec. VII,

$$\mathcal{R} = Q(E-\bar{H})^{-1}Q. \tag{160}$$

Since we know the eigenfunctions of $\bar{H}$ consist of $\{\langle 0|L_k$ and $R_k|0\rangle\}$, to refer the resolvent to the general state CC solution instead of the $|0\rangle$ reference implicit in $\mathcal{R}$, we have to exclude the left- and right-hand reference functions to define a modified resolvent $\tilde{R}_0$,

$$\tilde{R}_0 = \mathcal{R} - |0\rangle\langle 0|(1+\Lambda) = \sum_{k\neq 0}\frac{\hat{R}_k|0\rangle\langle 0|\hat{L}_k}{\omega_k}. \tag{161}$$

This enables representing the perturbed CC wave function in a generalized sum-over-states (SOS) form (Sekino and Bartlett, 1999),

$$\Delta E^{\alpha\beta} = \sum_k [\langle 0|(1+\Lambda)(\bar{h}^\alpha - E^\alpha)\hat{R}_k|0\rangle\omega_k^{-1}\langle 0|\hat{L}_k\bar{h}^\beta|0\rangle + \langle 0|(1+\Lambda)(\bar{h}^\beta - E^\beta)\hat{R}_k|0\rangle\omega_k^{-1}\langle 0|\hat{L}_k\bar{h}^\alpha|0\rangle], \tag{162}$$

to make the connection with ordinary perturbation theory. In practice, there can be no meaningful evaluation by using the SOS form, which for the examples we have discussed even at the EOM-CCSD level easily have $>10^6$ states. So, in practice, to avoid evaluation of the inverse resolvent, one solves the linear equation (Stanton and Bartlett, 1993a)

$$\begin{bmatrix} \langle \mathbf{h}_1|E-\bar{H}|\mathbf{h}_1\rangle & \langle \mathbf{h}_1|E-\bar{H}|\mathbf{h}_2\rangle \\ \langle \mathbf{h}_2|E-\bar{H}|\mathbf{h}_1\rangle & \langle \mathbf{h}_2|E-\bar{H}|\mathbf{h}_2\rangle \end{bmatrix}\begin{bmatrix} \mathbf{C}_1^\alpha \\ \mathbf{C}_2^\alpha \end{bmatrix} = \begin{bmatrix} \langle \mathbf{h}_1|(1+\Lambda)\bar{h}^\alpha|0\rangle \\ \langle \mathbf{h}_2|(1+\Lambda)\bar{h}^\alpha|0\rangle \end{bmatrix},$$

which can be accomplished much more efficiently using the same kind of numerical methods employed for the diagonalization of the EOM-CC equations, to get solutions for $\mathbf{C}^\alpha$. The second-order property can then be conveniently obtained from the matrix product

$$\Delta E^{\alpha\beta} = \langle 0|(1+\Lambda)(\bar{h}^\alpha - E^\alpha)|\mathbf{h}_1\mathbf{h}_2\rangle\mathbf{C}^\beta + \langle 0|(1+\Lambda)(\bar{h}^\beta - E^\beta)|\mathbf{h}_1\mathbf{h}_2\rangle\mathbf{C}^\alpha. \tag{163}$$

When the energies E^α and E^β remain in the expression, just as in ordinary RSPT there is the potential for size inextensivity, since their scaling for N units will be $E^\alpha(N)=NE^\alpha$, and without their cancellation, the final second-order result will not be size extensive except in the limit of all excitations (Kobayashi *et al.*, 1994; Rozyczko and Bartlett, 1997; Sekino and Bartlett, 1999). Hence, there is a slight difference between this perturbation (or propagator) -type approximation to a second-order property and the second derivative with respect to μ in the finite limit. The latter introduces a quadratic term in the perturbed T's,

$$E^{\alpha\beta} = \langle 0|(1+\Lambda)(\bar{h}^\alpha - E^\alpha)\bar{R}\bar{h}^\beta|0\rangle + \langle 0|(1+\Lambda)(\bar{h}^\beta - E^\beta)\bar{R}\bar{h}^\alpha|0\rangle + \langle 0|(1+\Lambda)(\bar{H}-E)|\mathbf{f}\rangle\langle \mathbf{f}|T^\alpha T^\beta|0\rangle, \tag{164}$$

where $|\mathbf{f}\rangle$ indicates all determinants beyond those in $|\mathbf{h}_1\mathbf{h}_2\rangle$. As a derivative of a size-extensive quantity, it must be size extensive. However, its evaluation is more difficult. For two electrons there is no $|\mathbf{f}\rangle$, so there is no quadratic term. Yet for more than two electrons, the quadratic term effects the cancellation of the energies E^α in the lead term among other things. To maintain the distinction between the two different approximations, we refer to the perturbation form as the CI-like approximation since we are using the EOM-CC eigenstates that are CI solutions to the $\bar{H}$ matrix. As a CI approximation for excited states, unlike a CC approximation that would use an exponential operator as in Fock space CC (see below), it will not be completely size extensive. We can simply remove the offending term and get excellent extensivity (Sekino and Bartlett, 1999), but that introduces an approximation. Results using the quadratic approximation, the perturbation, CI-like approximation, and its linearized, extensive form are shown elsewhere for dynamic polarizabilites (Rozyczko and Bartlett, 1997; Sekino and Bartlett, 1999). In general, for individual molecules the CI-like and quadratic form give quite close results. For NMR coupling constants they are virtually indistinguishable (Perera *et al.*, 1996).

It is a failing of standard CC theory that there are two ways to define second- and higher-order properties that are equivalent in the limit. We have recently shown that the more general unitary CC, $\exp(\tau)|0\rangle$, where $\tau = T - T^\dagger$ (Bartlett *et al.*, 1989), has to make them equivalent (Taube and Bartlett, 2006). However, the nontermination of the UCC ansatz has to still be addressed.

A. Numerical results

A few numerical examples of how well the EOM-CC methods perform for vertical excitation energies compared to full CI are shown in Tables IX–XII. For saturated atoms and molecules like Ne, HF, and H_2O, all

TABLE IX. Vertical excitation energies (in eV) of Ne with a cc-pVDZ basis set augmented by additional diffuse functions with exponents $s(0.04)$, $p(0.03)$. The active orbitals (lowest-lying unoccupied, highest occupied) are (4,4) for the FS and STEOM calculations.

State symmetry	STEOM CCSD[a]	FS		EOM		
		CCSD[a]	CCSDT[b]	CCSD[c]	CCSDT[b]	FCI[c]
$^1P^0$	16.162	16.153	16.380	16.158	16.372	16.398
^1D	17.975	17.968	18.225	17.963	18.185	18.213
^1P	18.013	18.003	18.231	18.005	18.228	18.256
^1S	18.261	18.242	18.553	18.248	18.450	18.485

[a]Meissner, 1998.
[b]Musiał and Bartlett, 2004b.
[c]Koch *et al.*, 1995.

excited states are Rydberg in character, meaning that they can be approximated by a one-electron atom energy formula $-Z_{\text{eff}}/(n-\delta)^2$ in terms of an effective atomic number with n the principal quantum number and δ the quantum defect. It also means that the electron is comparatively far from the molecule as measured by $\langle r^2 \rangle$, for example. When this is computed from the excited state's density matrix for a Rydberg state, it will be much larger than that in the ground state. On the other hand, for a valence excited state they will be comparable in size. To have lower-lying valence excited states typically requires some unsaturation in the molecule or other quasidegenerate behavior. Hence, Rydberg excited states are quite sensitive to the diffuseness in the Gaussian basis to describe them, but somewhat less sensitive to the description of electron correlation, while the valence states tend to reverse this behavior. To show one example of the former, results for EOM-CCSD and EOM-CCSDT for Ne are shown in Table IX along with Fock space (FS) and STEOM results to be discussed later. At the CCSD level, the error in a cc-pVDZ basis is a little more than ~0.2 eV. The EOM-CCSDT result reduces this to ~0.02 eV. Comparisons to experiment would not be good in this basis, as it lacks suitable diffuse functions, but when compared to full CI there is no ambiguity. If we make the same comparisons for the HF molecule's lowest 14 excited states and H_2O's lowest 9, we obtain average errors of 0.123 for EOM-CCSD and 0.035 for EOM-CCSDT, respectively.

TABLE X. Vertical excitation energies (in eV) of CH^+ (R =1.131 Å) with 6-31G^{**} basis set. The lowest and highest orbitals were frozen.

State symmetry	EOM[a]		FCI[a] ≡ EOM-CCSDTQ
	CCSD	CCSDT	
$^1\Sigma^+$	9.0742	8.6030	8.5304
$^1\Sigma^+$	14.3658	14.3070	14.3042
$^1\Sigma^+$	19.8063	18.0541	18.0224
$^1\Pi$	3.2366	3.2066	3.2087
$^1\Pi$	14.5036	14.2220	14.1595
$^1\Pi$	17.6963	17.1199	17.0573
$^1\Delta$	7.8325	6.9707	6.9335
$^1\Delta$	17.6687	16.8020	16.8460

[a]Hirata *et al.*, 2000.

For the more correlation-demanding excited states as in CH^+, shown in Table X, we see very large errors at the CCSD level for the third $^1\Sigma^+$ and $^1\Delta$ states. The reason for this is that these states have a large component of double excitation character, which can be judged by the large weight of double excitations in the excited-state wave function, perhaps most easily measured by the magnitude of the amplitudes from R_1 and R_2 (Stanton and Bartlett, 1993b). For these three states the singles contribution is, respectively, 0%, 0.22%, and 1.04%. Once we add the triple excitations fully into the calculation via EOM-CCSDT, the errors are greatly reduced to a few hundreths of an eV. The lowest-lying excited $^1\Sigma$ state is mostly a double excitation, as its % singles is 0.23, and as a valence state, its error at the CCSD level, ~0.5 eV, is reduced to ~0.07 with triples. Similar behavior is shown by the second and third $^1\Pi$ states.

Table XI shows how higher-order cluster amplitudes continue to modify the excitation energy for the methylene radical. In this case, the reference state is not the ground state, but the excited $^1A_1$. To get the ground state from EOM-CC, we deexcite to $^3B_1$. For all states, singlets or triplets, most of the error that remains at the CCSD level is removed by triple excitations. For the lowest $^1A_1$, $^1B_2$, and $^3B_2$ states, there is a significant contribution of double excitations that are again handled by the inclusion of triples.

For the C_2 molecule (Table XII), the inclusion of triples significantly improves the CCSD results, reducing the deviations from the FCI values even by several eV (cf. the $^3\Delta_g$ state). But the interesting observation is that EOM-CCSDT results in some cases are off by ~0.1 eV and only inclusion of quadruples cures the problem (see, e.g., the $^1\Delta_g$ state). For molecules like C_2, which has quasidegeneracy even at this equilibrium geometry, the cluster convergence of the EOM results is much slower

TABLE XI. Vertical excitation energies (in eV) of CH_2 (R=1.102 Å, $\angle_{HCH}$=104.7°) with 6-31G^* basis set. The lowest and highest orbitals were frozen.

State symmetry	EOM[a] CCSD	CCSDT	CCSDTQ	CCSDTQP	FCI[a]≡EOM CCSDTQPH
$^1B_1$	1.6677	1.6776	1.6787	1.6787	1.6787
$^1A_1$	5.8437	4.5629	4.5178	4.5168	4.5168
$^1A_2$	6.1006	6.0920	6.0926	6.0926	6.0926
$^1B_2$	9.6915	8.2780	8.2540	8.2536	8.2536
$^1A_1$	9.1202	9.0559	9.0531	9.0529	9.0529
$^3B_1$	−0.3443	−0.3120	−0.3101	−0.3101	−0.3101
$^3A_2$	5.3001	5.3143	5.3150	5.3150	5.3150
$^3B_2$	8.3816	6.9525	6.9054	6.9041	6.9041
$^3A_1$	8.3891	8.3291	8.3267	8.3265	8.3265
$^3B_2$	9.3035	9.1548	9.1504	9.1502	9.1502

[a]Hirata *et al.*, 2000.

than the previous examples, and to achieve good agreement with the reference values higher EOM models need to be considered.

Recognizing that we have different numbers of results at the various levels, and without further separation into Rydberg or valence, for all excited states we obtain average deviations from FCI shown in Table XIII. There we also show results from other approximations like CC2 and CC3 (Christiansen *et al.*, 1995a, 1995b), which are defined to be consistent through second- and third-order perturbation theory based upon the CCLR analysis.

In Tables XIV and XV, we show the same kind of full CI comparison for the EA-EOM-CC for CH^+ and the IP-EOM-CC for BH and C_2, where the accuracy is similar to that for excitation energies.

TABLE XII. Vertical excitation energies (in eV) of C_2 (R =2.348 a.u.) with a cc-pVDZ basis set augmented by additional diffuse functions with exponents s(0.0469), p(0.04041). The 1s orbitals were frozen.

State symmetry	EOM CCSD	CCSDT	CCSDTQ	FCI
$^1\Pi_u$	1.475[a]	1.419[a]	1.386[a]	1.385[b]
$^1\Delta_g$	4.347[a]	2.700[a]	2.317[a]	2.293[b]
$^1\Sigma_u^+$	5.799[a]	5.715[a]	5.615[a]	5.602[b]
$^1\Pi_g$	6.202[a]	4.582[a]	4.487[a]	4.494[b]
$a\ ^3\Pi_u$	0.280[c]	0.317[c]		0.305[c]
$c\ ^3\Sigma_u^+$	0.777[c]	1.143[c]		1.214[c]
$b\ ^3\Sigma_g^-$	3.566[c]	1.889[c]		1.385[c]
$d\ ^3\Pi_g$	4.290[c]	2.723[c]		2.589[c]
$g\ ^3\Delta_g$	10.712[c]	6.847[c]		6.670[c]

[a]Hirata, 2004.
[b]Christiansen *et al.*, 1996.
[c]Larsen *et al.*, 2001.

As we only have full CI results for small molecules in small basis sets, the more meaningful step toward experiment is offered by basis-set extrapolated results. For molecules, of course, unless one obtains at least the optimum geometry in each of the bound excited states to obtain an adiabatic excitation energy, which is what the spectroscopists should see, or better, even simulate the spectrum (Stanton and Gauss, 1999), theory comparisons are at the mercy of comparing with what the spectroscopists say is the correct vertical excitation energy. Also, the theorist has to be able to trust the basis-set extrapolation even though there are variants that will give different answers. With those caveats, such comparisons can be made and are illustrated for vertical excitation energies, vertical ionization potentials, and vertical electron affinities in Tables XVI–XIX. To offer one number to characterize the quality of the results, the mean absolute errors are 0.241 for CCSD and 0.089 for CCSDT for excitation energies, which are close to those deduced from the full CI comparisons. C_2, however, which is a very difficult molecule to treat due to its quasidegeneracies, does not compare as well as the other, very well studied systems. This might suggest an inaccurate vertical excitation energy for comparison. When the same C_2 molecule is studied in a small basis

TABLE XIII. Average deviations (in eV) from FCI[a] excitation energies for several methods. Results averaged over the series of small systems: Ne, HF, CH_2, H_2O, N_2, and C_2.

CC2	EOM-CCSD	CC3	EOM-CCSDT
	Singlet states		
0.50	0.25	0.07	0.05
	Triplet states		
0.42	0.13	0.03	0.02

[a]Koch *et al.*, 1995; Christiansen *et al.*, 1996; Hald *et al.*, 2001; Larsen *et al.*, 2001.

TABLE XIV. Vertical electron affinities (in eV) of CH^+ (R =1.120 Å) with 6-31G^* basis set. The lowest and highest orbital were frozen.

State symmetry	EOM[a]			FCI[a]
	CCSD	CCSDT	CCSDTQ	
1π	10.150	10.117	10.109	10.109
3σ	1.701	1.734	1.740	1.741

[a]Hirata *et al.*, 2000.

set where the full CI comparison is possible (Hirata *et al.*, 2000), $^1\Pi_u$ and $^1\Sigma_u^+$ at the EOM-CCSDT level differ by 0.03 and 0.11 eV, respectively, suggesting that at least the former vertical excitation energy is likely to be misassigned. At the EOM-CCSDTQ level, the difference from the full CI is 0.001 eV for the first state and 0.013 eV for the second. To make basis-set limit EOM-CCSDTQ calculations is beyond the state of the art at present.

As shown in Table XVII, the valence ionization potentials show less dependence on triple excitations regardless of whether the basis sets used in the extrapolation are the normal ones or those augmented with extra diffuse functions. The results appear to be quite close to the experimental ones. In Table XVIII, we have polyatomic molecules where the chances of missing the origin of the band in the experimental photoelectron spectrum are greater, potentially causing more apparent differences in the results. However, for the case of ethylene, where several different experimental results (Bieri and Asbrink, 1980; Holland *et al.*, 1997; Davidson and Jarzecki, 1998) have reached entirely different conclusions as to what the values are, we chose to turn the problem around and use theory to predict accurate vertical ionization potentials (Yau *et al.*, 2002; Musiał and Bartlett, 2004a). In Table XIX, we go to complete basis-set extrapolations for the difficult electron affinities of C_2 and the ozone molecule.

Matrices with rank $\sim 10^9$ for small molecules for EOM-CCSDT and $\sim 10^{12}$ for EOM-CCSDTQ clearly require simplifications before they can be widely applied. One can use EOM-CCSDT-3 as for the ground state, but except for a savings in that calculation there is little to gain for the excited state, as that would still require diagonalization using all triple excitations in the problem. Noniterative approximations should still be possible and were proposed (Watts and Bartlett, 1995; Watts *et al.*, 1996) to try to get workable methods. So far, however, none seem to work nearly as well as does CCSD(T) for ground states. The basic reason is that the description of the excited state has different demands from that for the ground state, and the demands for both the ground and excited states need to be satisfied to get accurate excitation energies. Using the same kind of analysis as shown in Sec. VI, an EOM-CCSD($\tilde{T}$) model can be extracted from EOM-CCSDT-3 for excited states (Watts and Bartlett, 1996). It tends to lower the excitation energy from EOM-CCSD and appears to improve the description of the excitation energy of valence excited states, but closer inspection shows that it also inappropriately lowers the excitation energy of Rydberg states. Hence, there is no good solution along these lines yet.

A better alternative is simply to limit higher excitations to those for a set of active orbitals, that is, to include triples iteratively, but only those that correspond to excitations involving the highest occupied orbitals into the lowest unoccupied ones. Then the rate-determining step in the EOM-CC calculation is almost that for CCSD. We call that EOM-CCSDt (Piecuch *et al.*, 1999) to indicate that the triple excitations are restricted to just those that can be made for a small number of active orbitals. Extensions to EOM-CCSDtq can obviously be done. Applications have been reported for such approximations (Kowalski and Piecuch, 2001; Piecuch *et al.*, 2002) with excellent results.

Another element that should be appreciated about EOM-CC methods is their use as a multireference target state method. That is, by adding or removing electrons, the method acquires the capability of treating multiple determinants in the target state. Consider two quasidegenerate MO's a and b. The target wave function has four $S_z=0$ determinants—$a\bar{a}$, $b\bar{b}$, $a\bar{b}$, and $\bar{a}b$—which should be treated equivalently. This is the essence of a MR-CC problem. Yet standard single-determinant reference CC would use $a\bar{a}$ as the reference, and the other determinants' weight in the wave function would have to be introduced from the Q space into the CC equations. This means their values would have to be attained through the iterations of the CC equations, and if some

TABLE XV. Vertical ionization potentials (in eV) of C_2 (R=1.262 Å) with 6-31G basis set and BH with 6-31G^{**} basis set. The two lowest and two highest orbitals were frozen.

Molecule	State symmetry	EOM[a]					FCI[a]
		CCSD	CCSDT	CCSDTQ	CCSDTQP	CCSDTQPH	
C_2	$1\pi_u$	12.662	12.314	12.151	12.130	12.132	12.131
	$2\sigma_u^-$	15.180	14.803	14.749	14.724	14.721	14.721
BH	3σ	9.418	9.384	9.383	9.383	9.383	9.383
	2σ	16.980	16.688	16.643	16.643	16.643	16.643

[a]Hirata *et al.*, 2000.

TABLE XVI. Extrapolated vertical excitation energies (in eV).

Molecule	Nominal state	CBS[a] EOM-CCSD	CBS[a] EOM-CCSDT	Expt.
N_2	$^1\Pi_g$	9.546[b]	9.301[b]	9.31[b]
	$^1\Sigma_u^-$	10.167[b]	9.844[b]	9.92[b]
	$^1\Delta_u$	10.604[b]	10.251[b]	10.27[b]
CO	$^1\Pi$	8.697[b]	8.540[b]	8.51[b]
	$^1\Sigma^-$	10.243[b]	10.044[b]	9.88[b]
	$^1\Delta$	10.379[b]	10.178[b]	10.23[b]
C_2	$^1\Pi_u$	1.287	1.268[c]	1.041[c]
	$^1\Sigma_u^+$	5.523	5.501[c]	5.361[c]

[a]For N_2 and CO: cc-pV∞Z; for C_2: aug-cc-pV∞Z.
[b]Musiał and Kucharski, 2004.
[c]Musiał *et al.* 2004.

are as large as that for the $a\bar{a}$ determinant (after accounting for the intermediate normalization), this would result in a badly converging calculation. Furthermore, there would still be a bias toward the $a\bar{a}$ reference since the excitations, say singles and doubles, are being taken from it, but not the same single and double excitations from the other three determinants. But because of the matrix diagonalization in EOM-CC, when these four determinants are in the manifold of EOM excitations, their coefficients have the flexibility to immediately become whatever they require. To achieve this in EOM, it might be useful to define the reference function to be a determinant with two fewer electrons, and then use the EOM double (DEA) operator $\hat{R}_{\mathrm{DEA}}$ to add two electrons to the problem. In that way, these four determinants would all be treated equivalently in $\bar{\mathbf{H}}$, being able to have their weights determined by diagonalization to whatever is appropriate. Similarly, we could start with a closed-shell reference determinant that has two more electrons than the target, and use the double (DIP) operator to eliminate two of them, which, once again, gives an equivalent treatment of all four determinants in the target state. This is the essence of a multireference problem as already discussed for ozone. This result for ozone was shown earlier. Because of CCSD's insensitivity to orbital choice, using orbitals for the $N-2$ determinant or the $N+2$ determinant reference is relatively reasonable for the description of the target state. However, as the EOM-CC equations are CI-like for the target state, as opposed to the CC ground state, we cannot always expect the same degree of orbital invariance as we have with help of the exponential $\exp(T_1)$ operator; see Tobita *et al.* (2003) for examples where orbital choice is still important.

Finally, another useful variant on the EOM-CC theme is that one can use high-spin reference determinants for CC, which may be UHF, ROHF, or QRHF, and are typically as good for such states as are the RHF ground-state references (Watts *et al.*, 1992; Comeau and Bartlett, 1993), and then deexcite from them to get a description of lower-spin states. This is the spin-flip approach of Krylov (Levchenko and Krylov, 2004). To illustrate, starting from a ROHF triplet whose reference determinant is $|A\alpha B\alpha|$, a deexcitation operator for $\hat{R}_{SF}=r_{B\alpha}^{B\beta}\hat{c}_{B\beta}^{\dagger}\hat{c}_{B\alpha}+r_{A\alpha}^{A\beta}\hat{c}_{A\beta}^{\dagger}\hat{c}_{A\alpha}$ will give the linear combination $r_{B\alpha}^{B\beta}|A\alpha B\beta|+r_{A\alpha}^{A\beta}|A\beta B\alpha|$, which depending upon the comparative signs of the amplitudes will provide the singlet eigenstates. In fact, the EOM-CC approach allows many routes to many different states by excitation, adding and removing electrons, and adding the spin-flipped components.

For an illustration of the EOM-CCSD approach for a second-order property, consider the scalar spin-spin coupling component of NMR. Its origin arises from interactions between nuclei that have magnetic moments and electrons. In the Ramsey nonrelativistic theory (Perera and Bartlett, 2005), there are four contributions: the diamagnetic spin-orbit (DSO) term

TABLE XVII. Extrapolated vertical ionization potentials[a] (in eV).

Molecule	Nominal state	cc-pV∞Z EOM-CCSD	cc-pV∞Z EOM-CCSDT	aug-cc-pV∞Z EOM-CCSD	aug-cc-pV∞Z EOM-CCSDT	Expt.
N_2	$3\sigma_g$	15.78	15.63	15.80	15.63	15.60
	$1\pi_u$	17.38	17.08	17.38	17.09	16.98
	$2\sigma_u$	19.01	18.82	19.02	18.82	18.78
CO	5σ	14.30	14.04	14.30	14.04	14.01
	1π	17.23	17.12	17.23	17.13	16.91
	4σ	19.95	19.69	19.95	19.70	19.72
F_2	$1\pi_g$	15.80	15.82	15.82	15.85	15.83
	$1\pi_u$	19.15	18.99	19.16	19.02	18.8
	$3\sigma_g$	21.30	21.20	21.32	21.23	21.1

[a]Musiał *et al.*, 2003.

TABLE XVIII. Extrapolated vertical ionization potentials[a] (in eV).

Molecule	Nominal state	cc-pV∞Z EOM-CCSD	cc-pV∞Z EOM-CCSDT	Expt.
C_2H_2	Π_u	11.66	11.52	11.49
	Σ_g^+	17.35	17.21	16.7
	Σ_u^-	19.24	19.08	18.7
C_2H_4	B_{3u}	10.77	10.75	10.95
	B_{3g}	13.22	13.18	12.95
	A_g	15.03	14.92	14.88
	B_{2u}	16.42	16.26	16.34
	B_{1u}	19.72	19.44	19.40
H_2CO	$1B_2$	10.96	10.92	10.9
	$1B_1$	14.48	14.42	14.5
	$2B_1$	15.98	15.89	16.1
	$2B_2$	18.09	17.70	17.0
	$3B_1$	22.06	21.63	21.4

[a]Musiał and Bartlett, 2004a.

$$h^{\alpha,\beta} \Leftrightarrow H_{NN'}(\mathrm{DSO})$$

$$= \frac{\mu_0^2 \mu_B e\hbar \gamma_N \gamma_{N'}}{8\pi^2} \times \sum_k \frac{(\mathbf{r}_{kN}\cdot\mathbf{r}_{kN'})(\mathbf{I}_N\cdot\mathbf{I}_{N'}) - (\mathbf{r}_{kN}\cdot\mathbf{I}_N)(\mathbf{r}_{kN'}\cdot\mathbf{I}_{N'})}{r_{kN}^3 r_{kN'}^3},$$

the paramagnetic spin-orbit (PSO)

$$h^{\alpha},h^{\beta} \Leftrightarrow H_N(\mathrm{PSO}) = \frac{\mu_0\mu_B\hbar\gamma_N}{2\pi i}\sum_k \mathbf{I}_N \cdot \frac{\mathbf{r}_{kN}\times\boldsymbol{\nabla}(k)}{r_{kN}^3},$$

the spin dipole (SD)

$$h^{\alpha},h^{\beta} \Leftrightarrow H_N(\mathrm{SD})$$

$$= \frac{\mu_0\mu_B\hbar\gamma_N}{2\pi} \times \sum_k \frac{3(\mathbf{S}_k\cdot\mathbf{r}_{kN})(\mathbf{I}_N\cdot\mathbf{r}_{kN}) - r_{kN}^2(\mathbf{S}_k\cdot\mathbf{I}_N)}{r_{kN}^5},$$

and the Fermi contact term (FC)

$$h^{\alpha},h^{\beta} \Leftrightarrow H_N(\mathrm{FC}) = \frac{4\mu_0\mu_B\hbar\gamma_N}{3}\sum_k \delta(\mathbf{r}_{kN})\mathbf{S}_k\cdot\mathbf{I}_N.$$

Here μ_0 and μ_B are the permeability of the vaccum and the Bohr magneton; γ_N and $\gamma_{N'}$ are the nuclear magnetogyric ratios of the nuclei N and N', respectively; and $\mathbf{I}_N$ and $\mathbf{I}_{N'}$ are the respective nuclear magnetic moments, k labels the electrons, and $\mathbf{r}_{kN}$ and $\mathbf{S}_k$ are the position vector and the total spin operator of the electron k. Predictive theory requires that all terms be evaluated. The DSO term is obtained from the generalized expectation value of $h^{\alpha,\beta}$ in Eq. (159). The others require the treatment of Eqs. (162) and (163).

In Table XX, we show the NMR spin-spin coupling constants using the CI-like approximation for several small molecules. We observe—comparing absolute errors for the coupled-perturbed HF (CPHF) and EOM-CCSD columns—that electron correlation effects are essential for the adequate description of the coupling constants. The CPHF average error of 28.1 Hz for the wide variety of coupling constants shown is significantly reduced to the value of 3.5 Hz. Before this work (Perera and Bartlett, 2000), such coupling constants could not be adequately described by electronic structure theory. EOM-CC now enables essentially predictive results to be obtained for situations that are not amendable to experimental observation. These include filling in the gaps in the experimental observation of carbocations like the 2-norbornyl cation that was instrumental in the long-term classical versus nonclassical carbocation controversy between Georg Olah and H. C. Brown (Perera and Bartlett, 1996); or in providing a universal curve that relates all secondary N-H-N coupling constants across H bonds to their distance apart, whether they belong to cations or neutrals (Del Bene *et al.*, 2000). The latter might have a role in identifying where protons are in biochemical structures, since they cannot be seen in x-ray crystallography.

The vector term in NMR, the chemical shift, has also been accurately described by CC theory (Gauss and Stanton, 1995). Unlike the scalar term it is necessary to use gauge including atomic orbitals (GIAO), which adds some complexity at the basis-set level.

IX. MULTIREFERENCE COUPLED-CLUSTER METHOD

The multireference (MR) formulation of the coupled-cluster theory is an important extension of the standard [single reference (SR)] approach. Basically, one employs

TABLE XIX. Extrapolated vertical electron affinities[a] (in eV) of $X\,^1\Sigma_g^+$ C_2 and $X\,^1A_1$ O_3.

Molecule	cc-pV∞Z EOM-CCSD	cc-pV∞Z EOM-CCSDT	aug-cc-pV∞Z EOM-CCSD	aug-cc-pV∞Z EOM-CCSDT	Expt.
C_2	3.36	3.23	3.39	3.24	3.27
O_3	1.86	1.60	1.97	1.87	2.10

[a]Musiał and Bartlett, 2003.

TABLE XX. Comparison of CPHF and EOM-CCSD indirect nuclear spin-spin coupling constants with experiment (in Hz).

Molecule	Coupling	CPHF	Abs. error	EOM-CCSD	Abs. error	Expt.
H_2	$^1J(^1H^2H)$	54.2	11.26	40.09	2.85	42.94±0.04
HF	$^1J(^{19}F^1H)$	654.1	125.1	526.4	2.6	529±23
CO	$^1J(^{13}C^{17}C)$	−5.1	11.3	15.6	0.8	16.4±0.1
N_2	$^1J(^{14}N^{15}N)$	−15.3	13.5	1.3	0.5	1.8±0.6
H_2O	$^1J(^1H^{17}O)$	−96.7	23.2	−76.88	3.38	−73.5
	$^2J(^1H^1H)$	−22.6	15.4	−10.61	3.41	−7.2
CH_3CN	$^1J(^{13}C^{15}N)$	−85.7	68.2	−16.99	0.51	±17.5±0.4
	$^1J(^{13}C^1H)$	172.6	36.6	126.20	9.8	±136.0±0.2
	$^2J(^{13}C^{15}N)$	12.2	9.2	3.01	0.01	±3.0±0.4
	$^2J(^{13}C^1H)$	−49.9	39.9	10.00	0.00	±10.00±0.2
	$^3J(^{15}N^1H)$	−12.9	11.1	−1.23	0.59	±1.80±0.1
CH_3F	$^1J(^{13}C^{19}F)$	−133.3	24.2	−169.56	12.56	−157.5±0.2
	$^2J(^1H^{19}F)$	62.9	16.54	46.8	0.44	46.36±0.1
	$^1J(^{13}C^1H)$	180.2	31.1	137.15	11.95	149.1±0.2
CH_3NH_2	$^1J(^{15}N^1H)$	−78.5	13.5	−61.33	3.67	−65.0±0.2
	$^1J(^{13}C^1H)$	159.5	27.3	120.62	11.58	132.2±0.2
	$^2J(^{15}N^1H)$	2.0	1.0	0.93	0.07	−1.0±0.1
Average			28.1		3.5	

the MR formalism for systems that are degenerate or quasidegenerate. In the single-determinant approach, the reference function is very often the Hartree-Fock determinant. The MR formulation assumes that instead of the single determinant we have a number of them forming a subspace denoted as $\mathbf{M}_0$. Thus the whole configurational space $\mathbf{M}$ is divided into two subspaces: the model space $\mathbf{M}_0$ defined through the projection operator $\mathbf{P}$ and the orthogonal one $\mathbf{M}_\perp$ defined through the action of the operator $\mathbf{Q}$. We may express the $\mathbf{P}$ operator as

$$P = \sum_m^{m_0} |\Phi_m\rangle\langle\Phi_m|,$$

where Φ_m is a model determinant and m_0 is the size of the model space. The projectors $\mathbf{P}$ and $\mathbf{Q}$ are related to each other through

$$P + Q = 1.$$

We have to introduce also the notion of the model function Ψ_k^0 defined through the action of the operator $\mathbf{P}$ on the exact wave function Ψ_k,

$$\Psi_k^0 = P\Psi_k.$$

Thus, Ψ_k^0 is a component of the function Ψ_k residing within the model space. This can be expressed as a linear combination of the model determinants,

$$\Psi_k^0 = \sum_m^{m_0} C_{mk}\Phi_m.$$

A principal quantity in the MR theories is the wave operator Ω, which is used to construct the exact wave function Ψ_k from the model function Ψ_k^0,

$$\Psi_k = \Omega\Psi_k^0 = \Omega\Psi_k. \tag{165}$$

Usually one also introduces the assumption of intermediate normalization, which can be expressed in operator language as

$$P\Omega = P. \tag{166}$$

The advantage of the multireference formalism relies on the fact that finding the exact energy of the system does not require solving the full Schrödinger equation,

$$H\Psi_k = E_k\Psi_k, \tag{167}$$

but instead solving the eigenvalue equation involving an effective Hamiltonian H^{eff},

$$H^{\text{eff}}\Psi_k^0 = E_k\Psi_k^0. \tag{168}$$

The H^{eff} operator is defined as

$$H^{\text{eff}} = PH\Omega P. \tag{169}$$

Equation (168) is obtained by applying the operator P to both sides of the Schrödinger equation, Eq. (167), and by exploiting the relations in Eqs. (165) and (166).

The last element of the multireference formalism is the Bloch equation (Bloch and Horowitz, 1958), obtained by the action of the operator Ω on the Schrödinger equation,

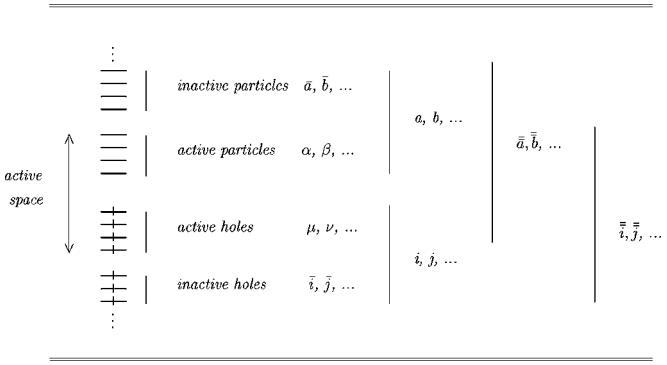

FIG. 37. Classification of the one-particle states.

$$\Omega H\Psi_k = E_k\Psi_k \tag{170}$$

and by subtracting from the last equation Eq. (167) to obtain the Bloch equation,

$$H\Omega P = \Omega PH\Omega P \tag{171}$$

or using the H^{eff} operator,

$$H\Omega P = \Omega PH^{\text{eff}}P. \tag{172}$$

The Bloch equation, as given by Eq. (172), is general enough to be applied to various forms of the multireference formalism. The text of Lindgren and Morrison (1986) discusses such approaches in depth. Their focus is the quasidegeneracy that occurs in open-shell atoms rather than the quasidegeneracy that occurs in bond breaking. The latter introduces what most call nondynamic correlation, also sometimes called left-right correlation. In our terminology (Bartlett and Stanton, 1994), static correlation means correlation encountered in the treatment of open-shell atoms and molecules that involves proper spin combinations of determinants and their interactions. Hence, static is not a synonym for nondynamic. However, both involve quasidegeneracy, although of a different kind. The multireference problem is meant to superimpose the essential effects of static or nondynamic correlation on top of the extremely efficient characterization of the dynamic correlation introduced by CC theory.

In order to define a model space, we need to introduce a formal classification of the one-particle states as presented in Fig. 37. The active space includes N_{ah} active hole levels and N_{ap} active particle levels. Since the number of active hole levels is equal to the number of electrons assigned to the active space N_{ae}, the complete N_{ae}-electron model space is constructed by considering determinants corresponding to all possible distributions of N_{ae} electrons among $N_{ah}+N_{ap}$ active levels. If some of determinants are excluded from the model space, then we have an incomplete model space.

Within the coupled-cluster theory, there are two principal definitions of the wave operator Ω, which leads to two different MRCC methods: the Hilbert-space MRCC approach and the Fock-space MRCC approach.

A. Hilbert-space formulation of the MRCC approach

In the first approach, the wave operator is a sum of operators defined independently for each model function (Jeziorski and Monkhorst, 1981; Lindgren and Mukherjee, 1987; Mukherjee and Pal, 1989; Balkova *et al.*, 1991a, 1991b; Kucharski and Bartlett, 1991b, 1992; Balkova, Kucharski, *et al.*, 1991; Kucharski *et al.*, 1992; Paldus *et al.*, 1993; Mašik and Hubač, 1999; Pittner *et al.*, 1999; Hubač *et al.*, 2000; Pittner, 2003; Li and Paldus, 2004). This can be expressed as

$$\Omega = \sum_\mu \Omega_\mu = \sum_\mu e^{S^\mu}P_\mu, \tag{173}$$

where P_μ is a projector onto the N_{ae}-valence-electron model determinant and the sum over μ runs over all model determinants Φ_μ. So the model space is an example of an N_{ae}-valence-electron Hilbert space and this approach is called a Hilbert-space MRCC (HS-MRCC) or state-universal MRCC (SU-MRCC) method.

The operator S_μ is a cluster operator,

$$S^\mu = S_1^\mu + S_2^\mu + \cdots \tag{174}$$

and

$$S_k^\mu = \frac{1}{(n!)^2}\Sigma'_{ij\cdots ab\cdots}s_{ij\cdots}^{ab\cdots}a^\dagger b^\dagger\cdots ji, \tag{175}$$

where the prime sign indicates that terms that generate excitations within the model space are excluded from the summation. The summation over $i,j,\ldots$ runs over all levels occupied in the Φ_μ determinants while $a,b,\ldots$ represents levels unoccupied in Φ_μ. Each of the Φ_μ determinants becomes, in turn, a Fermi vacuum that allows defining the appropriate particle $(a,b,\ldots)$ and hole $(i,j,\ldots)$ levels. Because of the complete active space, the definition of the wave operator given in Eqs. (173)–(175) is very similar to the definition of the T_n cluster operator in the single reference coupled-cluster theory. The main difference is that all terms in the summation in Eq. (175) that lead to the excitations within a model space are excluded. The equations for the amplitudes $s_{ij\cdots}^{ab\cdots}$ are obtained from the Bloch equation, Eq. (172), using the definition of the wave operator, Eqs. (173)–(175), and projecting against determinants $\Phi_{ij\cdots}^{ab\cdots}$ outside of the model space,

$$\langle\Phi_{ij\cdots}^{ab\cdots}(\mu)|He^{S_\mu}|\Phi_\mu\rangle = \sum_\nu \langle\Phi_{ij\cdots}^{ab\cdots}(\mu)|e^{S_\nu}|\Phi_\nu\rangle\langle\Phi_\nu|H^{\text{eff}}|\Phi_\mu\rangle. \tag{176}$$

The effective operator's elements are immediately obtained from Eq. (175), upon projection against the reference determinant Φ_ν,

$$\langle\Phi_\nu|He^{S_\mu}|\Phi_\mu\rangle = \langle\Phi_\nu|H^{\text{eff}}|\Phi_\mu\rangle = H_{\nu\mu}^{\text{eff}}. \tag{177}$$

As a matrix, the effective Hamiltonian is trying to describe m_0 states simultaneously. The set of amplitude equations given by Eq. (176) is solved for each reference determinant Φ_μ. Note that due to the renormalization term, i.e., that occurring on the right-hand side of Eq.

(176), the equations for each set of amplitudes are coupled and should be iterated simultaneously. The energy eigenvalues are obtained by diagonalization of the effective Hamiltonian matrix defined within the model space.

The problem of completness versus incompleteness of the model space is crucial in formulations of the MRCC theory. The completeness of the model space guarantees that the amplitude equations as well as the effective Hamiltonian elements include only connected terms, which ensures the size extensivity of the method. On the other hand, construction of the complete model space requires consideration of a large number of model determinants, particularly when large active spaces are used. In addition, large model spaces are plagued by the intruder state problem. The latter arises when determinants from the model space are close energetically to those belonging to the orthogonal space, and this causes severe divergences in the iteration process. Thus the preferable choice would be a development of an approach that would allow the use of a general model space (GMS), i.e., either complete or incomplete depending upon the problem.

Such a method was advocated by Mukherjee, which required relaxing the intermediate normalization in CC theory (Mukherjee and Pal, 1989). An alternative was proposed by Li and Paldus (2004), who introduced a general model space (GMS) SU-MRCC scheme based on connectivity (C) conditions. The C conditions recognize that in CI language $\Omega_\mu=(1+\hat{C}_1+\hat{C}_2+\cdots)P_\mu$. However, the intermediate normalization $\Omega=\Omega P$ requires the exclusion of internal excitations, i.e., those within the model space, from each $\hat{C}_\mu$. However, the exclusion of several excitations in $\hat{C}_n^\mu$ is not equivalent to their exclusion from S_n^μ, because of the usual relationship that $\hat{C}_2^\mu=\frac{1}{2}(S_1^\mu)^2+S_2^\mu$, etc. If the model space is incomplete, some of the lower excitations in the disconnected products can generate Q space determinants. The C conditions properly handle such terms. Hence, they force the cancellation of disconnected terms within both the amplitudes and effective Hamiltonian, which ensures the size-extensive property [see Refs. 20, 21, 27, 28 from Li and Paldus (2004) for details].

Li and Paldus (2004) tested the performance of the SU CCSD approach for several choices of model space by comparing the SU CCSD results with reference values (FCI or CISDTQ). In all cases studied (CH^+, HF, F_2, H_2O, and others), the SU-CCSD values remain close to the reference. Figure 38 presents potential-energy curves for the ground state and three excited states of CH^+ previously considered, obtained with 5R (five references in the model space) -SU CCSD. Comparisons with FCI PES [taken from Li and Paldus (2004)] show excellent agreement between FCI and SU CCSD results.

Returning to the problem of ozone's vibrational frequencies, we can compare the MR-CC results with those from SR-CC in Fig. 39 in the same DZP basis. The DIP-STEOM method has already been discussed as it falls

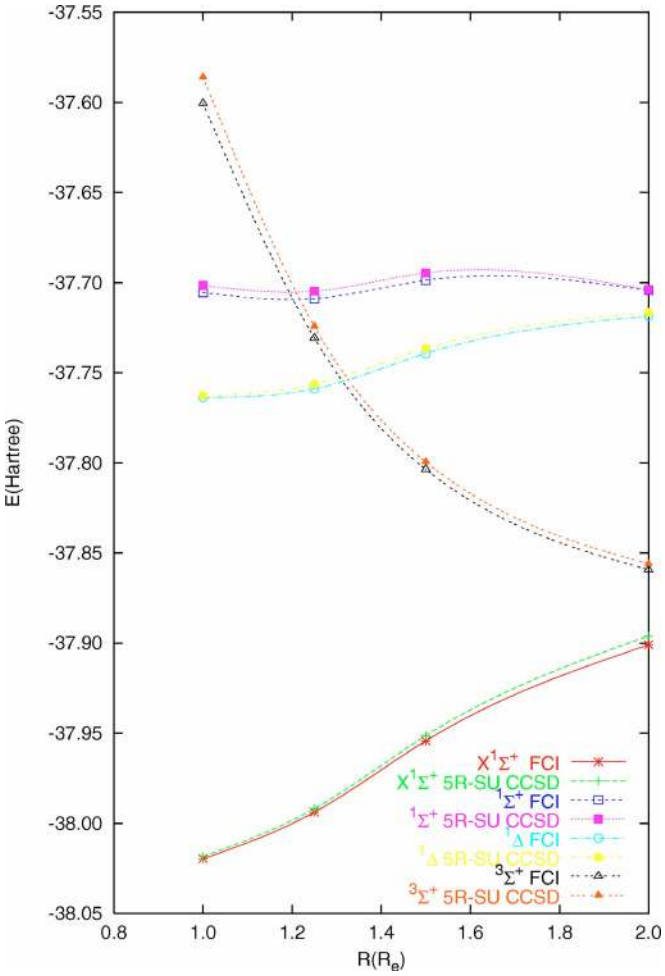

FIG. 38. (Color online) CH^+ potential-energy curves obtained with the FCI and 5R-SU CCSD methods.

between a true multireference approach and single reference theory, which it operationally is. Yet it is MR in that it treats all four of the revelant determinants (three configurations) equivalently. The MR(3)-CCSD results of Li and Paldus correspond to the true SU-CCSD re-

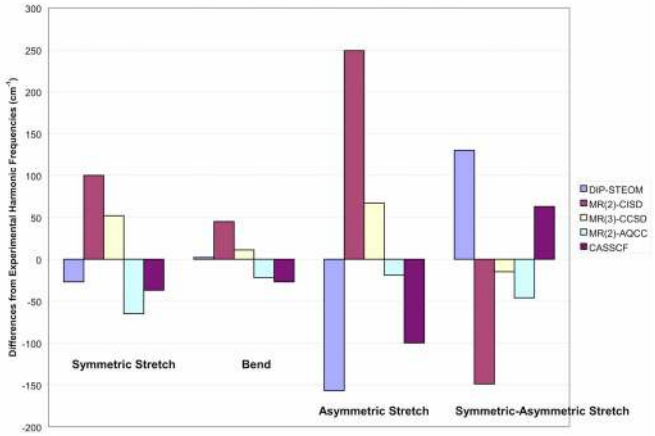

FIG. 39. (Color online) Vibrational frequencies of ozone (multireference methods, DZP basis set). See Fig. 23 for the experimental values.

sults, and they, too, are quite good and generally better than the SR-CC approximations. The poorest results are given by the MR(2)-CISD. The CASSCF includes nondynamic correlation, but no dynamic correlation is added. The final result is from a method termed MR-AQCC, which means multireference averaged quadratic CC (Szalay and Bartlett, 1993; Fusti-Molnar and Szalay, 1996; Szalay, 1997). This method follows the older multireference linearized CC method (Laidig *et al.*, 1987) and is close to the MR-ACPF (multireference averaged coupled-pair) (Gdanitz and Ahlrichs, 1988) method. Both are built upon the MR-CI structure and programs, as they benefit from the long-term development of CI technology, except in a few critical ways. The MR-AQCC method corrects for CI's lack of extensivity and introduces a functional, which makes it easy to do analytical gradients. The method is available in the COLUMBUS program system (Lischa *et al.*, 2001). It has been used in an extensive number of applications for complicated systems with outstanding success (Szalay, 1997). The two-reference variant shown here does rather well for ozone frequencies. As a final word on ozone frequencies, the tailored TCCSD discussed in Sec. VI.C for bond breaking has also been recently applied to this problem. Unlike for bond breaking, it was found (Hino *et al.*, 2006) that CAS-CI alone was not adequate for tailoring the SR-CC. Instead, the orbitals had to be rotated optimally too, to go from CAS-CI to CAS-SCF. Once this was done with a rather large CAS space consisting of 12 electrons into 9 orbitals, the final results in a cc-pVTZ basis were ω_1 (1137 cm^{-1} versus 1135 cm^{-1} expt.), ω_2 (1137 cm^{-1} versus 716 cm^{-1} expt.), and ω_3 (1098 cm^{-1} versus 1089 cm^{-1} expt.). All are less than 1% in error. It is unfortunate that no complete basis-set limit results are yet available for O_3 to bring the basis-set issue under control and to focus on the correlation problem unambiguously, but this attests to the limitations of such basis-set extrapolation techniques as they are encountered for even three atoms. This problem would be a worthy test for quantum Monte Carlo (QMC) calculations.

B. Fock-space formulation of the MRCC approach

The second MR-CC approach assumes the wave operator to be of the same form for all reference determinants, i.e., it is defined universally with respect to the whole model space. This version of the MRCC theory is often called a valence universal MRCC (VU-MRCC) approach (Lindgren, 1979; Haque and Mukherjee, 1984; Sinha *et al.*, 1986; Pal *et al.*, 1987, 1988; Jeziorski and Paldus, 1989; Rittby and Bartlett, 1991; Landau *et al.*, 1999, 2000).

The universal definition of the wave operator bears another important consequence: In order to have a well-determined set of amplitude equations, one has to include into the model space also determinants corresponding to variable numbers of active electrons, i.e., for a complete model space we have to include determinants with a number of valence electrons from 0 to $N_{ah}+N_{ap}$ distributed among all active levels. This type of Hilbert space includes, in addition to the N_{ah}-electron determinants, also those that correspond to the ionized (up to N_{ah}-tuple ionization) and electron attached (up to N_{ap} attached electrons) states. This is a Fock-space MRCC (FS-MRCC) approach.

In fact, it is more convenient to consider the model determinants as corresponding to a certain number of quasiparticles instead of a number of electrons (particles). That means that having N_{ah} electrons in the system with all hole levels occupied, i.e., Φ_0, we have zero quasiparticles or a zero-valence situation. Similarly, removing one electron from any occupied valence level in the Φ_0 or adding one electron to any unoccupied valence level, we have one quasiparticle in the system or one-valence problem; moving one electron from the occupied valence level to the unoccupied valence level, we have a two-valence problem (two quasiparticles: one hole and one particle).

In the FS-MRCC approach, the wave operator is given as

$$\Omega = \{e^{\tilde{S}}\}P, \tag{178}$$

$$\tilde{S} = \tilde{S}_1 + \tilde{S}_2 + \cdots + \tilde{S}_n, \tag{179}$$

and the $\tilde{S}_n$ operator in its most general form is expressed as

$$\tilde{S}_n = \frac{1}{(n!)^2} \sum_{\bar{\bar{a}}\bar{\bar{b}}\cdots\bar{\bar{\imath}}\bar{\bar{j}}\cdots}{}' s_{\bar{\bar{\imath}}\bar{\bar{j}}\cdots}^{\bar{\bar{a}}\bar{\bar{b}}\cdots} \bar{\bar{a}}^{\dagger}\bar{\bar{b}}^{\dagger}\cdots\bar{\bar{\imath}}\bar{\bar{\imath}}, \tag{180}$$

where the summation over $\bar{\bar{a}},\bar{\bar{b}},\ldots(\bar{\bar{\imath}},\bar{\bar{j}},\ldots)$ runs over inactive particles (inactive holes) and all valence levels, see Fig. 37, and the prime indicates that excitations within model determinants are excluded from the summation. It is important to note that the summation ranges for creation operators $(\bar{\bar{a}},\bar{\bar{b}},\ldots)$ and for annihilation ones $(\bar{\bar{\imath}},\bar{\bar{j}},\ldots)$ overlap within the valence levels, and because of this, contractions among $\tilde{S}$ operators are possible. To prevent that, a normal-ordered ansatz was introduced by Lindgren (1978)—indicated by $\{\}$—of the creation-annihilation operators in the expansion of $e^{\tilde{S}}$.

We may separate the P operator into zero-valence, one-valence, two-valence, etc., sectors depending on the number of valence quasiparticles present in the model determinant,

$$P = P^{(0)} + P^{(1)} + P^{(2)} + \cdots . \tag{181}$$

The n-valence sector can be further separated into the k-valence particle, l-valence hole $(k+l=n)$ sectors,

$$P^{(0)} = P^{(0,0)}, \tag{182}$$

$$P^{(1)} = P^{(1,0)} + P^{(0,1)}, \tag{183}$$

$$P^{(2)} = P^{(2,0)} + P^{(0,2)} + P^{(1,1)}, \tag{184}$$

$$\vdots.$$

As an example, we provide an explicit form of the projectors $P^{(1,0)}$, $P^{(0,1)}$, $P^{(1,1)}$,

$$P^{(1,0)} = \sum_{\alpha} |\Phi^{\alpha}\rangle\langle\Phi^{\alpha}|, \tag{185}$$

$$P^{(0,1)} = \sum_{\mu} |\Phi_{\mu}\rangle\langle\Phi_{\mu}|, \tag{186}$$

$$P^{(1,1)} = \sum_{\mu\alpha} |\Phi_{\mu}^{\alpha}\rangle\langle\Phi_{\mu}^{\alpha}|. \tag{187}$$

The same sector structure distinguishes the $\tilde{S}_n$ operator. Let us consider, for example, $\tilde{S}_2$,

$$\begin{aligned}\tilde{S}_2 &= \tfrac{1}{4}\sum_{\bar{a}\bar{b}ij}{}' s_{ij}^{\bar{a}\bar{b}} \bar{a}^{\dagger}\bar{b}^{\dagger}\bar{j}\bar{i} \\ &= \tfrac{1}{4}\sum_{abij} s_{ij}^{ab} a^{\dagger}b^{\dagger}ji + \tfrac{1}{2}\sum_{ab\alpha j} s_{\alpha j}^{ab} a^{\dagger}b^{\dagger}j\alpha + \tfrac{1}{2}\sum_{\mu bij} s_{ij}^{\mu b}\mu^{\dagger}b^{\dagger}ji \\ &\quad + \sum_{\mu\alpha bj}{}' s_{\alpha j}^{\mu b}\mu^{\dagger}b^{\dagger}j\alpha + \cdots \\ &= S_2^{(0,0)} + S_2^{(1,0)} + S_2^{(0,1)} + S_2^{(1,1)} + \cdots,\end{aligned}$$

where the terms for the sectors (2,0), (0,2), (2,1), (1,2), and (2,2) are skipped. To establish the summation ranges of the a,b,i,j,α,μ, indices, Fig. 37 should be consulted. In the general case, we have the following sector structure of the $\tilde{S}$ operator:

$$\tilde{S}^{(k,l)} = \sum_{i=0}^{k}\sum_{j=0}^{l} S^{(i,j)} \tag{188}$$

and by definition the $S^{(i,j)}$ operator includes i annihilation valence particle lines and j annihilation valence hole lines. It follows from that that there is a hierarchical structure of the S operator (Haque and Mukherjee, 1984; Chaudhuri *et al.*, 1989), which can be written as

$$S^{(m,n)}P^{(i,j)} = 0 \quad \text{if } m > i \text{ or } n > j. \tag{189}$$

For example,

$$S^{(1,0)}P^{(0,0)} = 0.$$

The maximum valence rank of the sector occurring for the N_{ah} valence holes and N_{ap} particles is $N_{ah}+N_{ap}$, i.e., for the complete model space we would need to consider the (N_{ap},N_{ah}) sector. However, in the majority of applications the valence rank of the $\tilde{S}^{(k,l)}$ operator, i.e., $k+l$, is much lower than the size of the model space N_a, which means that we deal with an incomplete model space.

In Fig. 40, we give algebraic and diagrammatic definitions of the S_1 and S_2 operators in the sectors (0,0), (1,0), (0,1), and (1,1). Note that the S operators for the (0,0) sector are identical with the T operator introduced in the single reference theory. The need for considering the lower sectors arises as follows. The $\tilde{S}$ operator for the (1,1) sector is defined as

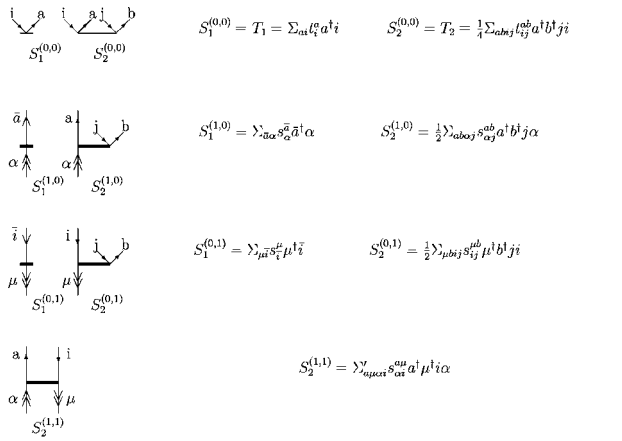

FIG. 40. A graphical representation and algebraic expressions for the $S^{(0,0)}$, $S^{(1,0)}$, $S^{(0,1)}$, and $S^{(1,1)}$ operators at the CCSD level. In the definition of the $S_2^{(1,1)}$ operator, the case in which both creation lines are active is excluded (this is denoted by $'$).

$$\tilde{S}^{(1,1)} = S^{(0,0)} + S^{(1,0)} + S^{(0,1)} + S^{(1,1)}.$$

The amplitude equations within the (1,1) sector are underdetermined, i.e., the number of equations is smaller than the number of the unknown amplitudes,

$$\begin{aligned}\langle\Phi_{\mu}^{\bar{a}}|\tilde{S}|\Phi_{\mu}^{\alpha}\rangle &= \langle\Phi_{\mu}^{\bar{a}}|\sum_{\bar{b}\beta} s_{\beta}^{\bar{b}}\bar{b}^{\dagger}\beta + \sum_{b\beta\nu} s_{\beta\nu}^{b\nu} b^{\dagger}\nu^{\dagger}\nu\beta|\Phi_{\mu}^{\alpha}\rangle \\ &= s_{\alpha}^{\bar{a}} + s_{\alpha\mu}^{\bar{a}\mu}.\end{aligned} \tag{190}$$

The above equation does not provide a single amplitude, unlike SR, but instead determines a sum of two amplitudes $s_{\alpha}^{\bar{a}}+s_{\alpha\mu}^{\bar{a}\mu}$. However, the value of $s_{\alpha}^{\bar{a}}$ can be determined from the lower sector, i.e., according to the relation

$$\langle\Phi^{\bar{a}}|\tilde{S}|\Phi^{\alpha}\rangle = \langle\Phi^{\bar{a}}|\sum_{\bar{b}\beta} s_{\beta}^{\bar{b}}\bar{b}^{\dagger}\beta|\Phi^{\alpha}\rangle = s_{\alpha}^{\bar{a}},$$

and due to the relation (189) the operators from the (1,1) sector do not enter the last equation. Thus from the solution of the FS-MRCC equations in the (1,0) and (0,1) sector, we obtain $s_{\alpha}^{\bar{a}}$ and s_{i}^{μ}, respectively, and we can then treat them as known quantities when solving the respective equations within the (1,1) sectors. Hence, $s_{\alpha\mu}^{\bar{a}\mu}$ is determined in Eq. (190) uniquely. This is a general feature of the FS-MRCC approach that in order to solve the equations for the (m,n) sector, solutions for all lower sectors (i,j) ($i=0,m$ and $j=0,n$) must be known. For example, for the (1,1) sector, solutions for (0,0), (0,1), and (1,0) sectors are required. This has sometimes been called the subsystem embedding condition (Chaudhuri *et al.*, 1989).

The general FS-MRCC equation for the (k,l) sector formulated in the operator form can be written as

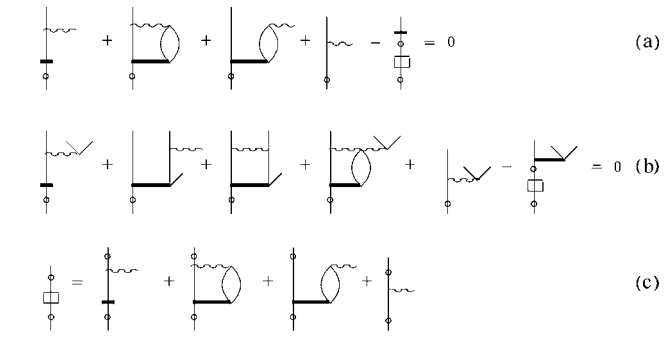

FIG. 41. The diagrammatic representation of the FS-CCSD equations for the (1,0) and (0,1) sectors in the skeleton form: (a) an equation for the S_1, (b) an equation for the S_2, and (c) an expression for the one-particle part of the H_{eff}. Active lines are designated by a circle.

$$H\{e^{\tilde{S}^{(k,l)}}\}P^{(k,l)} = \{e^{\tilde{S}^{k,l)}}\}P^{(k,l)}H^{\text{eff}}P^{(k,l)}. \tag{191}$$

It is convenient to separate from the $\tilde{S}$ operator that corresponding to the (0,0) sector,

$$\tilde{S}^{(k,l)} = \tilde{S}'^{(k,l)} + S^{(0,0)} = \tilde{S}'^{(k,l)} + T. \tag{192}$$

Rewriting Eq. (191) on the basis of the equality in Eq. (192) and multiplying from the left with e^{-T}, we obtain

$$e^{-T}He^{T}\{e^{\tilde{S}'^{(k,l)}}\}P^{(k,l)} = \{e^{\tilde{S}'^{(k,l)}}\}P^{(k,l)}H^{\text{eff}}P^{(k,l)}, \tag{193}$$

where $e^{-T}He^{T}=\bar{H}$ is the quantity introduced in previous sections. Thus the final form of the FS-MRCC equation is obtained upon projection of the last equation on the excited determinants in each sector represented by the projector $Q^{(k,l)}$,

$$Q^{(k,l)}\bar{H}\{e^{\tilde{S}'^{(k,l)}}\}P^{(k,l)} = Q^{(k,l)}\{e^{\tilde{S}'^{(k,l)}}\}P^{(k,l)}H^{\text{eff}}P^{(k,l)}, \tag{194}$$

where $\tilde{S}^{(k,l)}$ is defined according to Eq. (188), i.e., it includes all S components coming from the lower sectors.

The H^{eff} operator is defined in an analogous manner as in the HS variant, and, for instance, for the (k,l) sector we have

$$P^{(k,l)}H^{\text{eff}}P^{(k,l)} = P^{(k,l)}\bar{H}\{e^{\tilde{S}'^{(k,l)}}\}P^{(k,l)}. \tag{195}$$

In Fig. 41, we present the diagrammatic equation for the one-valence sectors, i.e., (1,0) and (0,1). Providing upward (downward) arrows to the annihilation lines in Fig. 41(a), we obtain equations for the $s_{\alpha}^{\bar{a}}$ ($s_{\bar{i}}^{\mu}$) amplitudes; applying the same procedure to Fig. 41(b), we obtain equations for the $s_{\alpha j}^{\bar{a}b}$ and $s_{\bar{i}j}^{\mu b}$ amplitudes. In Fig. 41(c), we present diagrammatic contributions to the effective Hamiltonian elements also for the one-valence sector. Note that only the linear term is present in the one-valence sector, as nonlinear terms contain more than one annihilation operator which makes them vanish when applied to the model determinants in the one-valence sector. The wiggly lines represent the elements of the $\bar{H}$ operator.

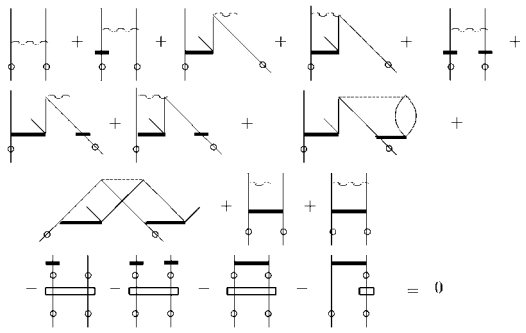

FIG. 42. The diagrammatic representation of the S_2 equation for the (1,1) sector in skeleton form.

The equation for the S_2 amplitudes in the (1,1) sector of the FS-CCSD model is given in Fig. 42. Here the S_1 and S_2 amplitudes determined in the one-valence sectors are used and they occur both in linear and quadratic terms, whereas the S_2 amplitudes in the (1,1) sector appear only via linear terms. This is a general feature of the FS equations that the $S^{(i,j)}$ amplitudes in the equations for the (i,j) sector occur linearly. The solution of the FS-MRCC equations presented in Figs. 41 and 42 is obtained in an iterative manner. In each iteration, a set of the S amplitudes is constructed as well as the elements of the H^{eff} operator [see Figs. 41(c) and 43], which are further diagonalized to obtain energy eigenvalues. The majority of applications of the FS-MRCC are limited to the (1,1) sector of the Fock space, while the cluster expansion, Eq. (179), is truncated at the S_2 operator (MRCCSD model). Just recently, an extension of the FS-MRCCSD model to full inclusion of the connected triple excitations has been reported (Musiał and Bartlett, 2004b). The FS-MRCCSDT approach requires determination of T_1,T_2,T_3 operators at the zero valence level, S_1,S_2,S_3 operators at the one-valence level, and S_2 and S_3 operators for the (1,1) sector. One should note that the rank of the computational procedure (based on the summation of inactive indices) decreases for higher sectors, i.e., we have an M^8,M^7,M^6 procedure for the FS-

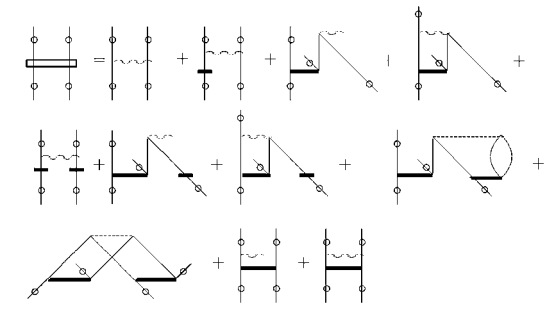

FIG. 43. The diagrammatic expression for the two-particle part of H_{eff}.

TABLE XXI. Vertical excitation energies (in eV) of N_2 (R=2.068 a.u.) with cc-pVDZ basis set. The 1s orbitals were frozen. The active orbitals (lowest-lying unoccupied, highest occupied) are (2,4) for the FS and STEOM calculations.

State symmetry	STEOM CCSD	FS		EOM		
		CCSD	CCSDT	CCSD	CCSDT	FCI[a]
$^1\Pi_g$	9.446[a]	9.409[a]	9.621[b]	9.665[c]	9.593[b]	9.584[c]
$^1\Sigma_u^-$	10.368[a]	10.315[a]	10.327[b]	10.465[c]	10.333[b]	10.329[c]
$^1\Delta_u$	10.833[a]	10.792[a]	10.722[b]	10.898[c]	10.726[b]	10.718[c]
$^1\Pi_u$	13.981[a]	14.010[a]	13.784[b]	14.009[c]	13.661[b]	13.608[c]
$^3\Sigma_u^+$	7.814	7.750		7.882[d]	7.883[d]	7.897[d]
$^3\Pi_g$	8.208	8.083		8.223[d]	8.174[d]	8.163[d]
$^3\Delta_u$	9.193	9.123		9.265[d]	9.192[d]	9.194[d]
$^3\Sigma_u^-$	10.155	10.109		10.192[d]	10.009[d]	9.999[d]
$^3\Pi_u$	11.555	11.435		11.539[d]	11.469[d]	11.441[d]

[a]Meissner, 1998.
[b]Musiał and Bartlett, 2004b.
[c]Christiansen *et al.*, 1996 (CCLR).
[d]Larsen *et al.*, 2001.

CCSDT model at zero-, one-, and two-valence sectors, respectively.

In Tables IX and XXI, we compare the performance of the EOM and FS methods up to triples (relative to the FCI values). For the Ne atom, the FS and EOM values are very close; for the N_2 molecule, the CCSD model provides slightly better results for the FS approach. In both cases, the inclusion of triples improves agreement with the FCI values remarkably. It should be emphasized, however, that the FS-MRCC results are rigorously size extensive, while the EOM ones, because of their dependence on a linear operator $\hat{R}$ instead of an exponential as in the Fock space case, mean that it retains certain elements of CI in its solutions. While EOM is fine for $(AB)^* \rightarrow A^* + B$ or $A + B^*$, it does not go smoothly to $A^+ + B^-$; FS-CC does (Meissner and Bartlett, 1995).

An intermediate approach between FS-CC and EOM-CC is the similarity transformed EOM (STEOM) (Nooijen and Bartlett, 1997a) method. In this approach, the (0,1) and (1,0) sector problems are solved to define a second similarity transformation $e^{\hat{S}}$ that is then applied to $\bar{H}$, i.e., $e^{-S}\bar{H}e^{S}=G$. By virtue of the second transformation, it can be shown that the single-excitation block of the (1,1) (excited-state) sector is approximately decoupled from both double and triple excitations. This gives a matrix of excited-state solutions whose rank is no

TABLE XXII. Vertical excitation energies (in eV) for the CH_2, H_2O, and C_2 molecules compared with the FCI values.

Molecule	State symmetry	STEOM-CCSD	FS-CCSD	EOM-CCSD	FCI
CH_2	$3\,^1A_1$	6.501[a]	6.493[a]	6.509[b]	6.514[b]
	$4\,^1A_1$	8.460[a]	8.454[a]	8.460[b]	8.479[b]
	$1\,^1B_1$	7.733[a]	7.725[a]	7.715[b]	7.703[b]
	$1\,^1B_2$	1.665[a]	1.616[a]	1.780[b]	1.793[b]
	$1\,^1A_2$	5.848[a]	5.801[a]	5.859[b]	5.853[b]
H_2O	$2\,^1A_1$	9.769[a]	9.755[a]	9.806[c]	9.874[c]
	$1\,^1B_2$	7.344[a]	7.325[a]	7.375[c]	7.447[c]
	$1\,^1B_1$	11.521[a]	11.505[a]	11.524[c]	11.611[c]
	$1\,^1A_2$	9.132[a]	9.108[a]	9.122[c]	9.211[c]
C_2	$^1\Pi_u$	1.420[a]	1.399[a]	1.474[c]	1.385[c]
	$^1\Sigma_u^+$	5.725[a]	5.717[a]	5.799[c]	5.602[c]

[a]Meissner, 1998.
[b]Koch *et al.*, 1995 (CCLR).
[c]Christiansen *et al.*, 1996 (CCLR).

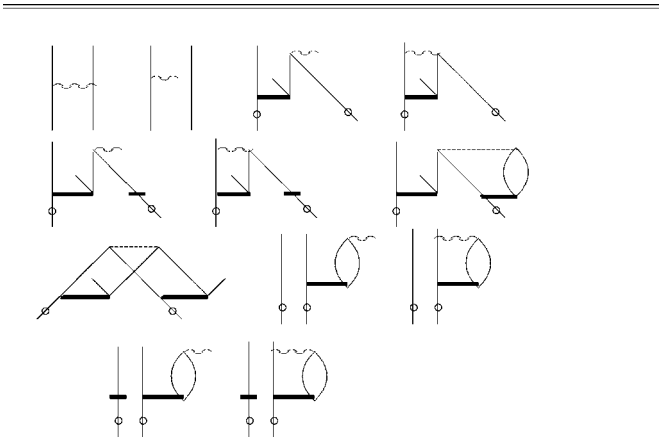

FIG. 44. Matrix representation of the intermediate Hamiltonian in diagrammatic form.

larger than the very small ($\sim nN$) number of single excitations. In a sense this is an exact, size-extensive CI singles theory for excited states that correspond to single excitations. The STEOM method also controls intruder states without further modification, unlike the FS-CC or HS-CC methods. Applications to free-base porphyrin illustrate its applicability (Nooijen and Bartlett, 1997b; Gwaltney and Bartlett, 1998). In Tables IX, XXI, and XXII, we compare the performance of the FS, EOM, and STEOM methods at the CCSD level relative to the FCI values. As we can see, the FS and STEOM methods give results that are of an overall quality comparable with EOM, but at substantially less cost because of the small matrix diagonalization.

The Fock-space approach, in particular, is plagued by the same complications as its Hilbert-space equivalent, i.e., by divergence problems in the iterative process when intruder states occur. That situation is more likely to occur when large model spaces are used. Intruder states constitute a serious limitation of the FS-MRCC approach.

C. Fock-space MRCC based on an intermediate Hamiltonian

In order to avoid the intruder state problem, a new version of the FS-MRCC method has been established that is based on the intermediate Hamiltonian theory of Malrieu *et al.*, (1985) and Meissner (Meissner and Bartlett, 1995; Meissner and Nooijen, 1995; Meissner, 1998; Landau *et al.*, 2000; Meissner and Malinowski, 2000; Malinowski *et al.*, 2002; Musiał and Meissner, 2005; Musiał *et al.*, 2005). The main idea of the intermediate Hamiltonian approach relies on selecting a part of the orthogonal space $M_\perp$ as an intermediate space M_I, connected with the projector P_I. The M_I space is achieved by the action of the operator Z operating on the model space P. The remaining part of the orthogonal space $M_{I\perp}$ is connected with the projector Q_I related to P_I by

$$Q = P_I + Q_I. \tag{196}$$

Within the FS-MRCCSD model in the expansion of the $e^{\tilde{S}'^{(1,1)}}$ operator,

$$\{e^{\tilde{S}'^{(1,1)}}\}P = (1 + Z + Y)P, \tag{197}$$

$$Z = \{(S_1^{(1,0)} + S_1^{(0,1)} + S_1^{(1,0)}S_1^{(0,1)} + S_2^{(1,1)})\}P^{(1,1)}, \tag{198}$$

TABLE XXIII. Vertical excitation energies (in eV) for N_2 as obtained with the IH-FS and EOM methods at the CCSD level[a] (R=2.068 a.u.)

State symmetry	aug-cc-pVQZ IH-FS (6,4)	aug-cc-pVQZ IH-FS (18,4)	aug-cc-pVQZ EOM	aug-cc-pVQZ+[b] IH-FS (18,4)	aug-cc-pVQZ+[b] EOM	Expt.
Singlet states						
$^1\Pi_g$	10.526	9.194	9.489	9.285	9.489	9.31
$^1\Sigma_u^-$	11.030	9.902	10.109	9.992	10.109	9.92
$^1\Delta_u$	11.504	10.395	10.547	10.477	10.546	10.27
$^1\Pi_u$	13.419	13.443	13.369	13.054	13.056	12.90
Triplet states						
$^3\Sigma_u^+$	8.666	7.638	7.818	7.733	7.818	7.75
$^3\Pi_g$	9.214	7.978	8.184	8.067	8.184	8.04
$^3\Delta_u$	9.859	8.843	9.038	8.931	9.038	8.88
$^3\Sigma_u^-$	10.976	9.816	9.950	9.914	9.950	9.67
$^3\Pi_u$	12.459	11.091	11.363	11.203	11.363	11.19
$^3\Sigma_g^+$	12.711	12.379	12.415	11.975	12.018	12.00

[a]Musiał *et al.*, 2005.
[b]Standard aug-cc-pVQZ basis set with additional s and p functions with exponents. s:0.0192, p:0.0136.

$$Y = \{(S_2^{(1,0)} + S_2^{(0,1)} + S_1^{(1,0)}S_2^{(0,1)} + S_1^{(0,1)}S_2^{(1,0)} + S_2^{(1,0)}S_2^{(0,1)})P^{(1,1)}\}. \quad (199)$$

We see that the operator Z operating on the model space $P^{(1,1)}$ generates determinants belonging to M_I space, while the Y operator connects the $P^{(1,1)}$ and $M_{I\perp}^{(1,1)}$ subspaces. Note that amplitudes of the $S^{(1,1)}$ operator that are sought in the equation for the (1,1) sector do not occur in the Y operator. We define the operator H_I,

$$H_I = P_0\{e^{-Y}\}\bar{H}\{e^{Y}\}P_0 = P_0(1-Y)\bar{H}(1+Y)P_0, \quad (200)$$

where $P_0 = P + P_I$ is a projection operator onto the model+intermediate space. Taking into account that Y generates configurations belonging to the $M_{I\perp}^{(1,1)}$ space, we replace the last equation with

$$H_I = P_0\bar{H}(1+Y)P_0. \quad (201)$$

Diagonalization of the H_I operator within the P_0 space provides a subset of eigenvalues that are identical with those obtained by diagonalization of the H^{eff} operator within the model space. We also observe that the Y operator used to construct the intermediate Hamiltonian is expressed exclusively through the operators known from lower sectors in the current case: $S^{(1,0)}$ and $S^{(0,1)}$. As a result, the FS-MRCC approach formulated in terms of the intermediate Hamiltonian does not require an iterative procedure and is free of the difficulties mentioned at the end of the previous subsection connected with intruder states. The diagrammatic contributions to the H_I elements are given in Fig. 44. Note that here, also, disconnected terms contribute but the result is size extensive due to the cancellation of disconnected terms in the diagonalization process.

The intermediate Hamiltonian formulation of the FS-MRCC theory has great advantages over the traditional FS approach. Being free from intruder states and divergence problems, it allows consideration of larger model spaces for which iterative solutions are impossible. In Table XXIII, we present IH-FS-MRCCSD results for the N_2 molecule obtained for two relatively large basis sets: the standard aug-cc-pVQZ basis set (Kendall *et al.*, 1992) and that with additional diffuse *s* and *p* functions. Two model spaces were considered: one containing 24 reference determinants and the other including 72 determinants. It may be seen from Table XXIII that the results depend on the type of model space. For the larger model space, the theoretical values are much closer to the experimental ones. Particularly good agreement with experiment is observed for the larger basis set: the diffuse basis functions allow for a proper treatment of the Rydberg states, and that combined with the sufficiently large model space gives results much closer to experimental data than the EOM values obtained for the same basis set. We believe that the intermediate Hamiltonian version of the FS-MRCC theory opens new and interesting possibilities for multireference CC theory.

ACKNOWLEDGMENTS

R.J.B. would like to acknowledge his teachers Per-Olov Löwdin, whose influence, many years later, can be seen throughout this paper; and John C. Slater, who first introduced him to electronic structure theory. Our contribution to the development of coupled-cluster theory has critically depended upon the exceptional students, postdocs, and visiting professors that joined us in this effort, many of whom are today's leaders in the field. Their names appear throughout the bibliography. M.M. owes a debt of gratitude to Professor Stanisław Kucharski, Dean of the School of Sciences, University of Silesia, Katowice, Poland, who first introduced her to diagrammatic CC methods. The authors particularly appreciate the long term support from the Air Force Office of Scientific Research, who supported the Bartlett's group development of coupled-cluster theory from the mid-1970s to the present. Special thanks go to Dr. Michael Berman, Dr. Larry Burgraff, Dr. Larry Davis, and Dr. Ralph Kelley.

REFERENCES

Adamowicz, L., and R. J. Bartlett, 1985, Int. J. Quantum Chem. **19**, 217.
Adamowicz, L., R. J. Bartlett, and E. A. Mccullough, 1985, Phys. Rev. Lett. **54**, 426.
Adamowicz, L., W. D. Laidig, and R. J. Bartlett, 1984, Int. J. Quantum Chem. **18**, 245.
Alexeev, Y., T. L. Windus, C. G. Zhan, and D. A. Dixon, 2005, Int. J. Quantum Chem. **104**, 379.
Almlöf, J., and P. R. Taylor, 1987, J. Chem. Phys. **86**, 4070.
Arponen, J. S., 1983, Ann. Phys. (N.Y.) **151**, 311.
Arponen, J. S., 1991, Theor. Chim. Acta **80**, 149.
Arponen, J. S., R. F. Bishop, and E. Pajanne, 1987a, Phys. Rev. A **36**, 2519.
Arponen, J. S., R. F. Bishop, and E. Pajanne, 1987b, Phys. Rev. A **36**, 2539.
Bak, K. L., J. Gauss, T. Helgaker, P. Jörgensen, and J. Olsen, 2000, Chem. Phys. Lett. **319**, 563.
Bak, K. L., P. Jörgensen, J. Olsen, T. Helgaker, and W. Klopper, 2000, J. Chem. Phys. **112**, 9229.
Balkova, A., and R. J. Bartlett, 1992, Chem. Phys. Lett. **193**, 364.
Balkova, A., and R. J. Bartlett, 1995, J. Chem. Phys. **102**, 7116.
Balkova, A., S. A. Kucharski, and R. J. Bartlett, 1991, Chem. Phys. Lett. **182**, 511.
Balkova, A., S. A. Kucharski, L. Meissner, and R. J. Bartlett, 1991a, Theor. Chim. Acta **80**, 335.
Balkova, A., S. A. Kucharski, L. Meissner, and R. J. Bartlett, 1991b, J. Chem. Phys. **95**, 4311.
Barbe, A., C. Secroun, and P. Jouve, 1974, J. Mol. Spectrosc. **49**, 171.
Bartlett, R. J., 1986, in *Geometrical Derivatives of Energy Surfaces and Molecular Properties*, edited by P. Jörgensen and J. Simons (Reidel, Dordrecht, The Netherlands), pp. 35–61.
Bartlett, R. J., 1989, J. Phys. Chem. **89**, 93, feature article.
Bartlett, R. J., 1995, in *Modern Electronic Structure Theory*, edited by D. R. Yarkony (World Scientific, Singapore), Vol. 2, pp. 1047–1131.
Bartlett, R. J., 2002, Int. J. Mol. Sci. **3**, 579.

Bartlett, R. J., 2004, in *Molecular Quantum Mechanics: Selected Papers of N.C. Handy*, edited by D. C. Clary, S. M. Colwell, and H. F. Schaefer III (Taylor & Francis, London), pp. 127–130.
Bartlett, R. J., 2005, in *Theory and Applications of Computational Chemistry: The First Forty Years*, edited by C. E. Dykstra, G. Frenking, K. S. Kim, and G. E. Scuseria (Elsevier, Amsterdam), pp. 1191–1221.
Bartlett, R. J., S. A. Kucharski, and J. Noga, 1989, Chem. Phys. Lett. **155**, 133.
Bartlett, R. J., and M. Musiał, 2006, J. Chem. Phys. **125**, 204105.
Bartlett, R. J., and J. Noga, 1988, Chem. Phys. Lett. **150**, 29.
Bartlett, R. J., and G. D. Purvis III, 1978, Int. J. Quantum Chem. **14**, 561.
Bartlett, R. J., and G. D. Purvis III, 1980, Phys. Scr. **21**, 225.
Bartlett, R. J., and D. M. Silver, 1974a, Phys. Rev. A **10**, 1927.
Bartlett, R. J., and D. M. Silver, 1974b, Chem. Phys. Lett. **29**, 199.
Bartlett, R. J., and D. M. Silver, 1975, Int. J. Quantum Chem., Symp. **9**, 183.
Bartlett, R. J., and D. M. Silver, 1976, J. Chem. Phys. **64**, 4578.
Bartlett, R. J., and J. F. Stanton, 1994, Rev. Comput. Chem. **5**, 65.
Bartlett, R. J., and J. D. Watts, 1998, *ACES II*, in *Encyclopedia of Computational Chemistry*, edited by P. von Schleyer *et al.* (Wiley, New York).
Bartlett, R. J., J. D. Watts, S. A. Kucharski, and J. Noga, 1990, Chem. Phys. Lett. **165**, 513.
Bauschlicher, C. W., Jr., S. R. Langhoff, P. R. Taylor, N. C. Handy, and P. J. Knowles, 1986, J. Chem. Phys. **85**, 1469.
Bauschlicher, C. W., Jr., and P. R. Taylor, 1986, J. Chem. Phys. **85**, 2779.
Bauschlicher, C. W., Jr., and P. R. Taylor, 1987a, J. Chem. Phys. **86**, 1420.
Bauschlicher, C. W., Jr., and P. R. Taylor, 1987b, J. Chem. Phys. **86**, 2844.
Beebe, N. H. F., and J. Linderberg, 1977, Int. J. Quantum Chem. **12**, 683.
Beste, A., and R. J. Bartlett, 2004, J. Chem. Phys. **120**, 8395.
Bieri, G., and L. Asbrink, 1980, J. Electron Spectrosc. Relat. Phenom. **20**, 149.
Bishop, R. F., 1991, Theor. Chim. Acta **80**, 95.
Bishop, R. F., 1998, in *Microscopic Quantum Many-Body Theories and Their Applications*, Lecture Notes in Physics Vol. 510, edited by J. Navarro and A. Polls (Springer, Berlin), pp. 1–70.
Bishop, R. F., T. Brandes, K. A. Germnoth, N. R. Walet, and Y. Xianm, 2002, *Recent Progress in Many-Body Theories, Advances in Quantum Many-Body Theories* (World Scientific, Singapore), Vol. 6.
Bishop, R. F., R. Guardiola, I. Moliner, J. Navarro, M. Partesi, A. Puente, and N. R. Walter, 1998, Nucl. Phys. A **643**, 258.
Bishop, R. F., and K. H. Lührmann, 1978, Phys. Rev. B **17**, 3757.
Bishop, R. F., and K. H. Lührmann, 1981, Physica B & C **108**, 873.
Bloch, C., and J. Horowitz, 1958, Nucl. Phys. **8**, 91.
Bogoliubov, N. N., and D. V. Shirkov, 1959, *Introduction to the Theory of Quantized Fields* (Wiley, New York) (English transl.).
Bomble, Y. J., J. F. Stanton, M. Kallay, and J. Gauss, 2005, J. Chem. Phys. **123**, 054101.
Boys, S. F., 1950, Proc. R. Soc. London, Ser. A **200**, 542.
Brueckner, K. A., 1955, Phys. Rev. **97**, 1353.
Chan, G. K.-L., M. Kallay, and J. Gauss, 2004, J. Chem. Phys. **121**, 6110.
Chaudhuri, R., D. Mukhopadhyay, and D. Mukherjee, 1989, Chem. Phys. Lett. **162**, 393.
Chawla, S., and A. G. Voth, 1998, J. Chem. Phys. **108**, 4697.
Chiles, R. A., and C. E. Dykstra, 1981, J. Chem. Phys. **74**, 4544.
Christiansen, O., H. Koch, and P. Jörgensen, 1995a, Chem. Phys. Lett. **243**, 409.
Christiansen, O., H. Koch, and P. Jörgensen, 1995b, J. Chem. Phys. **103**, 7429.
Christiansen, O., H. Koch, P. Jörgensen, and J. Olsen, 1996, Chem. Phys. Lett. **256**, 185.
Čížek, J., 1966, J. Chem. Phys. **45**, 4256.
Čížek, J., 1969, Adv. Chem. Phys. **14**, 35.
Čížek, J., 1991, Theor. Chim. Acta **80**, 91.
Čížek, J., and J. Paldus, 1971, Int. J. Quantum Chem. **5**, 359.
Coester, F., 1958, Nucl. Phys. **1**, 421.
Coester, F., and H. Kümmel, 1960, Nucl. Phys. **17**, 477.
Comeau, D., and R. J. Bartlett, 1993, Chem. Phys. Lett. **207**, 414.
Coriani, S., D. Marchesan, J. Gauss, Ch. Hattig, T. Helgaker, and P. Jörgensen, 2005, J. Chem. Phys. **123**, 184107.
Crawford, T. D., and H. F. Schaefer, III, 2000, in *Reviews of Computational Chemistry*, edited by K. B. Lipkowitz and D. B. Boyd (Wiley, New York), Vol. 14, pp. 33–136.
Crawford, T. D., and J. F. Stanton, 1998, Int. J. Quantum Chem. **70**, 601.
Dalgarno, A., and A. L. Stewart, 1958, Proc. R. Soc. London, Ser. A **247**, 245.
Davidson, E. R., 1975, J. Comput. Phys. **17**, 87.
Davidson, E. R., and A. A. Jarzecki, 1998, Chem. Phys. Lett. **285**, 155.
Del Bene, J. E., S. A. Perera, R. J. Bartlett, and J. Elguero, 2000, J. Phys. Chem. A **104**, 7165.
Dunning, T. H., Jr., 1989, J. Chem. Phys. **90**, 1007.
Dunning, T. H., and V. McKoy, 1967, J. Chem. Phys. **47**, 1735.
Eliav, E., and U. Kaldor, 1996, Chem. Phys. Lett. **248**, 405.
Eliav, E., U. Kaldor, and B. A. Hess, 1998, J. Chem. Phys. **108**, 3409.
Emrich, K., 1981, Nucl. Phys. A **351**, 379.
Fan, P.-D., K. Kowalski, and P. Piecuch, 2005, Mol. Phys. **103**, 2191.
Flocke, N., and R. J. Bartlett, 2003, Chem. Phys. Lett. **367**, 80.
Förner, W., R. Knab, J. Cizek, and J. Ladik, 1997, J. Chem. Phys. **106**, 10248.
Franke, R., H. Müller, and J. Noga, 1995, J. Chem. Phys. **114**, 7746.
Frantz, M., and R. L. Mills, 1960, Nucl. Phys. **15**, 16.
Freeman, D. L., 1977, Phys. Rev. B **15**, 5512.
Fusti-Molnar, L., and P. G. Szalay, 1996, J. Phys. Chem. **100**, 6288.
Gauss, J., 1998, in *Encyclopedia of Computational Chemistry*, edited by P. von R. Schleyer (Wiley, New York), Vol. I, pp. 615–636.
Gauss, J., and J. F. Stanton, 1995, J. Chem. Phys. **102**, 251.
Gauss, J., and J. F. Stanton, 2002, J. Chem. Phys. **116**, 4773.
Gdanitz, R. J., and R. Ahlricks, 1988, Chem. Phys. Lett. **143**, 413.
Geertsen, J., M. Rittby, and R. J. Bartlett, 1989, Chem. Phys. Lett. **164**, 57.
Gell-Mann, M., and K. A. Brueckner, 1957, Phys. Rev. **106**,

364.
Goldstone, J., 1957, Proc. R. Soc. London, Ser. A **239**, 267.
Guardiola, R., P. I. Moliner, J. Navarro, R. F. Bishop, A. Puente, and N. R. Walter, 1996, Nucl. Phys. A **609**, 218.
Gwaltney, S. R., and R. J. Bartlett, 1998, J. Chem. Phys. **108**, 6790.
Gwaltney, S. R., E. F. C. Byrd, T. Van Voorhis, and M. Head-Gordon, 2002, Chem. Phys. Lett. **353**, 359.
Gwaltney, S. R., and M. Head-Gordon, 2001, J. Chem. Phys. **115**, 2014.
Hald, K., Ch. Hattig, J. Olsen, and P. Jörgensen, 2001, J. Chem. Phys. **115**, 3545.
Handy, N. C., J. A. Pople, M. Head-Gordon, K. Raghavachari, and G. W. Trucks, 1989, Chem. Phys. Lett. **164**, 185.
Handy, N. C., and H. F. Schaefer III, 1984, J. Chem. Phys. **81**, 5031.
Haque, M. A., and D. Mukherjee, 1984, J. Chem. Phys. **80**, 5058.
Harris, T. E., H. J. Monkhorst, and D. L. Freeman, 1992, *Algebraic and Diagrammatic Methods in Many-Fermion Theory* (Oxford University, New York).
Heisenberg, J. H., and B. Mihaila, 1999, Phys. Rev. C **59**, 1440.
Helgaker, T., P. Jörgensen, and J. Olsen, 2000, *Molecular Electronic-Structure Theory* (Wiley, New York), pp. 817–883.
Hess, D. K., and U. Kaldor, 2000, J. Chem. Phys. **112**, 1809.
Hino O., T. Kinoshita, and R. J. Bartlett, 2004, J. Chem. Phys. **121**, 1206.
Hino, O., T. Kinoshita, G. K.-L. Chan, and R. J. Bartlett, 2006, J. Chem. Phys. **124**, 114311.
Hino, O., Y. Tanimura, and S. Ten-no, 2002, Chem. Phys. Lett. **353**, 317.
Hirao, K., and H. Nakatsuji, 1982, J. Comput. Phys. **45**, 246.
Hirata, S., 2003, J. Phys. Chem. A **107**, 10154.
Hirata, S., 2004, J. Chem. Phys. **121**, 5.
Hirata, S., P.-D. Fan, A. A. Auer, M. Nooijen, and P. Piecuch, 2004, J. Chem. Phys. **121**, 12197.
Hirata, S., I. Grabowski, M. Tobita, and R. J. Bartlett, 2001, Chem. Phys. Lett. **345**, 475.
Hirata, S., M. Nooijen, and R. J. Bartlett, 2000, Chem. Phys. Lett. **326**, 255.
Hirata, S., M. Nooijen, I. Grabowski, and R. J. Bartlett, 2001, J. Chem. Phys. **114**, 3919.
Hirata, S., R. Podeszwa, M. Tobita, and R. J. Bartlett, 2004, J. Chem. Phys. **120**, 2581.
Holland, D. M. P., D. A. Shaw, M. A. Hayes, L. G. Shpinkova, E. E. Rennie, L. Karlsson, P. Baltzer, and B. Wannberg, 1997, Chem. Phys. **219**, 91.
Hubač, I., J. Pittner, and P. Čarsky, 2000, J. Chem. Phys. **112**, 8779.
Hubbard, J., 1957, Proc. R. Soc. London, Ser. A **240**, 539.
Huber, K. P., and G. Herzberg, 1979, *Constants of Diatomic Molecules* (Van Nostrand Reinhold, New York).
Hurley, A. C., 1976, *Electron Correlation in Small Molecules* (Academic, New York).
Hylleraas, E. A., 1929, Z. Phys. **54**, 347.
Jeziorski, B., and H. J. Monkhorst, 1981, Phys. Rev. A **24**, 1668.
Jeziorski, B., and J. Paldus, 1989, J. Chem. Phys. **90**, 2714.
Kaldor, U., and B. A. Hess, 1994, Chem. Phys. Lett. **230**, 1.
Kallay, M., and J. Gauss, 2004, J. Chem. Phys. **120**, 6841.
Kállay, M., and P. Surjan, 2001, J. Chem. Phys. **115**, 2945.
Kato T., 1957, Commun. Pure Appl. Math. **10**, 15.
Kelly, H. P., 1962, Ph.D. thesis, University of California, Berkeley.
Kelly, H. P., 1969, Adv. Chem. Phys. **14**, 129.
Kendall, R. A., T. H. Dunning, Jr., and R. J. Harrison, 1992, J. Chem. Phys. **96**, 6796.
Kinoshita, T., O. Hino, and R. J. Bartlett, 2003, J. Chem. Phys. **119**, 7756.
Kinoshita, T., O. Hino, and R. J. Bartlett, 2005, J. Chem. Phys. **123**, 074106.
Kobayashi, R., H. Koch, and P. Jörgensen, 1994, Chem. Phys. Lett. **219**, 30.
Koch, H., O. Christiansen, P. Jörgensen, and J. Olsen, 1995, Chem. Phys. Lett. **244**, 75.
Koch, H., A. S. de Meras, and T. B. Pedersen, 2003, J. Chem. Phys. **118**, 9481.
Koch, H., H. J. Aa. Jensen, P. Jörgensen, and T. Helgaker, 1990, J. Chem. Phys. **93**, 3333.
Koch, H., and P. Jörgensen, 1990, J. Chem. Phys. **93**, 3333.
Kohn, W., and L. J. Sham, 1965, Phys. Rev. **140**, A1133.
Kowalski, K., D. J. Dean, M. Hjorth-Jensen, T. Papenbrock, and P. Piecuch, 2004, Phys. Rev. Lett. **92**, 132501.
Kowalski, K., and P. Piecuch, 2000a, J. Chem. Phys. **113**, 18.
Kowalski, K., and P. Piecuch, 2000b, J. Chem. Phys. **113**, 5644.
Kowalski K., and P. Piecuch, 2001, J. Chem. Phys. **115**, 643.
Krylov, A. I., C. D. Sherill, and M. Head-Gordon, 2000, J. Chem. Phys. **113**, 6509.
Kucharski, S. A., A. Balkova, P. G. Szalay, and R. J. Bartlett, 1992, J. Chem. Phys. **97**, 4289.
Kucharski, S. A., and R. J. Bartlett, 1986, Adv. Quantum Chem. **18**, 281.
Kucharski, S. A., and R. J. Bartlett, 1991a, Theor. Chim. Acta **80**, 387.
Kucharski, S. A., and R. J. Bartlett, 1991b, J. Chem. Phys. **95**, 9271.
Kucharski, S. A., and R. J. Bartlett, 1992, Int. J. Quantum Chem., Quantum Chem. Symp. **26**, 107.
Kucharski, S. A., and R. J. Bartlett, 1993, Chem. Phys. Lett. **206**, 574.
Kucharski, S. A., and R. J. Bartlett, 1998a, J. Chem. Phys. **108**, 5243.
Kucharski, S. A., and R. J. Bartlett, 1998b, J. Chem. Phys. **108**, 5255.
Kucharski, S. A., and R. J. Bartlett, 1998c, J. Chem. Phys. **108**, 9221.
Kucharski, S. A., and R. J. Bartlett, 1999, J. Chem. Phys. **110**, 8233.
Kucharski, S. A., M. Kolaski, and R. J. Bartlett, 2001, J. Chem. Phys. **114**, 692.
Kucharski, S. A., J. D. Watts, and R. J. Bartlett, 1999, Chem. Phys. Lett. **302**, 295.
Kümmel, 1991, Theor. Chim. Acta **80**, 81.
Kümmel, H., K. H. Lührmann, and J. Zabolitzky, 1978, Phys. Rep., Phys. Lett. **36**, 1.
Kutzelnigg, W., 1985, Theor. Chim. Acta **68**, 445.
Laidig, W. D., P. Saxe, and R. J. Bartlett, 1987, J. Chem. Phys. **86**, 887.
Landau, A., E. Eliav, Y. Ishikawa, and U. Kaldor, 2000, J. Chem. Phys. **113**, 9905.
Landau, A., E. Eliav, and U. Kaldor, 1999, Chem. Phys. Lett. **313**, 399.
Larsen, H., K. Hald, J. Olsen, and P. Jörgensen, 2001, J. Chem. Phys. **115**, 3015.
Lauderdale, W. J., J. F. Stanton, J. Gauss, J. D. Watts, and R. J.

Bartlett, 1992, J. Chem. Phys. **97**, 6606.
Lee, T. J., and G. E. Scuseria, 1995, in *Quantum Mechanical Electronic Structure Calculations with Chemical Accuracy*, edited by S. R. Langhoff (Kluwer, Dordrecht, The Netherlands), pp. 47–108.
Lee, Y. S., S. A. Kucharski, and R. J. Bartlett, 1984, J. Chem. Phys. **81**, 5906.
Levchenko, S. V., and A. I. Krylov, 2004, J. Chem. Phys. **120**, 175.
Li, X., and J. Paldus, 1994, J. Chem. Phys. **101**, 8812.
Li, X., and J. Paldus, 2004, J. Chem. Phys. **120**, 5890.
Lindgren, I., 1978, Int. J. Quantum Chem. **S12**, 33.
Lindgren, I., 1979, Int. J. Quantum Chem. **S12**, 3827.
Lindgren, I., and M. Morrison, 1986, *Atomic Many-Body Theory*, 2nd ed. (Springer, Berlin).
Lindgren, I., and D. Mukherjee, 1987, Phys. Rep. **151**, 93.
Lindgren, I., and S. Salomonsen, 2002, Int. J. Quantum Chem. **90**, 294.
Lischa, H., R. Shepard, I. Shavitt, R. M. Pitzer, M. Dallos, Th. Muller, P. G. Szalay, F. B. Brown, R. Ahlirchs, H. J. Bohm, A. Chang, D. C. Comeau, R. Gdanitz, H. Dachsel, C. Ehrhardt, M. Ernzerhof, P. Hochtl, S. Irle, G. Kedziora, T. Kovar, V. Parasuk, M. J. M. Pepper, P. Scharf, H. Schiffer, M. Schindler, M. Schuler, M. Seth, E. A. Stahlberg, J.-G. Zhao, S. Yabushita, and Z. Zhang, 2001, COLUMBUS, an *ab initio* electronic structure program, release 5.8.
Löwdin, P.-O., 1955, Phys. Rev. **97**, 1474.
Löwdin, P.-O., 1959, Adv. Chem. Phys. **2**, 207.
Löwdin, P.-O., 1968, Int. J. Quantum Chem. **2**, 867.
Lynch, B. J., and D. G. Truhlar, 2003, J. Phys. Chem. A **107**, 3898.
Malinowski, P., L. Meissner, and A. Nowaczyk, 2002, J. Chem. Phys. **116**, 7362.
Malrieu, J.-P., Ph. Durand, and J.-P. Daudey, 1985, J. Phys. B **18**, 809.
Manne, R., 1977, Int. J. Quantum Chem. **Y-11**, 175.
Maŝik A., and I. Hubač, 1999, Adv. Quantum Chem. **31**, 75.
McCurdy, C. W., Jr., T. N. Resigno, D. L. Yeager, and V. McKoy, 1982, in *The Equation of Motion Method: An Approach to the Dynamical Properties of Atoms and Molecules*, edited by G. A. Webb (Academic, New York), Vol. 12, pp. 339–386.
Meissner, L., 1998, J. Chem. Phys. **108**, 9227.
Meissner, L., and R. J. Bartlett, 1995, J. Chem. Phys. **102**, 7490.
Meissner, L., and R. J. Bartlett, 2001, J. Chem. Phys. **115**, 50.
Meissner, L., and P. Malinowski, 2000, Phys. Rev. A **61**, 062510.
Meissner, L., and M. Nooijen, 1995, J. Chem. Phys. **102**, 9604.
Mihaila, B., and J. Heisenberg, 2000, Phys. Rev. C **61**, 054309.
Monkhorst, H. J., 1977, Int. J. Quantum Chem., Quantum Chem. Symp. **11**, 421.
Mosyagin, N. S., A. V. Titov, E. Eliav, and U. Kaldor, 2001, J. Chem. Phys. **115**, 2007.
Moszyński, R., P. S. Żuchowski, and B. Jeziorski, 2005, Collect. Czech. Chem. Commun. **70**, 1109.
Mukherjee, D., and S. Pal, 1989, Adv. Quantum Chem. **20**, 291.
Musiał, M., and R. J. Bartlett, 2003, J. Chem. Phys. **119**, 1901.
Musiał, M., and R. J. Bartlett, 2004a, Chem. Phys. Lett. **384**, 210.
Musiał, M., and R. J. Bartlett, 2004b, J. Chem. Phys. **121**, 1670.
Musiał, M., and R. J. Bartlett, 2005, J. Chem. Phys. **122**, 224102.
Musiał, M., and S. A. Kucharski, 2004, Struct. Chem. **15**, 421.
Musiał, M., S. A. Kucharski, and R. J. Bartlett, 2001, J. Mol. Struct.: THEOCHEM **547**, 269.
Musiał, M., S. A. Kucharski, and R. J. Bartlett, 2002a, Mol. Phys. **100**, 1867.
Musiał, M., S. A. Kucharski, and R. J. Bartlett, 2002b, J. Chem. Phys. **116**, 4382.
Musiał, M., S. A. Kucharski, and R. J. Bartlett, 2003, J. Chem. Phys. **118**, 1128.
Musiał, M., S. A. Kucharski, and R. J. Bartlett, 2004, Adv. Quantum Chem. **47**, 209.
Musiał, M., and L. Meissner, 2005, Collect. Czech. Chem. Commun. **70**, 811.
Musiał, M., L. Meissner, S. A. Kucharski, and R. J. Bartlett, 2005, J. Chem. Phys. **122**, 224110.
Nakatsuji, H., 1978, Chem. Phys. Lett. **59**, 362.
Noga, J., R. J. Bartlett, and M. Urban, 1987, Chem. Phys. Lett. **134**, 126.
Noga, J., and W. Kutzelnigg, 1994, J. Chem. Phys. **101**, 7738.
Noga, J., W. Kutzelnigg, and W. Klopper, 1992, Chem. Phys. Lett. **199**, 497.
Noga, J., and P. Valiron, 2000, Chem. Phys. Lett. **324**, 166.
Noga, J., and P. Valiron, 2002, in *Computational Chemistry: Reviews of Current Trends*, edited by J. Leszczynski (World Scientific, Singapore), Vol. 7, pp. 131–185.
Noga, J., P. Valiron, and W. Klopper, 2001, J. Chem. Phys. **115**, 2022.
Nooijen, M., 2005, unpublished.
Nooijen, M., and R. J. Bartlett, 1997a, J. Chem. Phys. **106**, 6441.
Nooijen, M., and R. J. Bartlett, 1997b, J. Chem. Phys. **106**, 6449.
Nooijen, M., and R. J. Bartlett, 1997c, J. Chem. Phys. **107**, 6812.
Oliphant, N., and L. Adamowicz, 1992, J. Chem. Phys. **96**, 3739.
Olsen, J., 2000, J. Chem. Phys. **113**, 7140.
Pal, S., M. Rittby, and R. J. Bartlett, 1987, Chem. Phys. Lett. **137**, 273.
Pal, S., M. Rittby, R. J. Bartlett, D. Sinha, and D. Mukherjee, 1988, Chem. Phys. **88**, 4357.
Paldus, J., 1991, in *Methods in Computational Molecular Physics*, NATO Advanced Study Institute (Plenum, New York).
Paldus, J., 2005, in *Theory and Applications of Computational Chemistry: The First Forty Years*, edited by C. E. Dykstra, G. Frenking, K. S. Kim, and G. E. Scuseria (Elsevier, Amsterdam), pp. 115–147.
Paldus, J., and J. Čížek, 1975, Adv. Quantum Chem. **9**, 105.
Paldus, J., J. Cízek, and I. Shavitt, 1972, Phys. Rev. A **5**, 50.
Paldus, J., P. Piecuch, L. Pylypow, and B. Jeziorski, 1993, Phys. Rev. A **47**, 2738.
Parr, R. G., and B. L. Crawford, 1948, J. Chem. Phys. **16**, 526
Pawlowski, F., A. Halkier, P. Jörgensen, K. L. Bak, T. Helgaker, and W. Klopper, 2003, J. Chem. Phys. **118**, 2539.
Perera, S. A., and R. J. Bartlett, 1993, Chem. Phys. Lett. **216**, 606.
Perera, S. A., and R. J. Bartlett, 1996, J. Am. Chem. Soc. **118**, 7849.
Perera, S. A., and R. J. Bartlett, 2000, J. Am. Chem. Soc. **122**, 1231.
Perera, S. A., and R. J. Bartlett, 2005, Adv. Quantum Chem. **48**, 435.
Perera, S. A., M. Nooijen, and R. J. Bartlett, 1996, J. Chem. Phys. **104**, 3290.
Peterson, K. A., A. K. Wilson, D. E. Woon, and T. H. Dunning,

Jr., 1997, Theor. Chim. Acta **97**, 251.
Piecuch, P., K. Kowalski, I. S. Pimienta, and M. J. McGuire, 2002, Int. Rev. Phys. Chem. **21**, 527.
Piecuch, P., S. A. Kucharski, and R. J. Bartlett, 1999, J. Chem. Phys. **110**, 6103.
Piecuch, P., N. Oliphant, and L. Adamowicz, 1993, J. Chem. Phys. **99**, 1875.
Piecuch, P., M. Włoch, J. R. Gour, and A. Kinal, 2006, Chem. Phys. Lett. **418**, 467.
Pisani, L., and E. Clementi, 1995, J. Chem. Phys. **103**, 9321.
Pittner, J., 2003, J. Chem. Phys. **118**, 10876.
Pittner, J., P. Nachtigall, P. Carsky, J. Mašik, and I. Hubač, 1999, J. Chem. Phys. **110**, 10275.
Pople, J. A., J. S. Binkley, and R. Seeger, 1976, Int. J. Quantum Chem., Symp. **10**, 1.
Pople, J. A., R. Krishnan, H. B. Schlegel, and J. S. Binkley, 1978, Int. J. Quantum Chem., Quantum Chem. Symp. **14**, 545.
Purvis, G. D., III, and R. J. Bartlett, 1982, J. Chem. Phys. **76**, 1910.
Purvis, G. D., III, H. Sekino, and R. J. Bartlett, 1988, Collect. Czech. Chem. Commun. **53**, 2203.
Ragavachari, K., G. W. Trucks, J. A. Pople, and M. Head-Gordon, 1989, Chem. Phys. Lett. **157**, 479.
Rittby, M., and R. J. Bartlett, 1991, Theor. Chim. Acta **80**, 649.
Rowe, D. J., 1968, Rev. Mod. Phys. **40**, 153.
Rozyczko, P., and R. J. Bartlett, 1997, J. Chem. Phys. **107**, 10823.
Rozyczko, P., S. A. Perera, M. Nooijen, and R. J. Bartlett, 1997, J. Chem. Phys. **107**, 6736.
Ruden, T. A., T. Helgaker, P. Jörgensen, and J. Olsen, 2004, J. Chem. Phys. **121**, 5874.
Salter, E. A., and R. J. Bartlett, 1989, J. Chem. Phys. **90**, 1767.
Salter, E. A., G. W. Trucks, and R. J. Bartlett, 1989, J. Chem. Phys. **90**, 1752.
Sari, L., Y. Yamaguchi, and F. Schaefer III, 2001, J. Chem. Phys. **115**, 5932.
Schuetz, M., and H. J. Werner, 2000, Chem. Phys. Lett. **318**, 370.
Scuseria, G. E., A. C. Sheiner, T. J. Lee, J. E. Rice, and H. F. Schaefer III, 1987, J. Chem. Phys. **86**, 2881.
Sekino, H., and R. J. Bartlett, 1984, Int. J. Quantum Chem., Quantum Chem. Symp. **18**, 255.
Sekino, H., and R. J. Bartlett, 1999, Adv. Quantum Chem. **35**, 149.
Shavitt, I., 1998, Mol. Phys. **94**, 3.
Shavitt, I., and R. J. Bartlett, 2006, *Many-Body Methods in Quantum Chemistry: Many-Body Perturbation Theory and Coupled-Cluster Theory* (Cambridge University Press, in press).
Simons, J., and W. D. Smith, 1973, J. Chem. Phys. **58**, 4899.
Sinha, D., A. Mukhopadhyay, M. D. Prasad, and D. Mukherjee, 1986, Chem. Phys. Lett. **125**, 213.
Slater, J. C., 1929, Phys. Rev. **34**, 1293.
Sorouri, A., W. M. C. Foulkes, and N. D. M. Hine, 2006, J. Chem. Phys. **124**, 064105.
Stanton, J. F., 1994, J. Chem. Phys. **101**, 371.
Stanton, J. F., and R. J. Bartlett, 1993a, J. Chem. Phys. **99**, 5178.
Stanton, J. F., and R. J. Bartlett, 1993b, J. Chem. Phys. **98**, 7029.
Stanton, J. F., and J. Gauss, 1995, J. Chem. Phys. **103**, 8931.
Stanton, J. F., and J. Gauss, 1999, J. Chem. Phys. **110**, 6079.
Stanton, J. F., J. Gauss, and R. J. Bartlett, 1992, J. Chem. Phys. **97**, 5554.
Stanton, J. F., J. Gauss, J. D. Watts, M. Nooijen, N. Oliphant, S. A. Perera, P. G. Szalay, W. J. Lauderdale, S. A. Kucharski, S. R. Gwaltney, S. Beck, A. Balková, D. E. Bernholdt, K. K. Baeck, P. Różyczko, H. Sekino, C. Hober, J. Pittner, and R. J. Bartlett, 1993, ACES II program is a product of the Quantum Theory Project, University of Florida. Integral packages included are VMOL (J. Almlöf and P. Taylor); VPROPS (P. R. Taylor); and a modified version of the ABACUS integral derivative package (T. U. Helgaker, H. J. Aa. Jensen, J. Olsen, P. Jörgensen, and P. R. Taylor).
Stanton, J. F., W. N. Lipscomb, D. H. Magers, and R. J. Bartlett, 1989, J. Chem. Phys. **90**, 1077.
Szalay, P. G., 1997, in *Modern Ideas in Coupled-Cluster Methods*, edited by R. J. Bartlett (World Scientific, Singapore), pp. 81–123.
Szalay, P. G., and R. J. Bartlett, 1992, Int. J. Quantum Chem. **S26**, 85.
Szalay, P. G., and R. J. Bartlett, 1993, Chem. Phys. Lett. **214**, 481.
Szalay, P. G., and J. Gauss, 2000, J. Chem. Phys. **112**, 4027.
Szalay, P. G., J. Gauss, and J. F. Stanton, 1993, Theor. Chim. Acta **100**, 5.
Szalay, P. G., M. Nooijen, and R. J. Bartlett, 1995, J. Chem. Phys. **103**, 281.
Tajti, A., P. G. Szalay, A. G. Csaszar, M. Kallay, J. Gauss, E. F. Valeev, B. A. Flowers, J. Vazquez, and J. F. Stanton, 2004, J. Chem. Phys. **121**, 11599.
Tanaka, T., and Y. Morino, 1970, J. Mol. Spectrosc. **33**, 538.
Taube, A., and R. J. Bartlett, 2006, Int. J. Quantum Chem. (in press).
Thouless, D. J., 1961, *The Quantum Mechanics of Many Body Systems* (Academic, New York), p. 121.
Tobita, M., S. A. Perera, M. Musiał, R. J. Bartlett, M. Nooijen, and J. S. Lee, 2003, J. Chem. Phys. **119**, 10713.
Urban, M., I. Cernusak, V. Kello, and J. Noga, 1987, in *Methods in Computational Chemistry*, edited by S. Wilson (Plenum, New York), Vol. I, p. 117.
Urban, M., J. Noga, S. J. Cole, and R. J. Bartlett, 1985, J. Chem. Phys. **83**, 4041.
Van Voorhis, T., and M. Head-Gordon, 2000, Chem. Phys. Lett. **330**, 585.
Van Voorhis, T., and M. Head-Gordon, 2001, J. Chem. Phys. **115**, 7814.
Visscher, L., 1996, Chem. Phys. Lett. **253**, 20.
Visscher, L., J. Styszynski, and W. C. Nieuwpoort, 1996, J. Chem. Phys. **105**, 1987.
Watts, J. D., and R. J. Bartlett, 1994, Int. J. Quantum Chem. **28**, 195.
Watts, J. D., and R. J. Bartlett, 1995, Chem. Phys. Lett. **233**, 81.
Watts, J. D., and R. J. Bartlett, 1996, Chem. Phys. Lett. **258**, 581.
Watts, J. D., J. Gauss, and R. J. Bartlett, 1992, Chem. Phys. Lett. **200**, 1.
Watts, J. D., J. Gauss, and R. J. Bartlett, 1993, J. Chem. Phys. **98**, 8718.
Watts, J. D., S. R. Gwaltney, and R. J. Bartlett, 1996, J. Chem. Phys. **105**, 6979.
Werner, H. J., and F. R. Manby, 2006, J. Chem. Phys. **124**, 054114.
Wick, G. C., 1950, Phys. Rev. **80**, 268.
Wilson, K., 1989, *Ab Initio Quantum Chemistry: A Source of Ideas for Lattice Gauge Theorists, Nuclear Physics*

B—Proceedings of the Lattice Conference, Supplement, September, 1990, pp. 82–92.
Włoch, M., D. J. Dean, J. R. Gour, M. Hjorth-Jensen, K. Kowalski, T. Papenbrock, and P. Piecuch, 2005, Phys. Rev. Lett. **94**, 212501.
Woon, D. E., and T. H. Dunning, 1993, J. Chem. Phys. **98**, 1358.
Yau, A. D., S. A. Perera, and R. J. Bartlett, 2002, Mol. Phys. **100**, 835.